JCUA
International Journal of Contemporary Urban Affairs

Journal of Contemporary Urban Affairs

Vol. 01 Issue 03 2017 ISSN 2475-6156

In This issue:

ISSN 2475-6156 (print)
ISSN 2475-6164 (online)

Journal of Contemporary Urban Affairs

Volume 1, Issue 3, December 2017

Special issue on Climate Change Adaptation

www.ijcua.com

IMPRESSUM

International Journal of Contemporary Urban Affairs

Volume 1, Issue 3, December 2017

Special issue on Climate Change Adaptation

ISSN 2475-6156 (print) **ISSN** 2475-6164 (online)
URL: www.ijcua.com
Email: editor@ijcua.com
Publisher: Anglo-American Publications LLC
Address:
- No 13, Subat Sokak, Orkoz 1 Apartment, Flat 3, KKTC, Via Mersin 99302, Turkey.
- Girne American University, Karmi Campus, Mersin 10 Via, KKTC, Turkey.
Phone: +90 506 189 99 66
Circulation: 100 copies

Indexed & Abstracted:

Crossref, CNKI , BASE (Bielefeld Academic Search Engine) , Findplus , Scilit, Garba Rujukan Digital (GARUDA), ISSN International Centre, Dimensions, Powered by Digital Science, DRJI (Directory of Research Journals Indexing), TIB, IPI (Indonesian Publication Index), Polish Scholarly Bibliography (PBN), Osmikon Search , EZB, Index Copernicus, Genamics JournalSeek, SSRN, MAFIADOC, KUDOS, WorldCat, CiteFactote, UBL (Universitas Bibliotek Leipzig), SCIPIO, Elektronische Zeitschriften, TurkEgitiminDeksi, ResearchBib, SIS Index, Scientific world index, IIJIF, COSMOS, ESJI (Eurasian Scientific Journal Index), IP Indexing, JOURNAL FACTOR, IP Online Journal, Root Society for Indexing and Impact Factor, General Impact factor, I2OR, Saif Scholars Impact, Slideshare, Science Index , SPARC Indexing, Biojournal, Internation Scientific Indexing (ISI), sjifactor, International Citation Index (ICI), Calameo, LIVIVO - The Search Portal for Life Sciences, ZB MED – Informationszentrum Lebenswissenschaften, Opacplus, Beluga – Catalogue of Hamburg Libraries, Tpbin, ResearchGate

Note: *Journal of Contemporary Urban Affairs* (JCUA) has already been approved to be host by the libraries of Harvard University , Columbia University Libraries , University of Washington , University of Vechta and Technical University of Denmark.

Contemporary Urban Affairs

Journal of contemporary urban Affairs

www.ijcua.com Anglo-American Publications LLC

Review Board Members

Copy Editor:
Dr. Timothy O. Iyendo, European University of Lefke, KKTC, North Cyprus

Proofreader
Harry Jake Wadsworth, Girne American University, North Cyprus, Kyrenia, Turkey

Technical-Editor
Batuhan Yildiz, Girne American University, North Cyprus, Kyrenia, Turkey

Cover Design
Deren Raman, Girne American University, North Cyprus, Kyrenia, Turkey

****

Publisher:
Anglo-American Publications LLC
Address:
- No 13, Subat Sokak, Orkoz 1 Apartment, Flat 3, KKTC, Via Mersin 99302, Turkey.
- Girne American University, Karmi Campus, Mersin 10 Via, KKTC, **Turkey**.
Phone: +90 533 837 2598
Website: www.ijcua.com
E-mail: editor@ijcua.com

About the Journal

The journal of contemporary urban affairs is the interdisciplinary academic, refereed journal which publishes two times a year by Anglo-American Publications LLC. Journal of Contemporary Urban Affairs brings together all the theories, manifestoes and methodologies on contemporary urban spaces to raise the understanding for the future of urban planning. Overall, the journal of contemporary urban affairs aimed to establish a bridge between theory and practice in built environment. Thus, it reports on the latest research findings and innovative approaches, methodologies for creating, assessing, and understanding of contemporary built environments.

JCUA distinguishes itself by providing an international and interdisciplinary platform for the exchange of ideas and information among Architectures, urban planners, policy makers and urbanists from all disciplines to focus on seven main concern of this journal which are Housing studies, Emerging cities, urban ecology, Infra Habitation, Revitalization strategies, conflict, divided territories and overall contemporary urban issues about mentioned concerns. Submissions of empirical, comparative, theoretical research, critical review and manifestoes for the future of cities from different scholarly disciplines and methodological perspectives are encouraged.

Coverages

The journal explores a range of academic and policy concerns including, but not limited to:

- Conflict and divided territories.
- Emerging cities.
- Urban ecology, morphology and growing *concern on sustainability*.
- Infra Habitation (Slums / Affordable houses and Gated communities).
- Revitalization, regeneration and urban renewal.
- Housing studies (livability, responsive environment, quality of life and etc.)
- Contemporary urban issues (politics, strategies, sociology, Crime, Immigration and international labor migration and etc. New urbanism, Rapid urbanization, Urban sprawl).

Peer Review Statement

All research articles in this journal have undergone rigorous peer review, based on initial editor screening and anonymized refereeing by two referees.

The manuscript submission and peer review process is broken down into the following steps:

The Author submits a manuscript.
The Editor assigns Reviewers to the manuscript.
The Reviewers review the manuscript.
The Editor drafts a decision to be sent to the Author.

CrossCheck Plagiarism Screening System

The author bears the responsibility for checking whether material submitted is subject to copyright or ownership rights, e.g. figures, tables, photographs, illustrations, trade literature and data. The author will need to obtain permission to reproduce any such items, and include these permissions with their final submission. Where use is so restricted, the editorial office and Publisher must be informed with the final submission of the material. Please add any necessary acknowledgments to the typescript, preferably in the form of an Acknowledgments section at the end of the paper. Credit the source and copyright of photographs, figures, illustrations etc. in the supplementary captions.

Abstracting and Indexing

The journal is abstracted / indexed in:

Crossref
CNKI
BASE (Bielefeld Academic Search Engine)
Scilit
DRJI (Directory of Research Journals Indexing)
TIB
EZB
Index Copernicus
SSRN
MAFIADOC
KUDOS
WorldCat
CiteFactote
UBL (Universitas Bibliotek Leipzig)
SCIPIO
TurkEgitiminDeksi
ResearchBib
SIS Index
Scientific world index
IIJIF
COSMOS
ESJI (Eurasian Scientific Journal Index)
IP Indexing
IP Online Journal
Root Society for Indexing and Impact Factor
General Impact factor
I2OR
Saif Scholars Impact
Science Index

DOI number

Each paper published in the Journal of Contemporary Urban Affairs is assigned a DOI® number, which appears beneath the author's affiliation in the published paper.

Table of contents

Journal Of Contemporary Urban Affairs

2017, Volume 1, Number 3, pages 1– 6

Solar Radiation Projections of Cmip5 Models for South of Brazil

* **Elison Eduardo Bierhals** [1], **Francisco Pereira** [2], **Claudinéia Brazil** [3], **Elton Rossini** [4]

[1, 2, 3, 4] Energy Engineering, State University of Rio Grande do Sul, Brazil

[1] E mail: bierhalseduardo@gmail.com , [2] E mail: kiko.borgesp@gmail.com , [3] E mail: neiabrazil@gmail.com

ARTICLEINFO:

Article history:

Received 15 September 2017

Accepted 25 October 2017

Available online 3 November 2017

Keywords:

Climate Change;
Solar Radiation;
Energy Utilization.

ABSTRACT

The most critical factors in the acceleration of climate and environmental changes are related to the industrial development and consequently to an increase in the demand for electricity. Looking for measures that minimize impacts to the environment, alternative energy sources are gaining more and more space in the Brazilian energy matrix. Brazil presents a great solar potential for the generation of electric energy, so the knowledge of solar radiation and its characteristics are fundamental for the study of the energy use. Due to the above, this article aims to verify the climatic variability corresponding to the variations in solar radiation patterns, in the face of climate change scenarios. The database used in this research is part of the Phase 5 Intercomparison of Matching Models (CMIP5). Was used the RCP 8.5 that scenario is considered the most pessimistic for the 21st century and is consistent with no policy change to reduce emissions and strong dependence on fossil fuels. It is important, first of all, to determine its availability in order to enable the use of solar radiation as a source of energy in a given location and / or region. The climatic projections, based on the pessimistic scenario, in a 75-year period (2026-2100) showed a fall in solar radiation in all of Rio Grande do Sul, reaching 12% in the eastern region of the state. A concern with the factors that influence the pessimistic perspectives of this scenario, as it may affect a possible production of electric energy from solar radiation.

JOURNAL OF CONTEMPORARY URBAN AFFAIRS (2017) ***1***(3), 1-6.

https://doi.org/10.25034/ijcua.2018.36xx71

www.ijcua.com

1. Introduction

The acceleration of climate change is related to the industrial development and, consequently, to an increase in the demand for electricity. Looking for measures that minimize environmental impacts, the Brazilian energy matrix is gaining new formatting, becoming less and less dependent on non-renewable energy sources, such as oil and natural gas, while alternative sources of renewable energy increase its presence (Lima, 2012). By opting for a photovoltaic solar generation, the consumer also contributes to the mitigation of climate change, which is currently considered one of the biggest environmental problems.

The IPCC (Intergovernmental Panel on Climate Change) is the leading international scientific body for assessing climate change and

***Corresponding Author:**
Energy Engineering, State University of Rio Grande do Sul, Brazil
E-mail address: bierhalseduardo@gmail.com

was created to provide scientific information on the current state of knowledge of climate change and its possible socioeconomic and environmental impacts (Silveira *et al.,* 2016).

The results from this program have been an important tool for policies implementation as responses to climate change. The data are the results of global models simulations from several research centers, simulations of global models represent numerical and physical approximations of equations governing the movements of the atmosphere and their interaction with the Earth's surface (Sousa, 2010).

Since 1995, the IPCC reports have had an experimental framework to study the data provided by ocean-atmosphere general circulation models, the Coupled Model Intercomparison Project (CMIP). The combination of several readings of atmospheric data around the world makes it possible to evaluate certain patterns, which can predict events or evaluate deficiencies or even errors in the ways of analyzing these data (Le Treut *et al.,* 2007) .

The use of alternative sources of energy represents a major challenge in order to meet energy demand and reduce environmental damage. Faced with the need to diversify the energy matrix and try to minimize global warming, solar energy has been gaining space, being an important renewable source, even depending on the climatic conditions.

Compared to the European level, Brazil presents a great solar potential for the generation of electric energy, having more sun hours per year. The sun is an inexhaustible source of energy, allowing you to obtain a clean energy. According to Freitas (2008) quality information about the solar resource is fundamental for the sizing of solar systems, since the generation of electric energy depends on the availability of the resource.

Therefore, the knowledge about solar radiation and its characteristics are fundamental for the study of the energy utilization. Due to the above, this article aims to verify the climatic variability corresponding to the variations in solar radiation patterns by analyzing climate change scenarios.

2. Materials And Methods

2.1 Study area

The state of Rio Grande do Sul (Figure 1) is located in Brazil's extreme south, between latitudes 27 ° and 34 ° South (S) and longitudes 50 ° and 57 ° West (W). The state maintains borders to the West with Argentina, to the South with Uruguay, to the North with the Brazilian State of Santa Catarina and to the east, it is bathed by the Atlantic Ocean.

The territorial area of Rio Grande do Sul has 268,781,896 km²; the average population density is 38 inhabitants per km². Among the states of Brazil's southern region is the one with the lowest density (Gross, 2015).

The predominant climate is subtropical, being that in the region of the upper plateau the climate is subtropical of altitude.

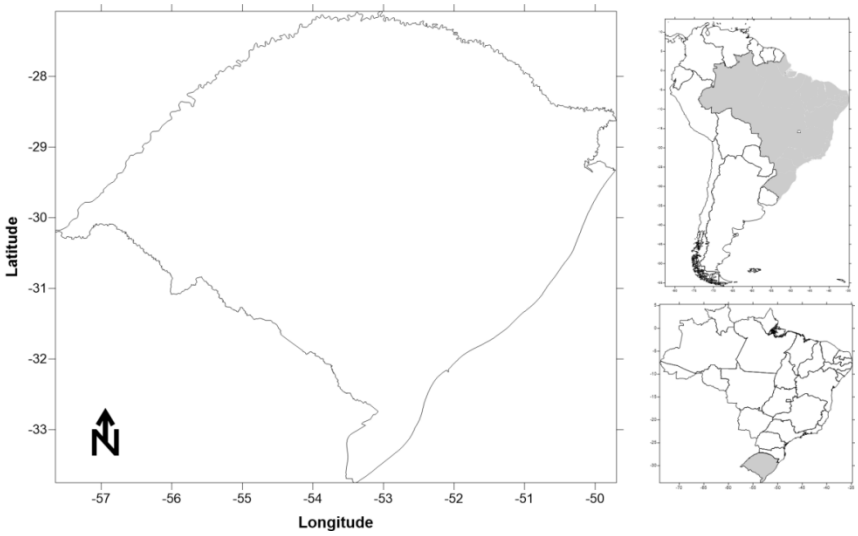

Figure 1. Map of the Study Region.

2.2 Description of the model used

The database used in this research is a part from the Phase 5 Intercomparison of Matching Models (CMIP5), and contributed to the preparation of the fifth IPCC-AR5 report. The data were extracted from ACCESS (The Australian Community Climate and Earth System Simulator) model.

According to Van Vuuren, and others in AR5 the scenarios are organized according to the RCPs. In this research, RCP 8.5 scenario was used which represents a scenario with a continuous population growth, resulting in high carbon dioxide emissions, with an increase Up to 4 ° C. (Van Vuuren, *et al.*, 2011)

In terms of greenhouse gas emissions, this scenario is considered to be the most pessimistic for the 21st century and is consistent with no policy change to reduce emissions and strong dependence on fossil fuels (Silveira, *et al.*, 2016).

3. Methodology

The work was carried out in steps, the monthly data of Solar radiation in KWh / m² were extracted from the IPCC-AR5 data base, this work stage was performed through GRADS software (Grid Analysis and Display System).

Grads is a data visualization and analysis systems in grid points, working with binary data matrices, in which variables can have up to four dimensions (longitude, latitude, vertical levels and time) (Souza, 2004).

After this stage, the historical data series and the data series with the climatic projections were organized. The projections were divided into three scenarios: Scenario-1 (2026-2050), Scenario-2 (2051-2075) and Scenario-3 (2076-2100).

The solar radiation anomaly was calculated from the following equation:

A_{Rad} (%) = ((R_{MM} – R_{MN})/ R_{MN})*100 (Equation 1)

At where:

ARad (%) is the radiation anomaly in percentage;

RMM is the average radiation of the month analyzed;

NMR is the normal climatological correlation for the analyzed month.

The World Meteorological Organization (WMO) defines climatological normal as averages of climatological data calculated for consecutive periods of 30 years

4. Results And Discussions

It is important, first of all, to determine its availability in order to enable the use of solar radiation as a source of energy in a given location and / or region.

Figure 3 shows the average solar radiation based on the IPCC projections for the state of Rio Grande do Sul from 2026 to 2100. The highest values are found in the Rio Grande do Sul'sthe western half of the state of Rio Grande do Sul, in the region of the Uruguayan's municipality with the maximum around 5 KWh / m², agreeing with the results obtained by Buriol and others that verified the availability of solar radiation from historical data. In the state's eastern region are located the lowest values of solar radiation (Buriol, *et. al.*, 2012).

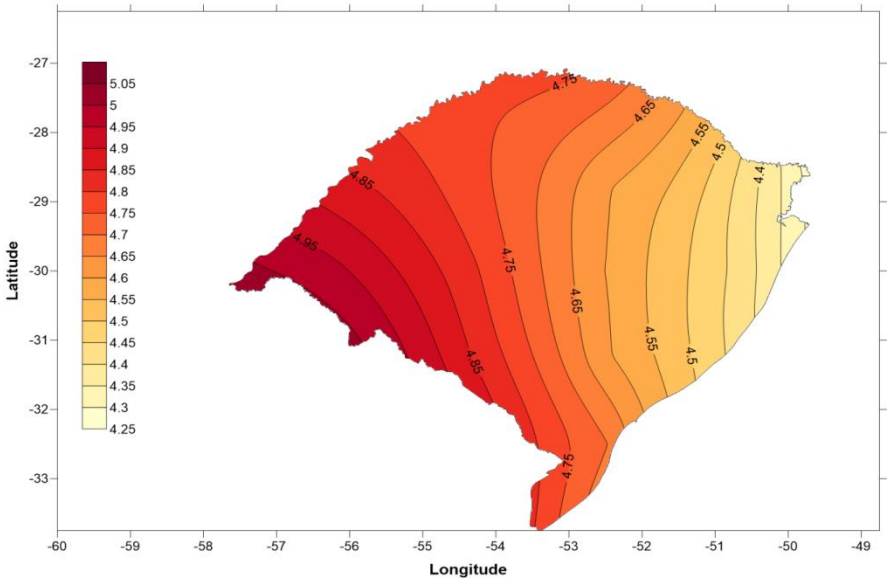

Figure 3. Average solar radiation KWh / m² - Projections (2026 - 2100)

From the historical series of Solar Radiation, the Climatic Radiation Norms were calculated, which are the long period averages of 1961-1990, for all months of the year. Based on

this information were recorded for each period the percentage of months that the Radiation was above or below Normal Climatological, according to Figure 4, it was verified that for all the scenarios analyzed Solar Radiation has a tendency to decrease over the next few years, in the scenario of 2076-2100 the tendency is that the radiation is 60% of the months below the normal climatological.

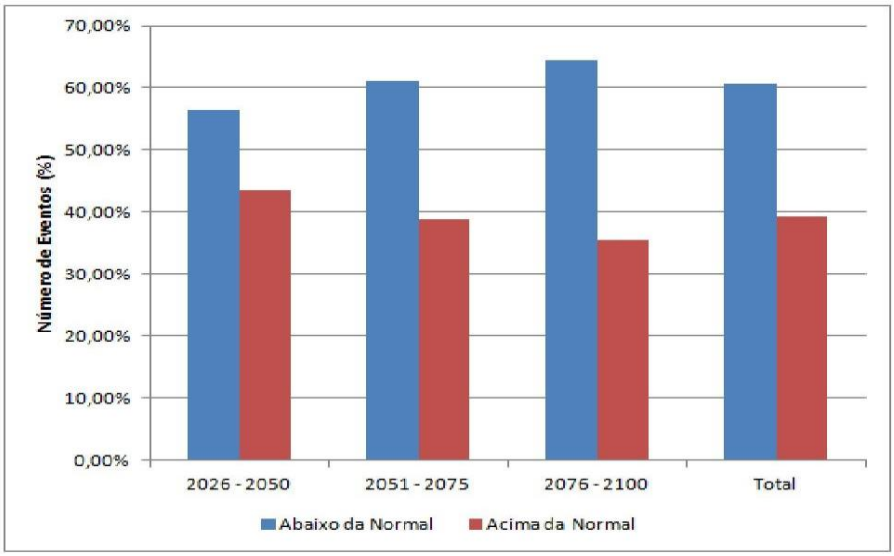

Figure 4. Graph percentage of number of events above(red) and below(blue) the Normal Climatological.

In order to verify the mean alteration trend over time, the anomalies of solar radiation that are the extreme fluctuations related to the historical averages were analyzed. Figure 5 shows the solar radiation anomaly for scenario 1 (2026-2100). In the coastal region, in addition to presenting the lowest values of solar radiation, the trend is that for this scenario there will be a fall around 5% compared to historical data, verifying the scenario 2(Figure 6) and scenario 3 (Figure 7), the tendency is to increase the fall of solar radiation, reaching a loss of 12% in the upper region of the East of the state of Rio Grande do Sul.

In general, negative anomalies were observed in the three scenarios, indicating a significant fall in radiation over the years, for the entire Gaucho territory.

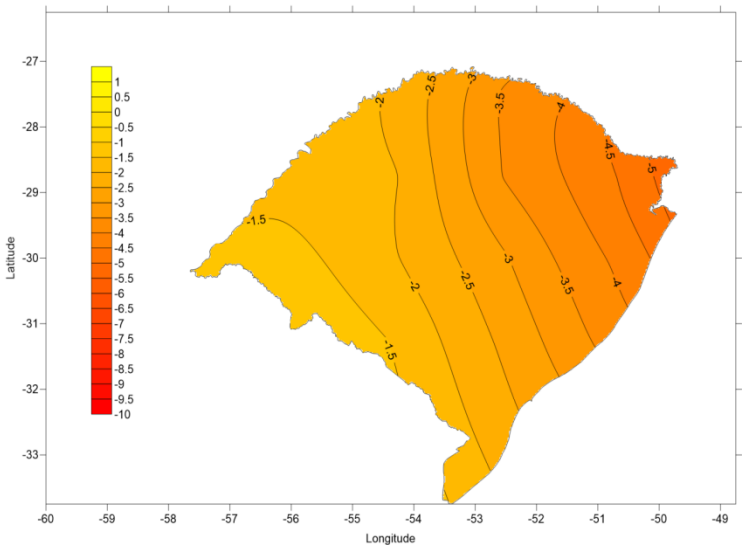

Figure 5. Averages of solar radiation anomalies KWh / m² (%)
Scenario 1 (2026 - 2050)

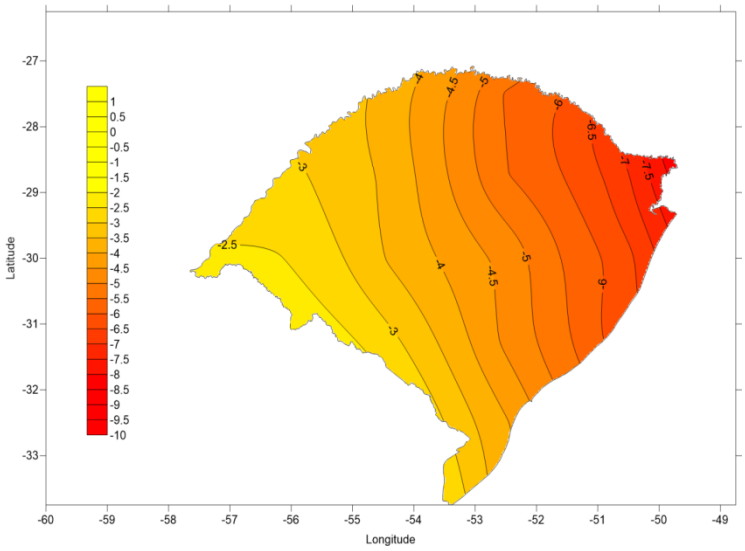

Figure 6. Averages of solar radiation anomalies KWh / m² (%) Scenario 2 (2051 - 2075)

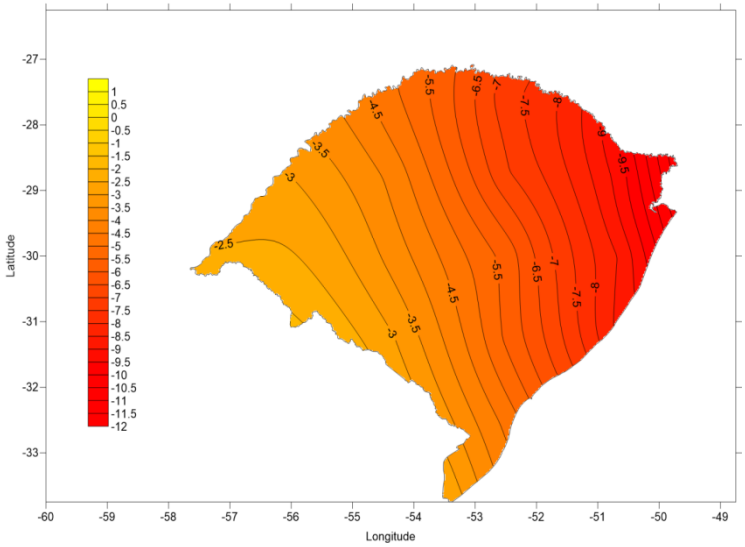

Figure 7. Averages of solar radiation anomalies KWh / m² (%) Scenario 2 (2076 - 2100)

5. Conclusions

Renewable energies, for the most part, are dependent on weather conditions, so adequate energy planning requires climate change knowledge. The climatic projections, based on the pessimistic scenario, showed in all Rio Grande do Sul a solar radiation fall, reaching 12% in the eastern region of the state. This data demonstrates the need for concern with the factors that influence the pessimistic perspectives of this scenario, as it will directly affect a possible production of electricity from solar radiation. In order to diversify the energy matrix and minimize future climate impacts, it is important to invest in an energy policy considering renewable energy sources.

Acknowledgement

This research did not receive any specific grant from funding agencies in the public, commercial, or not-for-profit sectors.

Referenes

Buriol, G. A., Estefanel, V., Heldwein, A. B., Prestes, S.D., Horn, J. F. C. (2012). Estimativa Da radiação solar global a partir dos dados de insolação, para Santa Maria - RS. *Ciência Rural, 42*, 1563-1567,

Freitas, S. S. A. (2008). Dimensionamento de sistemas fotovoltaicos**.**.*Bragança: ESTIG, Dissertação de Mestrado em Engenharia Industrial*.

Gross, J. A. (2015). *Índice de Anomalia de Chuva (IAC) dos municípios do Rio Grande do Sul afetados pelas estiagens no período de*

1991 a 2012. Dissertação de Mestrado. Universidade Federal de Santa Maria.

Lima, R. A. (2012) .A produção de energias renováveis e o desenvolvimento Sustentável: uma análise no cenário da mudança do clima. *Energy Law in Brazil, 5* (4).

Le Treut, H., R. Somerville, U. Cubasch, Y. Ding, C. Mauritzen, A. Mokssit, T. Peterson And Prather, M. (2007). Historical Overview of Climate Change. In: *Climate Change 2007: The Physical Science Basis. Contribution of Working Group I to the Fourth assessment Report of the Intergovernmental Panel on Climate Change* [Solomon, S., D. Qin, M. Manning, Z. Chen, M. Marquis, K.B. Averyt, M. Tignor and H.L. Miller (eds.)]. Cambridge, United Kingdom and New York, NY, USA: Cambridge University Press.

Silveira, S. S., Souza Filho, F. Martins, E. S., Oliveira, J. Costa, A., Nobrega, M. Souza, S. A. (2016). Climate change in the São Francisco river basin: analysis of precipitation and temperature**.** *RBRH, 21* (2), 416 - 428

Sousa, M. M. (2010). *Comparação Entre Ferramentas de Modelagem Unidimensional e Quasi-Bidimensional, Permanente e Não- Permanente, em Planejamento e Projetos de Engenharia Hidráulica.* Rio de Janeiro, Brazil: UFRJ/COPPE.

Souza, E. B. (2004) .*GrADS – Grid Analysis and Display System Fundamentos e rogramação Básica.* Universidade Federal do Pará. Retrieved from http://www.dca.iag.usp.br/www/material/ritaynoue/aca522/referencias/apostilagrads.pdf>.

Van Vuuren, D. P.; Edmonsds, J.; Kainuma, M.; Riahi, K.; Thomsonm, A.; Hibbard, K.; Hurtt, G. C.; Kram T.; Krey, V.; Lamarque, J. F.; Masui, T.; Meinshausen, M.; Nakicenovic, N.; Smith, S. J.; Rose, S. K. (2011). The representative concentration pathways: an overview. *Climatic Change, 109*,5-31.

Journal Of Contemporary Urban Affairs

2017, Volume 1, Number 3, pages 7– 12

Experimental analysis of a flat plate solar collector with integrated latent heat thermal storage

* Mauricio, Carmona[1], Mario Palacio[2], Arnold Martínez[3]

[1] Mechanical Engineering Department, Universidad del Norte, Colombia

[2] Faculty of Mechanical and Industrial Engineering, Universidad Pontificia Bolivariana, Colombia

[3] Mechanical Engineering Department, Universidad de Córdoba, Colombia

[1]E mail: mycarmona@uninorte.edu.co , [2]E mail: mario.palaciov@upb.edu.co

ARTICLEINFO:

Article history:

Received 2 August 2017

Accepted 10 August 2017

Available online 12 October 2017

Keywords:

Solar collector;
Thermal storage;
Latent heat storage.

ABSTRACT

In the present paper, an experimental analysis of a solar water heating collector with an integrated latent heat storage unit is presented. With the purpose to determine the performance of a device on a lab scale, but with commercial features, a flat plate solar collector with phase change material (PCM) containers under the absorber plate was constructed and tested. PCM used was a commercial semi-refined light paraffin with a melting point of 60°C. Tests were carried out in outdoor conditions from October 2016 to March 2017 starting at 7:00 AM until the collector does not transfer heat to the water after sunset. Performance variables as water inlet temperature, outlet temperature, mass flow and solar radiation were measured in order to determine a useful heat and the collector efficiency. Furthermore, operating temperatures of the glass cover, air gap, absorber plate, and PCM containers are presented. Other external variables as ambient temperature, humidity and wind speed were measured with a weather station located next to the collector. The developed prototype reached an average thermal efficiency of 24.11% and a maximum outlet temperature of 50°C. Results indicate that the absorber plate reached the PCM melting point in few cases, this suggests that the use of a PCM with a lower melting point could be a potential strategy to increase thermal storage. A thermal analysis and conclusions of the device performance are discussed.

JOURNAL OF CONTEMPORARY URBAN AFFAIRS (2017) ***1***(3), 7-12.

https://doi.org/10.25034/ijcua.2018.36zd72

www.ijcua.com

1. Introduction

Solar energy is the most widely available energy source in the world. However, it presents some obstacles to its implementation such as sensitivity to climatic conditions and intermittency. Therefore, it is necessary to develop technologies that allow storing solar energy for the periods in which it is not available, or its power is low. Two common methods of storing solar thermal energy are sensible and latent heat storage. While sensible heat is more common in practical applications, latent heat storage provides higher storage density, with narrow temperature variation. (Abhat, 1983) reported one of the earliest reviews on latent heat thermal storage. (Zalba *et al.*, 2003) reviewed thermal

***Corresponding Author:**
Mechanical Engineering Department, Universidad del Norte, Colombia
E-mail address: mycarmona@uninorte.edu.co

energy storage with PCM and its heat transfer analysis and applications. (Farid *et al.*, 2004; Kenisarin and Mahkamov, 2007; Nkwetta and Haghighat, 2014; Sharma *et al.,* 2009) reviewed solar energy storage using phase change materials. (Chandel and Agarwal, 2017) Reviewed the current state of research on energy storage, toxicity, health hazards and commercialization of phase changing materials. (Pandey and Chaurasiya, 2017) reviewed the analysis and development of solar flat plate collectors.

Although numerous works on latent heat storage, no commercial solar heaters with built-in PCM storage have been reported. However, preliminary studies in laboratory prototypes have shown considerable increases in efficiency and supply capacity. (Kürklü *et al.,* 2002) found a large difference between ambient temperature and water temperature both at day and at night. With the experimental techniques used, it was not possible to determine the phase change point at least in a general approach. No performance comparison is made against traditional devices. However they showed that its prototype has advantages in manufacturing cost and total weight for commercial devices, although it does not include an energy analysis. In countries with tropical climates, no scientific references have been found in studies of this kind of technology, in spite of the great capacity of available solar energy, quite possibly due to the lack of suitable commercial PCMs for this application. (Mehling *et al.,* 2003) presented experimental results and numerical simulation of a water tank with a PCM module using an explicit finite-difference method. Experiments and simulations indicated an increase in energy density of the tank of 20% to 45%. (Canbazoglu *et al*., 2005) Analyzed experimentally the time variations of the water temperatures at the midpoint of the heat storage tank of a solar heating system with sodium thiosulfate pentahydrate as PCM. It was obtained an increase in the produced hot water mass and total heat accumulated approximately 2.59–3.45 times of the conventional solar water-heating system. (Cabeza *et al.,* 2006) constructed an experimental solar pilot plant to test the PCM behavior in real conditions. It was obtained a discharge temperature stabilization near to 54 1C for a period of time between 10 and 12 h. (Mettawee and Assassa, 2006) performed parametric studies of different operating conditions, concluding that as the material melts, the heat transfer by convection increases the speed of the accumulation process. (Koca *et al.,* 2008) performed an analysis of energy and exergy a latent heat storage system with phase change material (PCM) for a flat-plate solar collector. The obtained experimental data showed that exergy efficiencies of latent heat storage systems with PCM are very low. However, the area of collector surface was smaller than that of the PCM surface area. As a result of this, the cost of the latent heat storage system was high and outlet temperature obtained was low. (Bouadila *et al.,* 2014) have developed an experimental study on a solar flat plate water heater with an accumulation of thermal energy in the collector using a PCM. Experimental measurements ascertain that the outlet temperature was not affected by the severe global solar radiation fluctuations. The solar collector remains a uniform useful heat around 400W during 5 h after sunset. (Serale *et al.,* 2014) present an approach to increase the performance of flat collectors based on the exploitation of the latent heat of the heat carrier fluid. The aim of this paper is to analyze experimentally the performance of a lab-scale solar collector built with commercial features and a latent heat storage unit inside it.

2. Method and materials

It was designed and constructed a flat plate solar collector prototype with a cavity to place macro-encapsulated PCM under the absorber plate. A schematic representation of the prototype is shown in Fig. 1. Further details of the collector are presented in Fig. 2 and described in Table 1.

The PCM was microencapsulated in 4 rectangular steel containers of 4000 X 4000 X 30 mm. Each container was filled with 3.35 kg of semi refined paraffin wax with a nominal melting point between 58-60 °C.

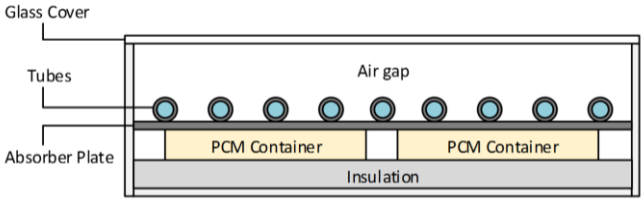

Figure 1. Schematic representation of the Solar Collector.

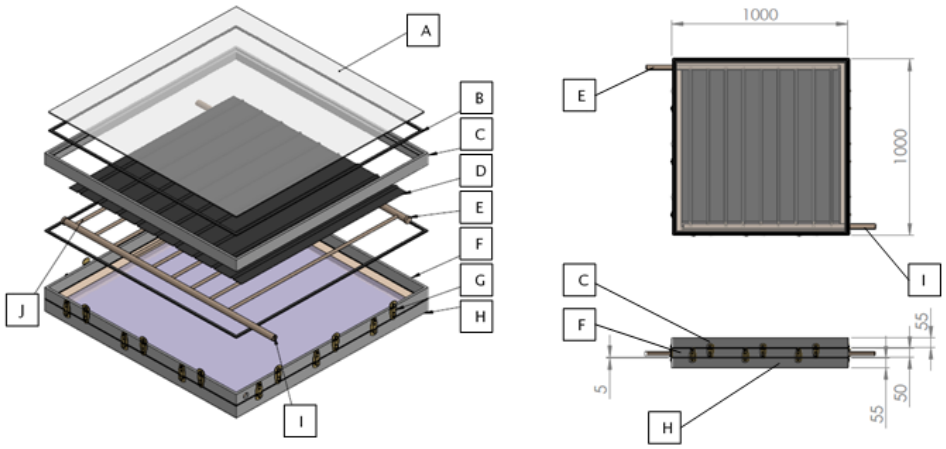

Figure. 1. Detailed view of the Solar Collector.

Table 1. Detailed component description of the collector

Item	Description	Specifications
A	Glass cover	Thickness: 4 mm
B	Gasket	--
C	Air cavity case	Thickness: 4 mm Aluminum
D	Absorber plate	Thickness: 1 mm Copper
E	Inlet line pipe	Diameter: 25.4 mm Copper
F	Plate Case	Thickness: 4 mm Aluminum
G	Lockers	--
H	PCM Cavity	Internal polyurethane insolation
I	Outlet line	Diameter: 25.4 mm Copper
J	Absorber pipes	Diameter: 12.7 mm Copper Separation: 100 mm

The experimental set-up is shown in **Error! Reference source not found.**. The water was supplied by an Aqua Pak LOOP 3V32-9/1115 pump with a fixed volumetric flow rate of 0.2 L/min and monitored by a rotameter Dwyer of 1.2 L/min. A weather station Davis Vantage Pro 2 Plus measured ambient temperature, wind speed, humidity and global solar radiation. Temperatures of the glass cover, confined air, absorber plate, water inlet, water outlet and PCM containers were measured with type-K thermocouples connected to a data acquisition unit Applent AT4532. 8 temperature channels were located on the absorber plate, 2 on the water inlet, 2 on the water outlet, 2 on the glass cover, 2 measured the confined air temperature, 4 on the top of the PCM containers and 4 at the bottom.

The experimental tests were carried out in 3 experimental campaigns with 20 days each one. The first campaign was performed in October 2016, the second in December 2016 and the third in February 2017. All at the test took place in Universidad del Norte campus, in Barranquilla Colombia (11°1'12.17"N,74°51'5.44"O). The test started at 7:00 AM monitoring all the variables every 5 minutes until the collector did not increase water temperature after sunset.

Figure 3. Experimental bank: 1. Water reservoir, 2. Pump, 3. Rotameter, 4. Solar collector, 5. Data acquisition unit, 6. Water reception tank, 7. Weather station.

3. Results & Discussion

Results of accumulated radiation, useful heat and efficiency during the 60 days of experimentation are presented in Figure 2 and summarized in Table 2. The highest efficiency of the collector was obtained in tests carried out in December while the lowest value during tests executed in October. As can be observed in Table 2, while low efficiencies are found both in rainy season with low radiation and clear season

with high radiation the highest efficiency values were obtained during medium radiation values.

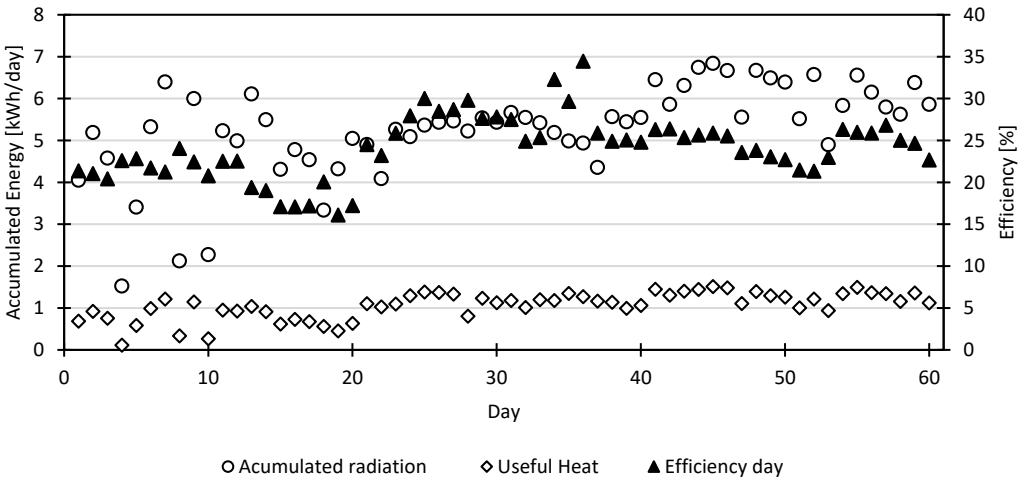

Figure 2. Experimental results by day.

Table 2. Results of the tests and weather conditions.

Exp. Campaign	Days in Figure X	Weather	Average Acc.rad [kWh/day]	Rad. Std. dev [kWh/day]	Average Efficiency [%]
Oct	01 - 20	Rainy	4.45	1.33	20.34
Dec	21 - 40	Scattered	5.22	0.41	27.44
Feb	41- 60	Clear	6.16	0.51	24.57
Total		-	5.27	1.10	24.11

The following graphs present the behavior of the collector on March 12, 2017. Figure 3 and Figure 4 shows respectively the solar radiation and wind speed measured by the weather station. This day has a high incidence of solar radiation with an accumulated radiation of 5.27 kWh. Figure 5 shows that the outlet temperature did not decrease too much during the cloudiness events of 11:00 and 15:00 which shows that the thermal energy storage system provides stability to the water supply.

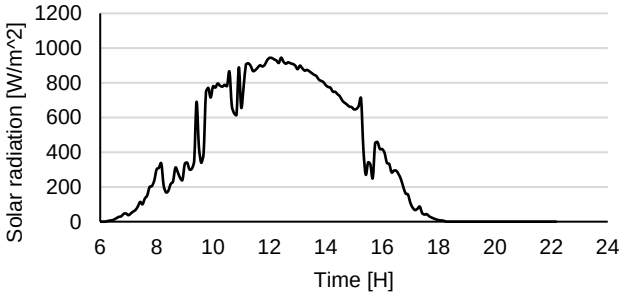

Figure 3. Solar radiation

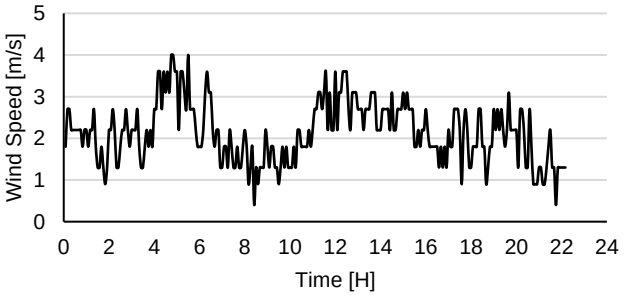

Figure 4. Wind speed

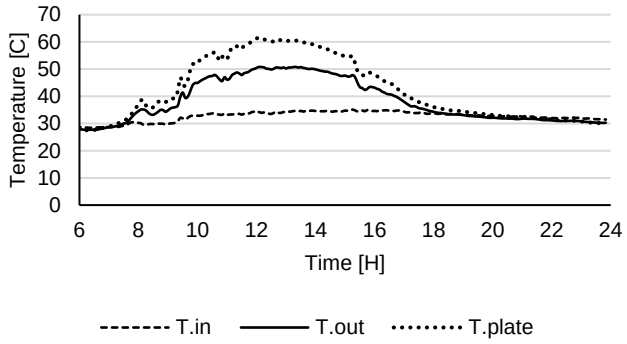

Figure 5. Temperatures of absorber plate, water inlet, and water outlet

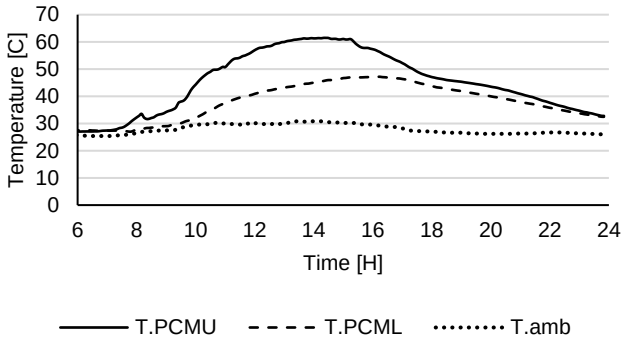

Figure 6. PCM Temperature and ambient temperature

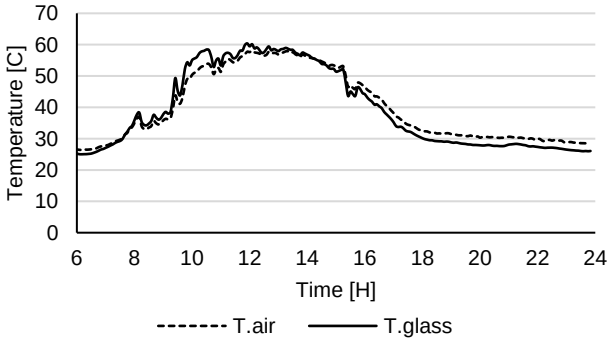

Figure 7. Temperature of air gap and glass cover

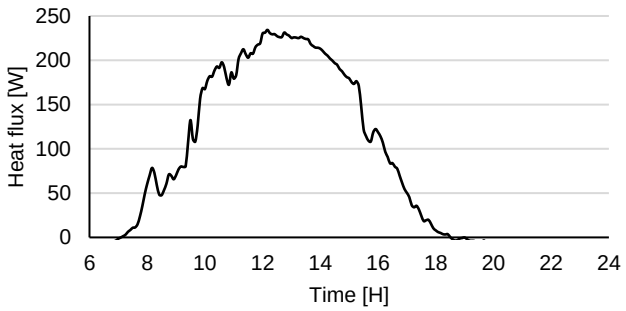

Figure 8. Useful Heat.

It can be observed in Figure 6 that the PCM containers store heat energy by sensible heat until 14:00, from where the temperature at container's top (T.PCMU) remains at 60°C until 16:00, indicating storage by latent heat. However, it should be noted in Figure 5 that the temperature of the absorber plate reaches the melting point of the PCM only for 2 hours, in many experimental tests the phase change temperature is never reached. This gives a short time to the PCM to accumulate energy by latent heat resulting in a PCM discharging process at a non-constant temperature. On the other hand, it can be seen in Figure 6 an asymmetric charge/discharge process. Despite the proper charging process during the morning the storage system was unable to provide thermal energy to the working fluid after 18:00 as can be seen in Figure 8 This may be due to an excess of PCM in the solar collector. In fact, Figure 6 shows that, although the upper part of the PCM reaches the phase change temperature, the lower part never reaches it and even its maximum temperature is reached about 2 hours later. Therefore, it can be inferred that during the night the molten PCM transfers heat to the solid PCM layers instead of the working fluid.

4. Conclusions

In this paper, an experimental analysis was carried out to evaluate the performance of a flat plate solar collector with integrated microencapsulated PCM as latent heat storage system. The highest efficiency of the prototype was obtained at accumulated radiation of 5.22 kWh/day. Values above or below this amount of radiation resulted in lower efficiency values. Asymmetric PCM charge/discharge process was observed. Therefore, reduce the PCM mass is recommended to avoid upper layers discharge thermal energy to lower layers instead of the absorber plate. It was obtained that the PCM modules provided stability to the outlet temperature against strong fluctuations in solar radiation. However, it was unable to supply thermal energy to the working fluid during the night. The short time the absorber plate reached the melting point of the PCM may be a cause of this. Thus, experimental analysis and simulation with PCM with lower phase change temperature is recommended.

Acknowledgments

This investigation has been partially funded by the Colombian Administrative Department of Science, Technology, and Innovation-COLCIENCIAS, through the program "es Tiempo

de Volver". Authors wish to express their acknowledgments to COLCIENCIAS and its excellent program.

Acknowledgement

This research did not receive any specific grant from funding agencies in the public, commercial, or not-for-profit sectors.

References

Abhat, A. (1983). Low-temperature latent heat thermal energy storage: Heat storage materials. *Sol. Energy, 30,* 313–332. doi:10.1016/0038-092X(83)90186-X

Bouadila, S., Fteïti, M., Oueslati, M.M., Guizani, A., Farhat, A. (2014). Enhancement of latent heat storage in a rectangular cavity: a Solar water heater case study. *Energy Convers. Manag*. *78*, 904–912. doi:10.1016/j.enconman.2013.07.094

Cabeza, L.F., Ibáñez, M., Solé, C., Roca, J., Nogués, M.(2006). Experimentation with a water tank including a PCM module. *Solar Energy Materials and Solar Cells,90* (9), 1273–1282. doi:10.1016/j.solmat.2005.08.002

Canbazoglu, S., Sahinaslan, A., Ekmekyapar, A., Aksoya, Y., Akarsu, F. (2005). Enhancement of solar thermal energy storage performance using sodium thiosulfate pentahydrate of a conventional solar water-heating system. *Energy Build, 37*, 235–242. doi:10.1016/j.enbuild.2004.06.016

Chandel, S.S., Agarwal, T. (2017). Review of current state of research on energy storage, toxicity, health hazards and commercialization of phase changing materials. Renew. Sustain. *Energy Rev,67*, 581–596. doi:10.1016/j.rser.2016.09.070

Farid, M.M., Khudhair, A.M., Razack, S.A.K., Al-Hallaj, S. (2004). A review on phase change energy storage: materials and applications. *Energy Convers. Manag. 45*, 1597–1615. doi:10.1016/j.enconman.2003.09.015

Kenisarin, M., Mahkamov, K. (2007). Solar energy storage using phase change materials. Renew. Sustain. *Energy Rev, 11*, 1913–1965. doi:10.1016/j.rser.2006.05.005

Koca, A., Oztop, H.F., Koyun, T., Varol, Y. (2008). Energy and exergy analysis of a latent heat storage system with phase change material for a solar collector. *Renew. Energy, 33.* doi:10.1016/j.renene.2007.03.012

Kürklü, A., Özmerzi, A., Bilgin, S. (2002). Thermal performance of water-phase change material solar collector. *Renew. Energy, 26*, 391–399. doi:10.1016/S0960-1481(01)00130-6

Mehling, H., Hippeli, S., Hiebler, S., Cabeza, L.F. (2003). PCM-module to improve hot water heat stores with stratification. *Renew. Energy, 28*, 699–711. doi:10.1016/S0960-1481(02)00108-8

Mettawee, E.B.S., Assassa, G.M.R.(2006). Experimental study of a compact PCM solar collector. *Energy ,31*, 2622–2632. doi:10.1016/j.energy.2005.11.019

Nkwetta, D.N., Haghighat, F., 2014. Thermal energy storage with phase change material - A state-of-the art review. Sustain. Cities Soc. 10, 87–100. doi:10.1016/j.scs.2013.05.007

Pandey, K.M., Chaurasiya, R. (2017). A review on analysis and development of solar flat plate collector. *Renew. Sustain. Energy Rev, 67*, 641–650. doi:10.1016/j.rser.2016.09.078

Serale, G., Baronetto, S., Goia, F., Perino, M. (2014). Characterization and energy performance of a slurry PCM-based solar thermal collector: A numerical analysis, in: *Energy Procedia, 48* .223–232. doi:10.1016/j.egypro.2014.02.027

Sharma, A., Tyagi, V.V., Chen, C.R., Buddhi, D. (2009). Review on thermal energy storage with phase change materials and applications. *Renew. Sustain. Energy Rev,13*, 318–345. doi:10.1016/j.rser.2007.10.005

Zalba, B., Marín, J.M., Cabeza, L.F., Mehling, H. (2003). Review on thermal energy storage with phase change: Materials, heat transfer analysis and applications. *Appl. Therm. Eng, 23*, 251–283. doi:10.1016/S1359-4311(02)00192-8

Journal Of Contemporary Urban Affairs

2017, Volume 1, Number 3, pages 13– 17

Livable City One Step Towards Sustainable Development

* Dr. **Farzaneh Sasanpour** [1]

[1] Department of Geography and Urban Planning, Kharazmi University, Tehran, Iran

E mail: f.sasanpour@gmail.com

ARTICLEINFO:

Article history:

Received 2 August 2017

Accepted 15 August 2017

Available online 12 October 2017

Keywords:

Livable City; Sustainable Development; Iran; Arak

ABSTRACT

Cities are the engines of economic growth. According to the United Nations, Today the global urban population is expected to reach 3 billion to 5 billion (61 percent) by 2030.The industrial revolution and the resulting economic-social changes led to the transformation of residential patterns and living patterns. Due to the increasing development of cities and its problems, the theory of sustainable development followed by the approach of the livable city was considered. Livable city environment with good planning is an attractive and safe environment for life, work and development, including good governance, competitive economy, high quality of life and environmental sustainability. The results indicate that the social, economic and environmental aspects of livability of the city of Arak are moderate and unfavorable. Also, the results of the Topsis model, which is a multi-criteria and decision-making model, show that in the environmental dimension of the region two with a score of 0.6859 and in the social dimension of the region of three with a score of 0.92 and in the economic dimension of the region three with a score of 1, the highest rank Have won. As a result, the city of Arak ranked 58th, is not livable and of the three city areas, zone 3 is closer to the surface of livable. And this process will not be in the path of sustainable development.

JOURNAL OF CONTEMPORARY URBAN AFFAIRS (2017) ***1***(3), 13-17.

https://doi.org/10.25034/ijcua.2018.3673

www.ijcua.com

1. Introduction

The cities can be recognized by scientific systems based on different views and theories. Among the new theories, is livable city, It is a term that describes a comfortable and sustainable environment and urban space as a place to live, work, visit for various aspects of the physical (urban facilities, infrastructure, spatial planning, etc.), as well as non-physical (relationships) Social, economic activities, etc. (Sasanpour *et al.* 2015). Until recently, initiatives to enhance livability and sustainability have been largely community-based, responding to issues of local concern (Miller, *et al.,* 2013). Livability and sustainability are popular concepts for urban planning and general public discourse, largely because they are representative of values, priorities, and behaviors to which many people and institutions subscribe. It is widely assumed that consumers should have a right to both livable and sustainable communities, which raises questions for planners and decision makers about how to satisfy the needs and desires of current and future residents. Yet, the conceptual linkages between livability and its counterpart

***Corresponding Author:**
Department of Geography and Urban Planning, Kharazmi University, Tehran, Iran
E-mail address: f.sasanpour@gmail.com

sustainability are not fully understood, limiting agreement on the policies to promote these ideals and their assessment (Portney, 2013; Van Kamp *et al.*, 2003). Livability, by contrast, brings a necessary pragmatism to the philosophical visions of sustainability. Livability is about now and here, focused on immediate and tangible conditions and interventions, and therefore interpreted as more achievable (Ruth and Franklin 2013). Understanding how livability sits next to sustainability will help planners bridge the desires of residents in the present moment with longer-term needs associated with a sustainability vision. Once basic needs, such as food, shelter, and security are fulfilled, individuals typically emphasize concern for matters over the short term, including livability preferences (Maslow, 1998; Ruth and Franklin, 2013; Gough, 2015). Although these notable distinctions between sustainability and livability imply competing normative and evaluation principles—and different remedies for their respective inherent concerns, there is an important nexus between the two concepts that may assist in the other's success. Livability interventions represent the incremental steps that collectively increase the potential for longer-term strides toward sustainability. "Livable sustainability" has been discussed elsewhere as the result of accommodating short-term, urgent needs or desires of community within a plan for larger scale, longer-term prospects of sustainability (Allen, 2010; Holden and Scerri 2013)

On the other hand, cities as the most important achievements of humans are places that, according to experts, have attracted the most studies to increase livability and achieve sustainable development. The city is a phenomenon that has evolved in history, the result of culture and spatial effects of playing the basic roles of man in the geographical environment and having various dimensions of the environmental, historical, cultural, political, economic, social, and psychological. Hence, comprehensive understanding of the city is possible by knowing all its dimensions and components. Livability encompasses a range of human needs ranging from food and security to beauty and cultural symbols and a sense of belonging to a community or place (Badland, *et al.*, 2014). The livability of the 1980s was due to the rapid development of urban areas relative to urban centers (in fact, at the same time as sustainable development).

In the meantime, Iranian cities, including the city of Arak, are confronted with issues of concern. The city of Arak, with an area of 5341 hectares, is located linearly along the east-west line. The city is located on the geographical coordinates of 42 and 49 longitude 5 and 34 latitudes on the central plateau of Iran, with an average height of 1755 meters above free sea level. The population of Arak city according to the official census of Iran's Statistics Center in 2016 is 571933. (Statistical Center of Iran in 2016). The expansion of Arak city has caused a lot of changes, and on the other hand, due to the rapid growth and development of the city, its migration and inefficiency, despite its advantages, has many problems in the economic, Social, environmental. Therefore, the purpose of this article this paper is search to study the livability of the city of Arak in three dimensions: economic, social, and environmental; on the other hand, it examines three urban areas and investigates the extent to which the city of Arak is in terms of its livable. It is more elaborate on which dimension is it and which region it is more livable to achieve with the achievement of the level of vitality of the city of Arak to achieve sustainable development of the city. The results of the research show that in general, the city of Arak is in poor condition in terms of its livability. The economic dimension of the city is better than the other two dimensions of livability. Of the three metropolitan areas, zone 3 is closer to the surface of livability.

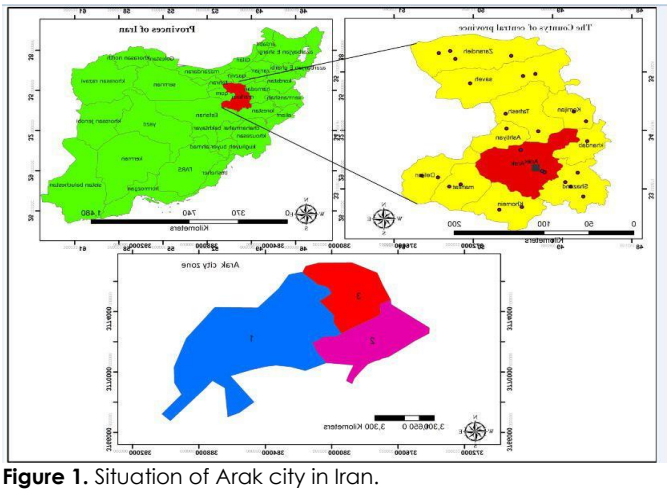

Figure 1. Situation of Arak city in Iran.

2. Method and Materials

This research is exploratory of type and is descriptive-analytic of method. The statistical population of the research includes urban authorities, citizens and private sector. The scope of this study is Arak city. To draw maps, ARC GIS software has been used. Information collection

through: (documentary method) at this stage, by referring to Latin articles and Persian books in the field of research, theoretical foundations are completed. (Field method) This step Includes objective observation, interview and also completion of the questionnaire. The sample size is used by the Cochran formula. In the current research, the population of Arak has 48,412 people. According to the Cochran formula, the sample size required is as follows:

$$n = \frac{\frac{(1.96)^2(0.5)(0.5)}{(0.05)^2}}{1 + \frac{1}{571933}(\frac{(1.96)^2(0.8)(0.2)}{(0.05)^2} - 1)} = 383$$

In this research, 14 indicators have been used as the main indicator of the livability of Arak city in three dimensions: social, economic and environmental. Social dimension: public education, leisure, medical and health care considerations, individual and social security, affinity, and partnership, partnership and solidarity. Economic dimension: consumer goods, employment and income, housing, infrastructure and infrastructure services, public transportation. Environmental dimension: Contamination, visual quality, green and clean. Then, Topsis multi-criteria model was used to assess the status of the livability rating of Arak city.

For each dimension, the stages of the topsis model have been calculated. But to avoid prolonging the steps, only the data matrix and then the ranking of the options are given. The steps of the topsis model

1. Data matrix
2. Non-scalable data
3. Non-scalable scaling
4. Determine the positive and negative ideals for each indicator
5. Getting the distance between each option from the positive and negative ideal
6. The relative closeness of each option or the ideal solution
7- Ranking Options

3. Results

The study of livability of Arak city was carried out in two stages. First, using the results of the questionnaires and applying the ranking of the Mercer Institute (100-80 highly livable, 80-70 = Durable, 60-70 = Acceptable, 50-60 = poor, -50 = non- livable). The results of the research show that Arak city with a rank of 58 is poorly located and is not biodegradable. Then, the research done in relation to livability of Arak's urban areas have been investigated with the Topsis model in three dimensions. Results in economic dimension are as follows. (Table 1)

Table 1. Economic Data Matrix.

	Consumer Goods	Employment and income	Housing	Facilities and infrastructure services	Public Transportation
1	31.5	25.89	8.28	11	34903
2	33.1	23.73	22.5	10.77	36325
3	35.4	48.03	67.04	41.86	31272

After completing the steps of the TOPSIS model, according to the CL values, the ranking of economic options can be made, so that the more livable is area 3 then the 2 and 1.

$$\text{Ranking Options} \quad A_3 > A_2 > A_1$$

The social dimension table was formed and social dimension indicators were also examined with the Topsis model (Table 2)

Table 2. Social Data Matrix.

	public education	free time	Medical and Health Care	Individual and Social Security	Affinity and Place of Honor	Partnership and solidarity
1	1.10	14.83	0.26	0.11	60	65
2	9.25	1.93	0.10	0.05	65	70
3	4.21	9.49	1.40	3.02	50	50

After completing the steps of the TOPSIS model, according to the CL values, the ranking of social options can be made, so that the more livable area 3 is then 1 and 2.

$$\text{Ranking Options} \quad A_3 > A_1 > A_2$$

The environmental dimension indicators for calculating the livability of Arak urban areas are specified in the table below (Table 3).

Table 3. Environmental Data Matrix.

	Pollution	*Visual quality*	*Green space*
1	0.53	129.79	30.86
2	21.16	35.52	16.28
3	21.18	114.83	15.06

After calculating the environmental dimension indices in the Topsis model, the results show that region 2 is more livable then 3 and 1

Ranking Options $A_2 > A_3 > A_1$

4. Discussion and conclusions

As it was said, livable cities are places where social life is communicated along with relationship. These cities are concerned with the creation of architecture, the street landscape and the design of public spaces, which facilitates the presence of city residents in the public domain and in the heart of the city. Such cities are committed to reducing traffic and solving safety, pollution and noise through a set of mechanisms (Lenard, 1997, 3).

The study of Arak city's livability in three dimensions of economic, social and environmental characteristics shows that this city has more livable environmental indicators of the economic dimension, but it is seen in the very poor environment of non-habitat. Total in three dimensions in Arak has a poorly-hit 58th place in the Mercer ranking. These studies were also studied in three areas of the city of Arak. The model used was a multi-criteria Topsis model. Also, the results of the Topsis model, which is a multi-criteria and decision-making model, show that in the environmental dimension of the region two with a score of 0.6859 and in the social dimension of the region of three with a score of 0.92 and in the economic dimension of the region three with a score of 1, the highest ranks have won. As a result, the city of Arak ranked 58th, is not livable. This study shows that the urban areas of Arak are not at the appropriate level of survival, but the 3rd district in other parts of the city has a better livable status. On the other hand, livability is a way to achieve sustainable development, but the results of the research show that Arak is not only livable, but is far from sustainable development.

Conclusions

Livability is a broad term consisting of four main elements: the pride of society, the desire to work, jobs and workgroups, human development and regional solutions, and empowerment of society. Livability becomes reality. If citizens accept the responsibility actively, this is the key to initiating change. The study of Arak city in 14 indicators and three dimensions of livability shows that this city is not only non-livable, but it has not been able to make environmentally clean, economically efficient, and occupationally urban and socially sense of belonging to location and identity To create citizens in Arak.

Therefore, it is far from sustainable development, and it seems that to reduce this gap and increase the livability, these should be done: increasing social awareness, increasing popular participation, empowerment, reducing pollution, increasing green space, increasing employment and income. And with increasing the level of livability, a step towards sustainable development of the city of Arak could be taken.

Acknowledgement

This research did not receive any specific grant from funding agencies in the public, commercial, or not-for-profit sectors.

References

Allen, T. F. H. (2010). "Making Livable Sustainable Systems Unremarkable." *Systems Research and Behavioral Science,* 27 (5), 469–79.

Badland, H. Whitzman, C., Aye, L., Butterworth, H. (2014) Urban Liveability: Emerging Lesson from Australian for exploring the potential for indicators to measure the social determinants of health. *Social Science and Medicine*, (111), 64-73.

Gough, M. Z. (2015). Reconciling Livability and Sustainability: Conceptual and Practical Implications for Planning. *Journal of Planning Education and Research*, *35*(2), 145–160.

Holden, M., and Scerri, A. (2013). "More Than This: Liveable Melbourne Meets Liveable Vancouver." *Cities, 31*, 444–53.

Lennard, H. L. (1997)."Principles for the Livable City" In Lennard, S.H., S Von UngernSternberg, H.L.Lennard (Eds), *Making Cities Livable. International Making Cities LivableConferences.* California, Usa: Gondolier Press.

Maslow, A. H. (1998). *Toward a Psychology of Being*, 3rd edition. New York: John Wiley.

Miller, H. J., Witlox, F., and Tribby, C. P. (2013). Developing Context-Sensitive Livability Indicators for Transportation Planning: A Measurement Framework." *Journal of Transport Geography* 26, 51–64.

Portney, K. (2013). *Taking Sustainable Cities Seriously: Economic Development, the*

Environment, and Quality of Life in American Cities. Cambridge: MIT Press.

Ruth, M., and Franklin, R. S. (2013). Livability for All? Conceptual Limits and Practical Implications. *Applied Geography 4*9, 18–23.

Sasanpour, F., Simin, T., Hamza, J.A. (2015), Measuring and assessing urban livability in twenty-two regions of Tehran metropolitan area. *Regional Planning Quarterly, 18*, 42-27.

Statistical Center of Iran. (2016). Arak Population Census.

Van Kamp, I., Leidelmeijer, K., Marsman, G., and de Hollander, A.(2003). Urban Environmental Quality and Human Well-Being. *Landscape and Urban Planning, 65* (2), 5–18.

Journal Of Contemporary Urban Affairs

2017, Volume 1, Number 3, pages 18– 23

Feasibility of a Carbon Consumption Tax for sustainable development – A case study of India

* Dr. **Singh Kanwal Deepinder Pal** [1]

[1] University School of Law and Legal Studies, Guru Gobind Singh Indraprastha University New Delhi, India

E mail: kdps@ipu.ac.in

ARTICLEINFO:

Article history:

Received 2 August 2017

Accepted 8 October 2017

Available online 12 October 2017

Keywords:

Carbon Consumption Tax;
Sustainable development;
Global climate change;
India

ABSTRACT

Global climate change is a major issue confronting policymakers worldwide, and there is widespread scientific acceptance of the reality of climate change and its adverse consequences In terms of economic analysis, greenhouse gas emissions (GHG), which cause planetary climate changes, represent both an environmental externality and the overuse of a common property resource. The paper is premised around the hypothesis that tax policy can be used to address climate concerns by making less Green House Gas intensive purchases and investments more financially attractive. However, in the absence of an international framework capping GHG emissions, countries adopting mitigation policies incur costs that would not exist under global cooperation such as the loss of competitiveness and emissions leakage. A consumption tax based on the carbon footprint of a product levied on all products at the point of purchase by the final end-user, regardless of where the goods are produced using a Credit-method would be capable of addressing these concerns of emissions leakage and loss of competitiveness, while being WTO compliant. The author intends to test the feasibility and effectiveness of such a carbon consumption tax in the Indian Context. The author shall test the feasibility of levy of such a consumption tax in the context of India and evaluate the effectiveness in mitigating climate change and catering to the goal of sustainable development.

JOURNAL OF CONTEMPORARY URBAN AFFAIRS (2017) ***1***(3), 18-23.

https://doi.org/10.25034/ijcua.2018.3674

www.ijcua.com

1. Introduction

Climate change is a major environmental issue that is affecting the policy decisions worldwide. The world is aware of this grim reality and adverse consequences of global warming (Harris, *et al.*, 2015) Greenhouse gas emissions (GHG), cause climate changes, and are adversely affecting economies also. This is because of overuse of a common property resource. (Harris, *et al.*, 2015). The paper is premised around the hypothesis that tax policy can be used to address climate concerns by making less GHG intensive purchases and investments financially attractive. (Moarif, and Rastogi, 2012)· However, in the absence of an international framework capping GHG emissions, countries adopting mitigation policies incur costs that would not exist under global cooperation such as the loss of competitiveness and emissions leakage. A consumption tax based on the carbon footprint of a product levied on all products at the point of purchase by the final end-user, regardless of where the goods are produced would be

***Corresponding Author:**
University School of Law and Legal Studies, Guru Gobind Singh Indraprastha University New Delhi, India
E-mail address: kdps@ipu.ac.in

capable of addressing these concerns of emissions leakage and loss of competitiveness, while also being WTO compliant. The paper intends to test the feasibility and effectiveness of such a carbon consumption tax in the Indian context. The author shall test the feasibility of levy of such a consumption tax in the context of India and evaluate the effectiveness in mitigating climate change and catering to the goal of sustainable development.

A carbon tax is a levy imposed on fossil fuels and other primary products based on the amount of GHG they emit. To explain it with an example, carbon tax places a fee on coal, proportionate to the amount of carbon dioxide (CO2) released when coal is burned. This tax can also be seen as a cost for emitting GHGs into the atmosphere. The environmental friendly people can also use it as a financial incentive for reducing GHG emissions. A carbon tax policy can also be designed to include tax credits for activities that reduce GHGs in the atmosphere.

A carbon tax can also be seen as explicit carbon pricing because it is a tax linked to the level of carbon dioxide (CO2) emissions. This can be used as an economic instrument and can contribute to an effective reduction in emissions. The carbon tax is a price on each tonne of GHG emitted, and therefore the price signal causes a response in an entire economy. The emitters feel that it would be economically beneficial to shift to less GHG method production and this feeling of profitability results in reduced emissions. Carbon taxes can be introduced independently or alongside other carbon pricing instrument, like an energy tax. Introduction of a direct carbon tax is a new concept, but its acceptability is coming at a fast pace. (Congressional Budget Office Policy Options for Reducing CO2 Emissions, 2012.) . A carbon tax can also be seen as an alternative or a supplement to a cap-and-trade program.

A carbon tax and a cap-and-trade program are both market-based and have a concept of financial incentive to reduce GHG emissions. The main difference between the two concepts is on the establishment of price and reduction of emissions. A carbon tax imposes a direct levy called the "carbon price" on activity based on the amount of GHGs they emit. It puts no restriction on GHG emissions. On the other hand, the cap-and-trade program sets a limit, or "cap," on emissions, but the price for emission is determined by the demand and supply. Current climatic conditions force a relook on existing policy efforts related to global warming issues. The main premise of this paper is a plan that provides clean environment by the introduction of a small carbon tax or a GHG tax. The proceeds of this tax could be used to support research efforts on energy sources, energy use, and reduction of emission. The scenario prevailing in different countries is examined along with the position in India. The evidence shows that carbon taxes may be an interesting policy option and that their main negative impacts may be compensated through the design of the tax and the proper use of the generated revenues.

2. International Legal Scenario

Kyoto Protocol was earlier considered to be the strongest international agreement on the topic of climate change wherein 182 nations had committed to minimizing GHGs. Critics of the Kyoto Protocol felt that it was premised on setting national emissions targets and did not deal with the actual problem of global warming caused by emissions. It also created "common but differentiated responsibilities." It put little to no responsibility for developing nations to check emissions. Unchecked growth of emissions in the developing world was having a larger impact on the environment. It was beginning to overcome the developed world, the best example being India and China. Countries like Canada and Russia feel that it was not a way forward, and declined to take on additional obligations. Dealing with these issues is expensive and inconvenient, and it carries high monetary and sociological costs. Cost of environmental degradation already has a negative effect on the economy. There is a need for international coordination on environmental issues as much as international coordination is required in trade liberalization.

Carbon taxes are seen as a cost-effective instrument for reducing emissions. However, in practice, only a few countries have implemented taxes based on the carbon content of energy products. Some countries that have imposed carbon taxes are discussed subsequently. The methodology adopted by them in discussed briefly so as to weigh it in relation to the Indian scenario.

In British Columbia, carbon tax applies to the purchase or use of fuels. This tax is revenue neutral, and all funds generated by the tax are used to provide reductions to citizens for other taxes. Denmark imposed a carbon tax in 2014 covering consumption of natural gas, oil, and coal. There are partial exemption and refund for

EU coverage and certain other activities. Fuels used in the production of electricity are not subject to the carbon tax. But there is a tax on production of electricity. French parliament approved consumption tax on energy products in December 2013. It is based on the content of CO2 in consumption of fossil fuel. On the consumption of gas, heavy fuel oil, and coal carbon tax was imposed in 2014. In 2015 carbon tax was extended to transport fuels and heating oil. In Iceland importers of gas and diesel oils, petrol, aircraft, and jet fuels are liable for the carbon tax. It is also applicable to retail use. The funds collected are deposited in the treasury In Ireland the carbon tax applies to petrol, heavy oil, auto-diesel, kerosene, liquid petroleum gas (LPG), fuel oil, natural gas, and coal since 2010. In Japan, CO2 emission factor is used for each sector since 2012. It has imposed a levy named Japan's Tax for Climate Change Mitigation on use of fossil fuels. In May 2013 the South African government published a policy paper for public comment on before introducing a carbon tax. The government has introduced a fuel input tax based on the carbon content of the fuel. It covered all direct GHG emissions and had been imposed from January 2016. Sweden introduced a carbon tax in 1991. It was a part of energy sector reform, and tax was imposed on natural gas, gasoline, and coal, Switzerland introduced carbon since 2008, and this tax is applicable on all fossil fuels. They are exempted if they are used for energy. The United .Kingdom has introduced carbon price floor (CPF) tax on fossil fuels used to generate electricity since 2013. This changed the Climate Change Levy (CCL) regime, by applying carbon price support (CPS) rates of CCL to gas, solid fuels, and liquefied petroleum gas (LPG) used in electricity generation. (OECD Environment Policy paper, 2013).

3. Utility of carbon tax and its impact

World economists understand that to reduce the impact of climate change; it is necessary to tax production and use of fossil fuels. The taxation scheme should encourage efficient use of existing resources so that the negative result of such uses is reduced. A tax would lower fossil fuel consumption as they become more expensive. It will make it cost efficient and also encourage the use of alternative technologies. It leads to internalizing the costs of emissions. Carbon taxes affect all industry with the capacity to pollute, but the burden falls upon the energy and transportation sectors. Therefore it is advisable to levy it on all sectors as needed.

3.1 Impact of carbon tax on companies

Companies and individuals pay higher prices for GHG-intensive energy. Costs of a carbon tax are passed down to consumers. High energy prices impact the overall income of companies and individuals. This impact is dependent on the utility of tax revenues. The overall impact also depends on the use of energy, and on the ability of the company to minimize costs. This can be done by using clean fuel and by making the carbon tax "revenue neutral." This can also be done through rebates or changes in the tax code like reducing capital gains taxes. A carbon tax policy can also make provisions to provide funding for research or transportation infrastructure (Stef, and Van Dender, 2011).

3.2 Impact on lower-income consumers

Impact of a carbon tax on lower-income consumers depends on the use of tax revenues. A basic carbon tax is regressive. Lower-income consumers pay a higher percentage of their total income for goods and services (Lin, and Li, 2011). Some carbon tax programs address this by "recycling" tax revenues. or allow reductions in other regressive taxes, such as state sales taxes or federal payroll taxes.

3.3 Impact on international competitiveness

Impacts on an industry depend on the level of the tax, recycling of revenue, use of energy by the industry and competitiveness of the industry. The competitiveness varies by sector. One thought process treats it as cost penalty for doing business whereas the other line of thought feels that a carbon tax encourages innovation and efficiency. This leads to long-term competitiveness.

Environmental challenges, like climate change, and pollution, occur when there is a burden on the assimilative capacity of environmental resources. If a society is affected by pollution, and the polluter is not held accountable for it, then all this cost of pollution is not reflected in the final prices of the goods and services. This leads to market failure and government intervention. The government regulates it or introduces market-based instruments. These instruments influence the decision-making processes of producers and consumers. (Liu , *et al.,* 2015). The government may also regulate by formulating emissions standards, levying taxes, or allocating pollution rights and granting subsidies to contribute to cleaning the environment. Market-based instruments set a price on the pollution

causing market distortion, IPCC (2013). A carbon price can drive changes in producer and consumer behavior, and can address climate change. Carbon pricing encourages a shift to low-carbon and energy-efficient technologies. This requires replacement with low-carbon-emitting alternatives and mitigation and adaptation strategies (Burniaux *et al.,* 2010). A carbon price also creates an environment for research, development and technology innovation. It reduces the price gap between carbon-intensive technologies and low-carbon alternatives.

4. Indian Scenario

The Government of India published its response to climate change in June 2010 which was titled "India: Taking on climate change." The government has approved the Perform, Achieve, and Trade (PAT) mechanism for energy efficiency. The first cycle of this mechanism commenced in 2014–15. This scheme works towards enhancing cost-effectiveness through tradable energy saving certificates (ESCerts) (Cropper *et al.,* 2012). The PAT scheme covers 478 energy consumers, representing 40 percent of total industrial consumption in sectors like thermal power, steel, cement, fertilizer, pulp and paper, textile, aluminum and chlor-alkali. National Action Plan on Climate Change has been formulated which provides for generating 20 000 MW of solar power by 2022 and 2 000 MW from off-grid solar plants. India's Green initiative has been part of International Solar Alliance (ISA) that will provide a special platform for mutual cooperation among 121 solar-resource-rich countries lying fully or partially between the Tropic of Cancer and Tropic of Capricorn. India aims to have 40 percent cumulative electric power from non-fossil fuel- based energy resources by 2030. India has cut subsidies and increased taxes on fossil fuels. This is the movement from carbon subsidy to carbon taxes. Fossil fuel subsidy on diesel and petrol has been phased out, and reforms are being carried out in kerosene and LPG subsidies. The government of India has decontrolled diesel prices. Excise duty on petrol and diesel has been increased periodically to match the declining global prices. Since October 2014, excise duties have been imposed on diesel and petrol. Also, the coal cess has been continuously increased from 50 per ton to 400 per ton.

Excise duties on petrol or diesel act as an implicit carbon tax. They put an effective price on emissions. For example, more fuel car burns, and the greater the emissions, the greater the tax paid. In India, the change from subsidization to the taxation of fossil fuels is related to revenue and macro-economic considerations. They also impact climate change. This is important in the context of global efforts to deal with climate change because India is the third largest emitter of GHG emission.

While India has made substantial progress recently in decontrolling price of petrol and diesel and in calibrating excise duty to compensate for the declining world oil prices, there is still room for further reform of petroleum pricing policies (Schipper *et al.,* 1997).

5. Translating coal cess into carbon tax to GST compensation

Recently, the Government of India revised its coal cess from *50 per ton to 400 per ton.* Translating this into a carbon tax equivalent using the emission factor, the government is able to mop up a significant amount of revenue. Any rationalization of coal pricing must take account of the implications for power prices and hence access to energy for the poorest in India which is and must remain a fundamental objective of policy.

Since Modi took office in 2014, the coal cess has been raised with an idea was to dedicate the revenue to greening the economy. However, only 37% of the money collected between 2010 and 2017 was allocated to the clean energy and environment fund. The rest sat idle, creating a surplus that reached 56,700 crore rupees ($8.8 billion) at the beginning of this financial year, more than 20 times the annual budget of the environment ministry. That surplus has now been allocated to compensate states that will lose out in the GST reform. More than 1 lakh crore rupees ($15.5bn) of revenue due to being channeled into clean energy over the next five years will go the same way.

About 55 ongoing clean energy projects will continue to be funded through general taxation, "But this fund, for now, is over. After five years the government can rethink if it wants to spend 50% of the cess collected again for renewable energy and environment." GST, a big blow to clean energy financing. It was India's carbon tax; it was thought to be a source of funding clean energy projects, to combat climate change. Now it is being thrown out of the window. In the last six years, the government of India has

collected around Rs 54,000 crore by levying a cess on every tonne of coal mined or imported.

6. Conclusion

International coordination is the prerequisite to deal with climate change. There should be an international regime of harmonized domestic carbon taxes. If there is a minimum amount of taxation on domestic producers, the revenue can be used for setting up of alternative means of energy production (Washington DC. World Bank, 2012). This shall also overcome the problem of non-participation of countries in agreements like the Kyoto Protocol. There are large ramifications of emitting harsh pollutants into the air. Though these supplies are supplies are cheap and come from long-utilized sources these options do not have longevity (Holden et al., 2016). Human actions have caused too many environmental disasters. Although the states would like to choose the use of resources to produce electricity their primary duty is to look after health and welfare of citizens. Use of cheap power plants is holding the states from meeting their responsibilities. This reflects a monumental threat" to the prosperity of the greatest number for the longest time. Reducing carbon dioxide emissions and mitigating climate change, the states can ensure best for their citizens best serve the people. To ensure the greatest good for future generations, society must take responsibility for its actions-starting now (Pachauri, and. Reisinger, 2007).

India has turned a carbon subsidy regime into one of carbon taxation. This has increased petrol and diesel price and reduced annual harmful emissions. India has to go a long way to get the gains from reform of coal pricing and petroleum pricing policies. Substantial carbon taxation and solar power program can lead to substantial contributions to climate change by India. Climate policies can also influence the, but the amount of influence shall depend upon a policy of exchange rate. A fixed exchange rate is beneficial for the economy.

The rapid development of the renewable energy sector is also very important for India to turn into a green economy. The costs of mitigation policies can be more if affordable renewable energy is absent.

To reduce emission levels, the renewable energy sector needs to grow, and carbon mitigation policies are required. Technological and financial resources are required to develop the renewable energy sector. Emission trading permits can also be a source of finance. The level of emissions needs to be lower than the allowance. If emissions are higher than the allowance, the country will have to buy permits, involving the outflow of capital. Therefore, the choice of mitigation strategy is important. To conclude the transition to a green economy depends crucially on the rapid development of the renewable energy sector and the design of appropriate carbon mitigation policies (Basanta, and Ghosh, 2013).

Acknowledgement

This research did not receive any specific grant from funding agencies in the public, commercial, or not-for-profit sectors.

References

Basanta K., and Ghosh, P.J. (2013). *The Impact of Carbon Taxes on Growth Emissions and Welfare in India: A CGE analysis I*. Retrieved from www.iegindia.org/upload/publication/Workpap/wp315.pdf IEG Working Paper No. 315G Working Paper No. 315

Burniaux, J.M., Chateau, J. and Duval, R. (2010). *Is there a Case for Carbon-Based Border Tax Adjustment? An Applied General Equilibrium Analysis*Ⅱ. OECD Economics Department Working Papers 794.Paris, France: OECD Publishing

Congressional Budget Office Policy Options for Reducing CO2 Emissions. (2012). Retrieved from http://www.cbo.gov/ftpdocs/89xx/doc8934/02-12-Carbon.pdf last accessed on 06.07.2017

Cropper. M., Gamkhar, S., Malik, K., Limonov, A., and Partridge, I. (2012). The Health Effects of Coal Electricity Generation in India. *RFF Working Paper*.

Harris, M. J., Roach, B., and Codur, M. A. (2015) *The Economics of Global Climate Change*. Global Development and Environment Institute Tufts University. Retrieved from http://www.ase.tufts.edu/gdae/education_materials/modules/The_Economics_of_Global_Climate_Change.pdf last accessed on 04.10.2016.

Holden, E., Harball, E., & Gilmer, E.M. (2016). *SCOTUS halts Clean Power Plan, stuns states planning carbon cuts.* E&E PUBLISHING

IPCC (2013). *Climate Change 2013, —The Physical Science Basis*. Working Group I Contribution to the IPCC Fifth Assessment Report, Summary for Policymakers,

Intergovernmental Panel on Climate Change, Geneva.

Lin, B.Q., Li, X.H. (2011). The Effect of Carbon Tax on Per Capita CO2 Emissions. *Energy Policy, 39*(9), 5137–46.

Liu, X.B., Wang, C., Niu, D.J. (2015), ―An Analysis of Company Choice Preference to Carbon Tax Policy in China. *Journal of Clean Prod*; doi:10.1016/j.jclepro.2014.12.084.

Moarif, S., Rastogi, N.P. (2012). *Market-based climate mitigation policies in emerging economies*, Center for Climate and Energy Solutions. Retrieved from http://www.c2es.org/docUploads/market-based-climate-mitigation-policies-emerging-economies.pdf last accessed on 04.10.2016.

OECD Environment Policy paper. (2013). *Climate and Carbon Aligning prices and policies.*

Pachauri, R.K and. Reisinger A. (2007). *Climate Change 2007, ―Synthesis Report, Contribution of Working Groups I, II and III to the Fourth Assessment Report of the Intergovernmental Panel on Climate Change*. Geneva:IPCC,

Stef, P. and Van Dender, K. (2011). What Long-term Road Transport Future? Trends and Policy Options. *Review of Environmental Economics and Policy, 5*(1): 44-65.

Schipper, L., Ting, M., Khrushch, M., Golove, W. (1997), ―The Evolution of Carbon Dioxide Emissions from Energy Use in Industrialized Countries: An End-Use Analysis‖. *Energy Policy, 25* (7), 651–672.

Washington DC. World Bank. (2012). *4˚ Turn Down the Heat: Why a 4˚ Warmer World Must Be Avoided.* Washington DC., USA: World Bank

Journal Of Contemporary Urban Affairs

2017, Volume 1, Number 3, pages 24– 30

Interrelationship Between Nutrients And Chlorophyll-A In An Urban Stormwater Lake During The Ice-Covered Period

* **Kejian Chu** [1], **Yuntong She** [2], **Jeff Kemp** [3], **Mark Loewen** [4], **Evan Davies** [5]

[1] College of Environment, Hohai University, Nanjing, P. R. China

[1, 2, 3, 4, 5] Department of Civil and Environmental Engineering, University of Alberta, Edmonton, Canada

[1] E mail: kejian@ualberta.ca , [2] E mail: yuntong.she@ualberta.ca

ARTICLEINFO:

Article history:

Received 2 August 2017

Accepted 10 October 2017

Available online 12 October 2017

Keywords:

Ice-covered;
Chlorophyll-a;
Nutrients;
Urban Stormwater Lake.

ABSTRACT

Urban stormwater lakes in cold regions are ice-covered for substantial parts of the winter. It has long been considered that the ice-covered period is the "dormant season," during which ecological processes are inactive. However, little is known about this period due to the historical focus on the open-water season. Recent pioneering research on ice-covered natural lakes has suggested that some critical ecological processes play out on the ice. The objective of this study was to investigate the active processes in ice-covered stormwater lakes. Data collected during a two-year field measurement program at a stormwater lake located in Edmonton, Alberta, Canada were analyzed. The lake was covered by ice from November to mid-April of the following year. The mean value of chlorophyll-a during the ice-covered period was 22.09% of the mean value for the open-water season, suggesting that primary productivity under ice can be important. Nitrogen and phosphorus were remarkably higher during the ice-covered period, while dissolved organic carbon showed little seasonal variation. Under ice-covered conditions, the total phosphorus was the major nutrient controlling the ratio of total nitrogen to total phosphorus, and a significant positive correlation existed between total phosphorus and chlorophyll-a when the ratio was smaller than 10. The results provide preliminary evidence of the critical nutrient processes in the Stormwater Lake during the ice-covered period.

JOURNAL OF CONTEMPORARY URBAN AFFAIRS (2017) ***1***(3), 24-30.

https://doi.org/10.25034/ijcua.2018.3675

www.ijcua.com

1. Introduction

Stormwater lakes support urban runoff management and prevent flooding and downstream erosion in urban areas. In cold regions, these lakes are ice-covered for substantial part or the entire winter. It has long been considered that the ice-covered period is the "dormant season" for lakes (Hampton et al., 2015), during which ecosystems subjected to low temperatures are "on hold" and most ecological processes are inactive until the environmental conditions become more conducive to the growth of aquatic organisms (Bertilsson et al., 2013). In the original Plankton Ecology Group's (PEG) model (an influential freshwater

***Corresponding Author:**
College of Environment, Hohai University, Nanjing, P. R. China
E-mail address: kejian@ualberta.ca

ecological model), the ice-covered period is described as a physical suppressor of the ecosystem and essentially a "reset" button for renewal in the following spring (Sommer et al., 1986). From this perspective, most historical research had focused on the open-water period as the "growing" season, and few studies have included winter research on ice-covered lakes; thus, little is known about the physics, geochemistry, and biology under ice in these systems (Hampton et al., 2017).

More recently, some pioneering winter lake research has shown increasing evidence that some critical ecological processes are playing out under the ice (Salonen et al. 2009, Bertilsson et al., 2013). For example in Lake Erie, the under-ice phytoplankton growth and loss rates in mid-winter were found to be as high as those of the summer months (Twiss et al., 2014). Lenard and Wojciechowska (2013) compared the phytoplankton community composition of two lakes in two consecutive winters. Both lakes favored the development of nanoplankton when they were ice covered in one winter, but produced microplankton when they were completely ice-free in the second winter. Phytoplankton community structure was found to be strongly correlated with ice thickness (Ozkundakci et al., 2016). High species diversity has been found under ice despite unfavorable conditions, including limited light availability, low water temperatures, restricted air-water gas exchange and prevention of wind-induced mixing (Salonen et al., 2009, Schröder, 2013). The concentration of nutrients and dissolved organic carbon may help to drive the plankton dynamics (Babanazarova et al., 2013). Griffiths et al. (2017) examined the shifts in diatom assemblages from ten High Arctic lakes, lakes and concluded that ice cover is likely the principle driver of some of the most important ecological changes, resulting in increased diversity and the emergence of novel growth forms and epiphytic species. With respect to winter stormwater lakes, previous studies have mostly focused on the hydrodynamic, water quality, pollutant removal performances, and operational environmental risk (e.g., Marsalek et al., 2000, 2003; Semadeni-Davies, 2006; Tixier et al., 2012). However, ecological processes in ice-covered stormwater lakes have not received the same level of attention as the natural lakes.

The objective of this study was to investigate the active processes in an ice-covered stormwater lake. Data including concentrations of nutrients, dissolved carbon, and chlorophyll-a collected during a two-year field measurement program at a stormwater lake located in Edmonton, Alberta, Canada were analyzed. The Stormwater Lake was covered by ice from November to mid-April in the following year. The differences in concentrations of total nitrogen (TN), total phosphorus (TP), dissolved organic carbon (DOC), dissolved inorganic carbon (DIC) and chlorophyll-a (Chl-a) between ice-covered and open-water seasons were explored. The correlations between these variables were analyzed using the Pearson correlation test and their correlative behaviors in ice-covered and open-water periods were compared to reveal the pattern of nutrient processes occurring under ice in the study lake.

2. Study Lake and methodology

The study Stormwater Lake is located in southwest Edmonton and has an average depth of 1.78 m and a storage volume of 39,000 m^3. The bathymetry of the lake together with the inlet and outlet locations are shown in Figure 1. A total of 162 water samples were collected during a two-year field measurement program between October 2013 and October 2015. Sampling locations were at the inlet and outlet locations, as well as at the corner and center of the lake. 26 samples were collected during the ice-covered period by drilling holes at monthly intervals. The water samples were sent to the Biogeochemical Analytical Service Laboratory (BASL) at the University of Alberta for measurement of the pertinent water quality parameters, including TN, TP, DOC, DIC, and Chl-a. TN and TP were analyzed by Lachat QuickChem QC8500 FIA Automated Ion Analyzer (American Water Works Association, 2004, 1999), DOC and DIC by Shimadzu TOC-5000A Total Organic Carbon Analyzer (EPA 415.1 (Modified)), and Chl-a by Shimadzu RF-1501 Spectrofluorophotometer (Welschmeyer, 1994) and Varian Cary 50 Probe UV-Visible Spectrophotometer (EPA 446.0 (Modified)). The detection limits of the BASL test results are 7 ppb for TN, 1.4 ppb for TP, 0.1 ppm for DOC, 0.2 ppm for DIC and 0.2 µg/L for Chl-a.

3. Results and discussion

The sampling results for TN, TP, DOC, DOC, and Chl-a in the stormwater lake are presented in Figure 2. Ice-covered periods are indicated by dashed rectangles. Descriptive statistics were calculated to describe the main characteristics of the variable measurements (Table 1). During the monitoring period, the concentrations of

DOC and DIC were relatively stable, with coefficients of variation of 24.41% and 31.80% respectively. Daily averages for the different sampling locations (± standard deviation) ranged from 4.92 ± 3.17 mg/L to 13.58 ± 0.67 mg/L for DOC and 10.89 ± 3.02 mg/L to 31.0 ± 0.93 mg/L for DIC. The concentrations of Chl-a, TN and TP fluctuated more, with corresponding coefficients of variation of 83.79%, 57.89%, and 65.48%, and daily averages ranging between 1.45 ± 1.09 µg/L and 300.9 ± 75.12 µg/L, 549.71 ± 16.71 µg/L and 3438.4 ± 897.19 µg/L, 89.4 ± 8.74 µg/L and 650.2 ± 321.99 µg/L respectively.

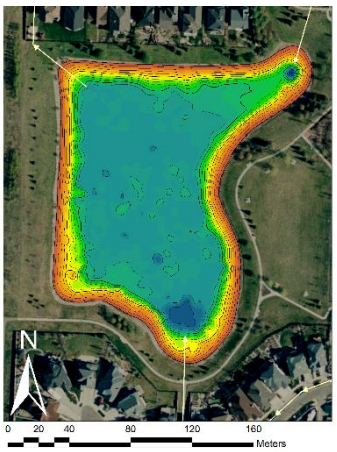

Figure 1. Bathymetry of the study Stormwater Lake, arrows indicate incoming and outgoing storm sewer.

a)

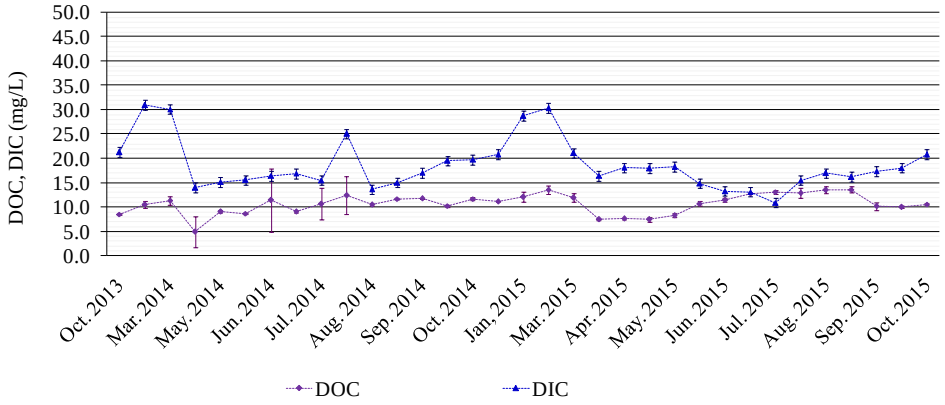

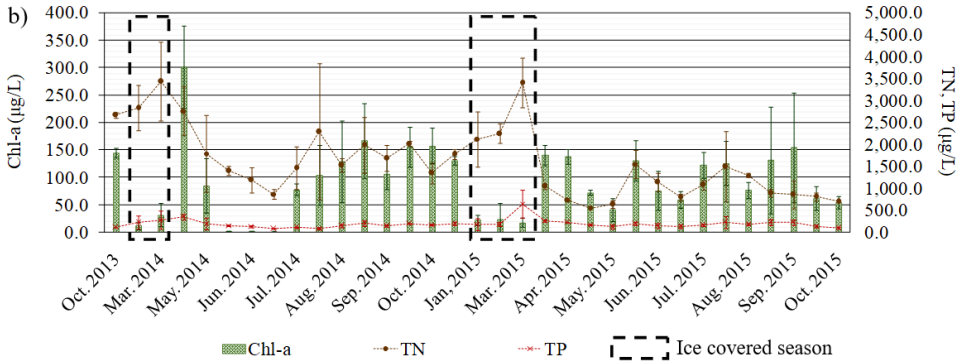

Figure 2. Measured concentration of a) DOC, DIC; b) Chl-a, TP, TN during the two-year monitoring period.

Table 1. Descriptive statistics of the measurements during the monitoring period.

Variable	Min	Max	Mean	SD	CV
Chl-a (µg/L)	1.45	300.90	87.59	73.39	83.79%
TN (µg/L)	549.71	3438.40	1518.67	879.10	57.89%
TP (µg/L)	89.40	650.20	194.82	127.56	65.48%
DOC (mg/L)	4.92	13.58	10.55	2.57	24.41%
DIC (mg/L)	10.89	31.00	18.34	5.83	31.80%

Notes: Min=minimum of daily average value of all sampling locations; Max=maximum of daily average value of all sampling locations; Mean=average value during monitoring period of all sampling locations; SD=standard deviation; CV=coefficient of variation.

Table 2 provides descriptive statistics for the measurements during the ice-covered and open-water seasons. The corresponding periods in both monitoring years were combined for this

analysis. Average Chl-a under ice-covered conditions (22.11 ± 17.48 µg/L) was significantly lower, but still approximately a quarter (22.09%) of the open-water average (100.1 ± 73.37 µg/L). Therefore, primary productivity under ice should be considered an important part of the whole-year productivity.

TN, TP and DIC were remarkably higher under ice-covered conditions (2788.31 ± 783.60 µg/L, 302.19 ± 247.79 µg/L and 28.34 ± 4.02 mg/L) compared to open-water conditions (1275.95 ± 661.92 µg/L, 174.29 ± 73.42 µg/L and 16.43 ± 3.83 mg/L), whereas DOC concentrations showed little seasonal variation (11.92 ± 1.34 mg/L under ice-covered condition and 10.29 ± 2.67 mg/L under open-water condition). The higher concentrations of TN and TP under the ice likely reflect nutrient input from the municipal storm sewer network, roadway and roadside deposit, deicing and anti-skid agents (Oberts et al., 2000), as well as leaf litter (Bratt et al., 2017). The seasonal difference was most prominent for TN, where the ratio of the under-ice average to the open-water average reached 2.19:1. This ratio was 1.73:1 for TP, 1.72:1 for DIC and 1.16:1 for DOC.

Table 2. Descriptive statistics for variable measurements under ice-covered and open-water conditions

		Chl-a (µg/L)	TN (µg/L)	TP (µg/L)	DOC (mg/L)	DIC (mg/L)
Ice-covered	Min	12.28	2124.00	186.60	10.50	21.06
	Max	32.23	3438.40	650.20	13.53	31.00
	Mean	22.11	2788.31	302.19	11.92	28.34
	SD	17.48	783.60	247.79	1.34	4.02
	CV	79.05%	28.10%	82.00%	11.23%	14.17%
Open water	Min	1.45	549.71	89.40	4.92	10.89
	Max	300.90	2763.33	349.67	13.58	25.05
	Mean	100.10	1275.95	174.29	10.29	16.43
	SD	73.37	661.92	73.42	2.67	3.83
	CV	73.30%	51.88%	42.12%	25.98%	23.30%

The correlation coefficient values among TN, TP, DOC, DIC and Chl-a are presented in Table 3. There were significant positive relationships between TN and TP under ice-covered (0.59, $p<0.01$) and open-water conditions (0.42, $p<0.01$). This suggests that both nutrients have the same input sources and outputs to the water area. During the ice-covered period, significant negative correlations existed between DOC and TN (-0.53, $p<0.01$), and DIC and TP (-0.58, $p<0.01$), whereas these correlations were very weak under open-water conditions. No statistically significant correlations were found among DOC, DIC and Chl-a under both ice-covered and open-water conditions. Chl-a appeared to vary independently from dissolved carbon during the monitoring period in the study lake.

A significant correlation existed between TP and Chl-a (0.68, $p<0.01$) as well as TN and Chl-a (0.50, $p<0.01$) during the open-water periods, while both nutrients were statistically uncorrelated to Chl-a under ice (-0.26, $p=0.20$ for TN; -0.13, $p=0.53$ for TP). The interaction patterns of nutrients with Chl-a differ between ice-covered and open-water conditions in the study lake. Under open-water conditions, TP had a stronger positive correlation with Chl-a than TN, indicating that TP plays a more important role in algal growth. The relationship between TP and Chl-a, shown in Figure 3 on a log-log scale, demonstrates a predominantly positive trend. Under ice-covered conditions, the overall weak relationships of TN and TP to Chl-a suggest that the stormwater lake is not primarily nutrient limited.

Table 3. Pearson's correlation among the measured variables for the study lake.

		TN	TP	DOC	DIC	Chl-a
Ice-covered	TN	1	0.59**	-0.53**	-0.43*	-0.26
	TP		1	-0.38	-0.58**	-0.13
	DOC			1	-0.06	0.34
	DIC				1	0.09
	Chl-a					1
Open water	TN	1.00	0.42**	-0.11	0.18*	0.50**
	TP		1.00	-0.22*	-0.04	0.68**
	DOC			1.00	-0.06	-0.16
	DIC				1.00	-0.14
	Chl-a					1

Note: * significant (two-tailed) at p≤0.05 level; ** significant (two-tailed) at p≤0.01 level.

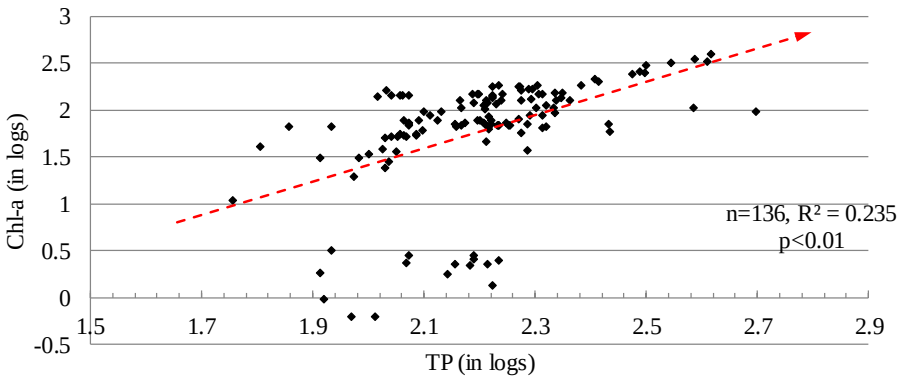

Figure 3. Log (TP) vs. Log (Chl-a) under open-water conditions.

For the study lake, the value of TN/TP was calculated to range from 2.64 to 24.62 under ice-covered conditions and from 2.31 to 47.08 under open-water conditions respectively. TP and TN/TP were more significantly correlated than TN and TN/TP under ice, but the opposite was found during the open-water period (Figure 4). This indicates that the major nutrient controlling the TN/TP level is TP during the ice-covered period, and it shifts to TN in the open-water seasons.

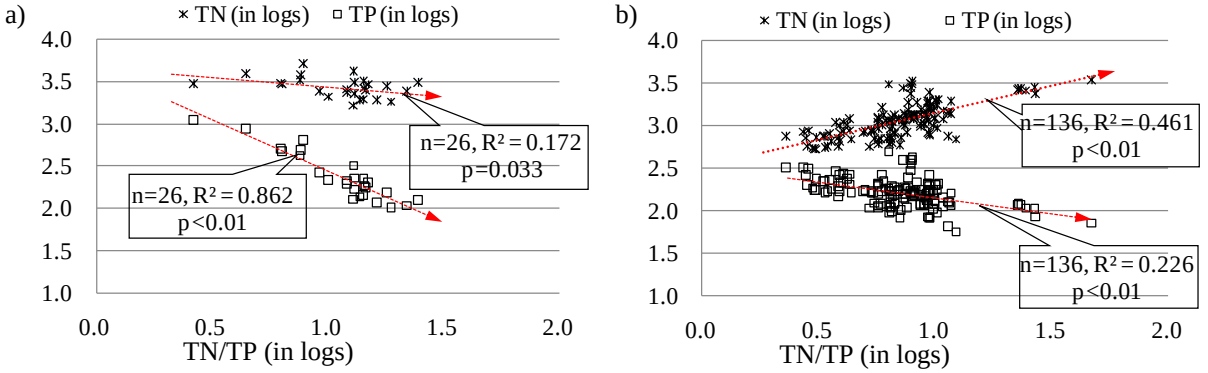

Figure 4. Log (TN/TP) vs. Log (TN) and Log (TP) under a) ice-covered conditions; b) open-water conditions.

Generally, a lake is considered nitrogen-limited when TN/TP < 10; nitrogen- or phosphorus-limited or phosphorus-limited when TN/TP > 10. The relationships between TN, TP and Chl-a at different TN/TP levels are presented in Figure 5. Significant positive correlations existed between TP and Chl-a under both ice-covered conditions (0.73, p<0.05) and open-water conditions (0.73, p<0.01) when TN/TP<10. The Chl-a concentration increased dramatically with respect to the TP concentration under open-water conditions, and gradually under ice. When TN/TP>10, TP was positively related to Chl-a under open-water conditions (0.58, p<0.01), but the correlation was

non-significant during the ice-covered period (0.26, p=0.30). The correlations between TN and Chl-a were significantly positive in open-water season (0.55, p<0.01 when TN/TP<10; 0.56, p<0.05 when TN/TP>10); however, during the ice-covered period, the situation differed strongly: when TN/TP<10, TN had a non-significant negative correlation with Chl-a (-0.37, p=0.36); when TN/TP>10, the relationship was very weak (-0.002, p=0.99).

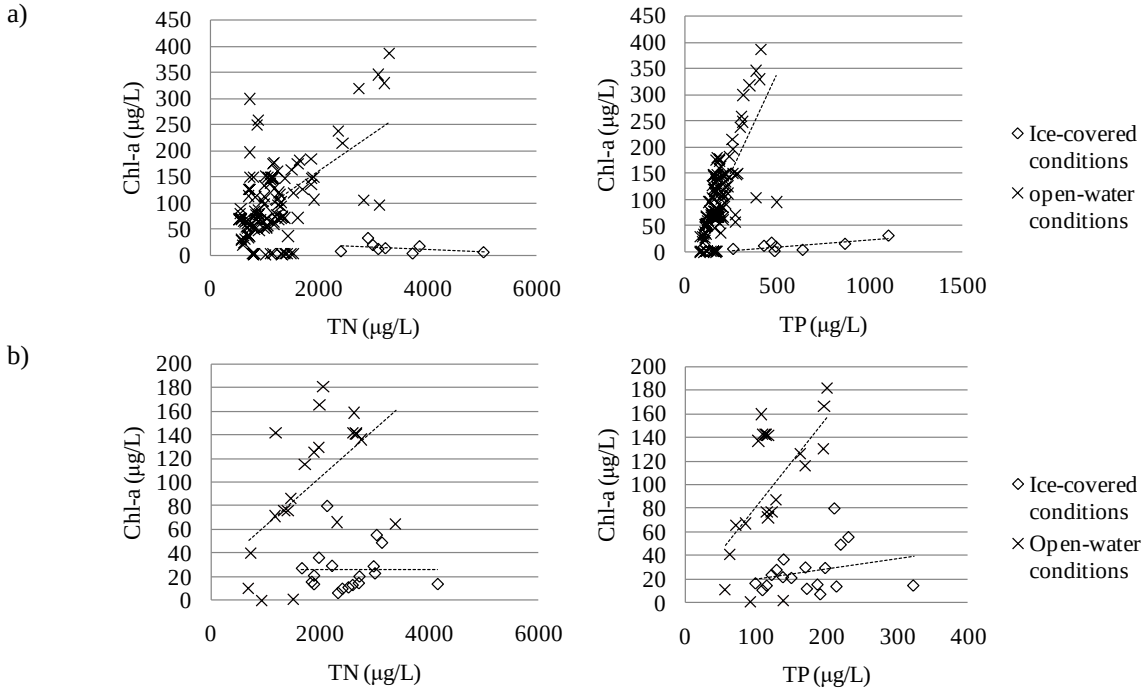

Figure 5. Relationships between TN, TP and Chl-a at a) TN/TP < 10; b) TN/TP > 10

4. Conclusion

The nutrient processes in a study stormwater lake were investigated. Data analyzed included the concentrations of TN, TP, DOC, DIC, and Chl-a collected during a two-year field measurement program. The Stormwater Lake was covered by ice from November to mid-April in the following year for both winters, allowing a comparison between ice-covered and open-water conditions. The results indicated that the mean value of Chl-a under ice-covered condition was 22.09% of the mean value under open-water conditions, suggesting the potential importance of primary productivity under ice. Concentrations of TN, TP, and DIC were remarkably higher under ice-covered conditions, while DOC showed little seasonal variation. The correlation trends of nutrients with Chl-a also varied seasonally. TP was found to be more determinative of Chl-a concentrations in open-water season. During the ice-covered period, TP was the major nutrient controlling the ratio of TN to TP, and the relationships between nutrients and Chl-a were remarkably different under different TN/TP.

Acknowledgement

This work was financially supported by the Natural Sciences and Engineering Research Council of Canada (NSERC) Collaborative Research and Development Grant, the City of Edmonton, and the China Scholarship Council (CSC). Their support is gratefully acknowledged.

References

American Water Works Association. (1999). *TP Standard methods for the examination of water and wastewater*. 20th Ed, 4500-P.

American Water Works Association. (2004). *TN Standard methods for the examination of water and wastewater*. 22nd Ed, 4500-N-B.

Babanazarova, O., Sidelev, S., Schischeleva, S. (2013). "*The structure of winter phytoplankton in Lake Nero, Russia, a hypertrophic lake dominated by Planktothrix-like Cyanobacteria*". *Aquatic Biosystems*, 9(18). doi: 10.1186/2046-9063-9-18.

Bertilsson, S., Burgin A., Carey C., Fey S., Grossart, P., Grubisic, L., Jones, I., Kirillin, G., Lennon, J., Shade, A., Smyth, R. (2013). "The under-ice micro biome of seasonally frozen lakes" *Limnol. Oceanogr*, *58* (6), 1998-2013.

Bratt, A. R., Finlay, J. C., Hobbie, S. E., Janke, B. D., Worm, A. C., Kemmitt, K. L. (2017). "Contribution of leaf litter to nutrient export during winter months in an urban residential watershed." *Environmental Science & Technology*,*51*(6),3138–3147. https://doi.org/10.1021/acs.est.6b06299

Griffiths, K., Michelutti, N., Sugar, M., Douglas, M., Smol, J. (2017). "Ice-cover is the principal driver of ecological change in High Arctic lakes and lakes." *PLOS ONE*, *12*(3). doi:10.1371/journal.pone.0172989.

Hampton, S., Moore, M., Ozersky T., Stanley, E., Polashenski, C., Galloway, A. (2015). "HORIZONS heating up a cold subject: prospects for under-ice plankton research in lakes." *J. Plankton Res*, *37*(2), 277–284.

Hampton, S., Galloway, A., Powers, S., Ozersky, T., Woo, K., Batt, R., Labou, S., O'Reilly, C., Sharma, S., Lottig, N., Stanley, E., North, R., Stockwell, J., et al. (2017). "Ecology under lake ice." *Ecology Letters*, *20*, 98–111.

Lenard, T., Wojciechowska, W. (2013). "Phytoplankton diversity and biomass during winter with and without ice cover in the context of climate change." *Polish Journal of Ecology*, *61*, 739–748.

Marsalek, P. M., Watt, W. E., Marsalek, J., Anderson B. C. (2000). "Winter flow dynamics of an on-stream stormwater management pond." *Water Qual. Res. J. Canada*, *35*(3), 505-523.

Marsalek, P. M., Watt, W. E., Marsalek, J., Anderson B. C. (2003). "Winter operation of an on-stream stormwater management pond." *Water Science and Technology*, *48*(9), 133-143.

Oberts, G.L., Marsalek, J., Viklander, M. (2000). "Review of water quality impacts of winter operation of urban drainage." *Water Qual. Res. J. Canada*, *35*(4), 881-808.

Ozkundakci, D., Gsell, A.S., Hintze, T., Tauscher, H., Adrian, R. (2016). "Winter severity determines functional trait composition of phytoplankton in seasonally ice-covered lakes." *Glob. Change Biol, 22*, 284-298.

Salonen, K., Lepparanta, M., Viljanen, M., Gulati, R. (2009). "Perspectives in winter limnology: closing the annual cycle of freezing lakes." *Aquat. Ecol , 43*, 609–616.

Semadeni-Davies, A. (2006). "Winter performance of an urban stormwater pond in southern Sweden." *Hydrol. The process*,*20*, 165–182.

Sommer, U., Gliwicz, M., Lampert, W., Duncan A. (1986). "The PEG-model of seasonal succession of planktonic events in fresh waters." *Arch. Hydrobiol.*, *106*(4), 433–471.

Schröder, A. (2013). "Density-and size-dependent winter mortality and growth of late Chaoborus flavicans larvae." *PLOS ONE*, *8*(10), e75839.

Tixier, G., Rochfort, Q., Grapentine, L., Marsalek, J., Lafont, M. (2012). "Spatial and seasonal toxicity in a stormwater management facility: Evidence obtained by adapting an integrated sediment quality assessment approach" *Water Research*, vol. 46, pp. 6671-6682.

Twiss, M.R., McKay, R.M.L., Bourbonniere, R.A., Bullerjahn, G.S., Carrick, H.J., Smith, R.E.H., Winter J.G., D'souza, N.A., Furey, P.C., Lashaway, A.R., Saxton, M.A., Wilhelm, S.W. (2012). "Diatoms abound in ice-covered Lake Erie: an investigation of offshore winter limnology in Lake Erie over the period 2007 to 2010". *J. Great Lakes Res.*, *38*, 18–30.

Welschmeyer, N. A. (1994). "Fluorometric Analysis of chlorophyll an in the presence of chlorophyll b and pheopigments." *Limnol. Oceanogr.*, *39*(8), 1985-1992.

Journal Of Contemporary Urban Affairs

2017, Volume 1, Number 3, pages 31– 37

Power Quality Improvement by Using Statcom Control Scheme in Wind Energy Generation Interface to Grid

* Dr. **Sheeraz Kirmani** [1], **Brijech Kumar** [2]

[1, 2] Department of Electrical Engineering, Jamia Millia islamia, New Delhi, India

E mail: sheerazkirmani@gmail.com , E mail: bknsea@icloud.com

ARTICLEINFO:

Article history:

Received 2 August 2017

Accepted 26 August 2017

Available online 12 October 2017

Keywords:

Power quality Improvement;
Statcom control scheme;
Wind energy Generation.

ABSTRACT

"Electric Power Quality (EPQ) is a term that refers to maintaining the near sinusoidal waveform of power distribution bus voltages and currents at rated magnitude and frequency." Today customers are more aware of the seriousness that the power quality possesses, this prompts the utilities to assure good quality of power to their customer. The power quality is basically customer-centric. The increased focus on utilities toward to maintaining reliable power supply by employing power quality improvement tools has reduced the power outages and blackout considerably. Good power quality is the characteristic of reliable power supply. Low power factor, harmonic pollution, load imbalance, fast voltage variations are some common parameters which are used to define the power quality. If the power quality issues are not checked, i.e., the parameters that define power quality doesn't fall within the predefined standards than it will lead to high electricity bill, high running cost in industries, malfunctioning of equipments, challenges in connecting renewables. Capacitor banks, FACTS devices, harmonic filters, SVC's, STATCOM are the solutions to achieve the power quality. The performance of Wind turbine generators is affected by poor quality power, at the same time these wind power generating plant affects the power quality negatively. This paper presents the STATCOM system with the BESS and studies the impact on the power quality in a system which consist of wind turbine generator, nonlinear load, hysteresis controller for controlling the operation of STATCOM and grid. The model is simulated in the MATLAB/Simulink. This scheme mitigates the power quality issues, improves voltage profile and also reduces harmonic distortion of the waveforms. BESS level out the imbalances caused by real power due to intermittent nature of wind power available due to varying wind speeds.

JOURNAL OF CONTEMPORARY URBAN AFFAIRS (2017) ***1***(3), 31-37.

https://doi.org/10.25034/ijcua.2018.3676

www.ijcua.com

I. Introduction

Power is the very crucial input for the growth of any economy. Therefore, it is considered as a core industry as it facilitates development across various sectors, such as agriculture,

***Corresponding Author:**

Department of Electrical Engineering, Jamia Millia islamia, New Delhi, India

E-mail address: sheerazkirmani@gmail.com

manufacturing, railways, education, commercial, etc. to expel economic development. To meet the high GDP rates, the energy needs of the country are inevitable.

Renewable energy is characterized as intermittent and variability which presents various challenges in its grid integration for maintaining grid stability and security.

Intermittent/variable nature of RE source results in wide variation in quantum and direction of power flow on the inter-state high capacity transmission corridors. This requires placement of dynamic reactive compensation in the form of dynamic reactive compensation in the form of STATCOM/svc at strategic locations to provide dynamic support for smooth operation and to maintain grid security.

The integration wind into existing electrical power system induces power quality problems like voltage regulation, stability, harmonic distortion, voltage sag/swell and also power factor. The power quality is always customer-focused measure and is greatly affected by the operation of a distribution and transmission network. In this

proposed scheme one of the Flexible AC transmission system (FACTS) device, i.e., Static-Compensator (STATCOM) is connected at the point of common coupling (PCC) with a battery energy storage system (BESS) to mitigate power quality problems. Since STATCOM connected to the grid provides reactive power support to wind generator and to load. The BESS is integrated to sustain real power source under fluctuating wind or solar power.

In the event of if there is any sudden load change or change in voltage profile like a short circuit in point of common coupling (PCC), a Distribution-STATCOM responds fast and stabilizes the voltage and also helps in order to maintain power quality.

II. Problems Related To Power Quality

A. Power Quality Issues of Grid Side:

At the grid side, the power quality is the responsibility of utility. The utility should make sure that the power matches the customer requirements and should not violate the limits that are specified for the parameters which define the power quality. From the customer point of view, the voltage variations and high content of harmonics in the grid power are highly undesired as they affect the performance of the end equipment. For the IIP's who have planned the wind power project, the voltage profile of evacuating substation and nearby substations is of prime concern.

1) Voltage variation:

Intermittent nature of wind power causes several problems, and one is a variation of the voltage of buses in the region of high wind penetration. Wind generators mostly employed induction generators and power electronic circuits which demand reactive power for operation. Voltage sag/swell is observed where ineffective methods of reactive power management are employed. If the voltage rises beyond the controllable limit, forced tripping of lines carried out, cascaded tripping may destabilize a weak power system. Generally, the power factor of evacuating substation is maintained near to unity preferably slightly lagging.

2) Voltage Transients:

B. Power Quality Issues of WTG Side

In the wind energy generating system the power quality primarily concerned with the quality of current waveform which is being drawn or generated by the wind turbine. Poor power quality affects the performance of the loads connected to the grid.

1) Reactive Power Consumption:

Induction generators draw reactive power to produce its working flux while generating active power at the same time. As induction generators are most widely preferred in wind turbine generators, collectively a wind farm demand a huge amount of reactive power. As the wind speed is not constant, in such a case the use of electronic power conversion devices in wind turbine generators becomes inevitable to achieve a rotor speed for maximum extraction of energy from wind. The operation of power electronic devices also requires reactive power. To avoid voltage stability problem either STATCOM or capacitor arrangement is used to supply this demand of reactive power.

2) Current Harmonics Generation:

Capacitors are used as an essential part of the wind turbine generators for supplying reactive power demand. Capacitor switching may cause large voltage transient. The frequency and amplitude of such transient are enormous, particularly when back to back switching is involved, for instance, capacitor bank switching. The overvoltages may damage the insulation, moreover, electronic equipment such as controllers are very sensitive to these transients, may produce incorrect commands. In addition,

lightning strikes will cause an overvoltage in the electrical system of the wind turbine.

III. Topology for Power Quality Improvement

The STATCOM based current control voltage source inverter injects the current into the grid in such a way that the source current is harmonic free and their phase-angle with respect to source voltage has a desired value. The injected current will cancel out the reactive part and harmonic part of the load and induction generator current, thus it improves the power factor and the power quality. To accomplish these goals, the grid voltages are sensed and are synchronized in generating the current command for the inverter. The proposed grid-connected system is implemented for power quality improvement at the point of common coupling (PCC), as shown in Figure 1.The connected grid system in Figure 1, consists of wind energy generation system and battery energy storage system withSTATCOM.

B. Bess-Statcom

The battery energy storage system (BESS) is used as an energy storage element to support the wind farm during intermittencies it also supports grid during any disturbance and loss of generation. The BESS will naturally maintain dc capacitor voltage constant and is best suited in STATCOM since it readily manages demand and supply of real power and also injects or absorbed reactive power to stabilize the grid system. It also controls the distribution and transmission system at a very fast rate. When power fluctuations occurs in the system, the BESS can be used to level the power fluctuations by charging and discharging operation. The BESS system is connected in parallel to the dc capacitor of STATCOM (Salamah *et al.,* 1992; Yang *et al.,* 2001; Black, and Strbac, 2007; Spahic *et al.,* 2007; Mohod, and Aware, 2008)

STATCOM comes from the family of FACTS devices. These are basically solid-state devices which are having the capability to respond to the reactive power demand. STATCOM have the edge over the SVC's as the former have constant current characteristics while in the SVC's the capacitive current drops linearly with the voltage. STATCOM can easily be interfaced with real power sources like the battery systems, fuel cells, etc. STATCOM effectively control the system voltage and avoid voltage collapse.

STATCOM are solid-state shunt connected devices. STATCOM's strategically placed in the power system to make the grid robust to the disturbances. STATCOM are finding applications in the renewable energy integration.

C. System Operation

In the system under study, STATCOM is interfaced with the BESS system. The STATCOM-BESS system is then connected to the PCC in the grid where non-linear loads and induction generator based wind turbine are also interfaced.The current control strategy is adapted to control the statcom-BESS system. The control strategy controls the output of station in such a manner so as to achieve power quality norms in the electrical grid.The statcom is intended here to support both reactive as well as real power demand of the other sub-systems.The main block diagram of the operational system scheme is shown in Figure 2.

IV Control Scheme

A. Bang-Bang Current Controller

The current control scheme is implemented using a bang-bang current controller. In this control scheme, the source current is detected by a current sensor, and these are compared with the reference current to obtain the current error for the hysteresis-based bang-bang controller.

Thus the ON/OFF switching signals for IGBT of STATCOM are derived from hysteresis controller. The switching function S_A for phase 'an' is expressed as.

$$i_{sa} < (i_{sa}^{*} - HB) \rightarrow S_A = 0$$

$$i_{sa} > (i_{sa}^{*} - HB) \rightarrow S_A = 1$$

where HB is a current hysteresis band, similarly the switching functionS_B ,S_C can be derived for phases "b" and "c" (Mohod, and Aware, 2008; Mohod, and Aware, 2006)

B. Gird Synchronisation

In three-phase balance system, the RMS voltage source ampl-

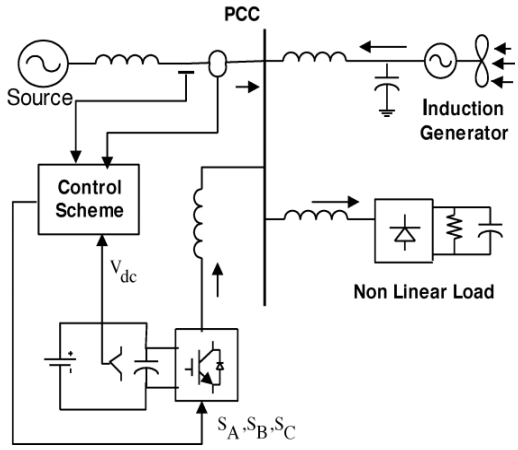

Figure 1. Diagrammatic representation of operating scheme.

-studies calculated at the sampling frequency of the source phase voltage (V_{sa}, V_{sb}, V_{sc}) and is expressed as sample template V_{sm}, sampled peak voltage, as in (1).

$$V_{sm} = \sqrt{\{\frac{2}{3}(V_{sa}^2 + V_{sb}^2 + V_{sc}^2)\}} \qquad (1)$$

The in-phase unit vectors are obtained from AC source-phase voltage and the RMS value of unit vector u_{sa}, u_{sb}, u_{sc} as shown in (2).

$$u_{sa} = \frac{V_{sa}}{V_{sm}},\ u_{sb} = \frac{V_{sb}}{V_{sm}},\ u_{sc} = \frac{V_{sc}}{V_{sm}} \qquad (2)$$

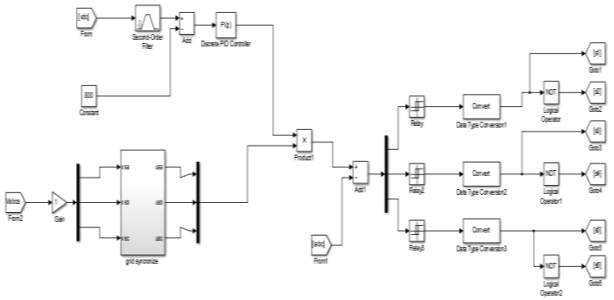

Figure 2. Hysteresis controller (Matlab Model).

The in-phase generated reference currents are derived using in-phase unit voltage template as, in (figure 3)

$$i_{sa} = I.u_{sa},\ i_{sb} = I.u_{sb},\ i_{sc} = I.u_{sc} \qquad (3)$$

Where *I* am proportional to the magnitude of filtered source voltage for respective phases. This ensures that the source current is controlled to be sinusoidal. The unit vectors implement the important function in the grid connection for the synchronization for STATCOM. This method is simple, robust and favorable as compared with other methods (Milands *et al.,* 2007).

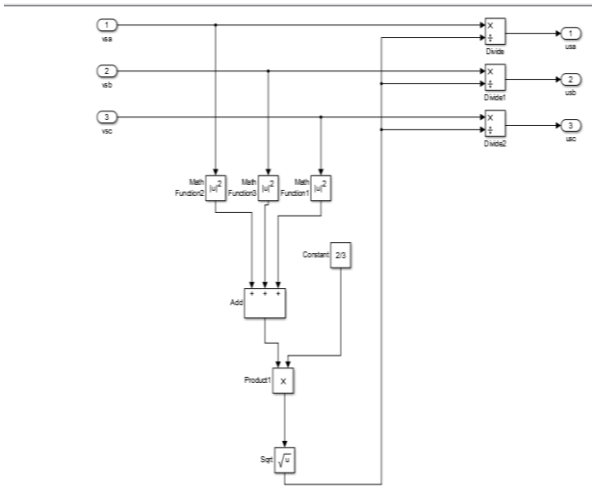

Figure 3. Unit Vector Block for Grid Synchronisation.

V. System P Performance

The proposed control scheme is simulated using Simulink power system block set. The system parameter for given system is given Table I.

A. *Voltage Source Current Control—Inverter Operation*

STATCOM in its basic structure is a voltage source inverter and is composed of IGBT's. Igbt based three-phase inverter is connected to the grid at PCC through the interconnecting transformers. The statcom inject the three phase currents to level out the distortions due to nonlinear loads and wind turbine generating system in the grid power supply. The control signals with a hysteresis band of 0.08 for switching of igbts are simulated from the comparison made between reference currents and actual three-phase source currents. Hysteresis band is generally kept low for better combating capabilities of statcom.The control signal of switching frequency within its operating band, as shown in Figure. 4.

The choice of the current band depends on the operating voltage and the interfacing transformer impedance. The compensated current for the nonlinear load and demanded reactive power is provided by the inverter. The real power transfer from the batteries is also supported by the controller of this inverter. The three-phase inverter injected current are shown in Figure 5.

B. *STATCOM—Performance under Load Variations*

The system is modeled in MATLAB to investigate the performance of STATCOM based BESS system under dynamic loads and peak wind generation

or fixed wind generation. Induction generator based wind turbine generator demand reactive power. Therefore when the STATCOM is switched on at time 0.7sec, it starts supplying this reactive power demand. Additionally, it also injects current such that harmonics at the supply side current reduces considerably. To investigate the performance under varying

Table I. Rating and parameters.

S.N.	Parameters	Ratings
1	Grid Voltage	3-phase ,415V,50 Hz
2	Induction Motor/Generator	3.35 kVA,415V, 50 Hz, P = 4, Speed = 1440 rpm, Rs = 0.01Ω, Rr=0.015Ω,Ls =0.06H,Lr=0.06H
3	Line Series Inductance	0.05mH
4	Inverter Parameters	DC Link Voltage = 800V, DC link Capacitance = 100 µF. Switching frequency = 2 kHz,
5	IGBT Rating	Collector Voltage =1200V, Forward Current =50A,Gate voltage =20V, Power dissipation = 310W
6	Load Parameter	Non-linear Load 25kW.

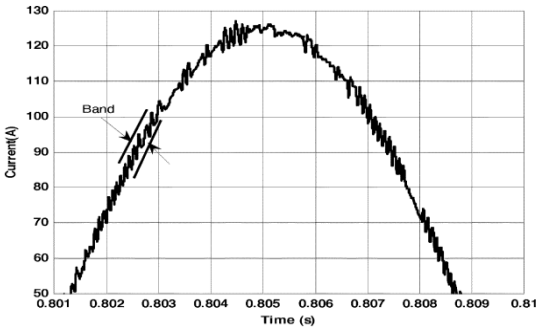

Figure 4. Switching signal and control hysteresis band.

loads the provisions are made in the MATLAB program to increase the load at time 1sec. For increased load STATCOM based system effectively compensate the increased demand for real and reactive power. The result of source current, the load current is shown in Figure 6(a) and (b) respectively. While the result of injected current from STATCOM are shown in Figure 6(c) and the generated current from wind generator at PCC are depicted in Figure 6(d).

The DC link voltage regulates the source current in the grid system, so the DC link voltage is maintained constant across the capacitor as shown in Figure 7(a). The current through the dc link capacitor is indicating the charging and discharging operation as shown in Figure 7(b)

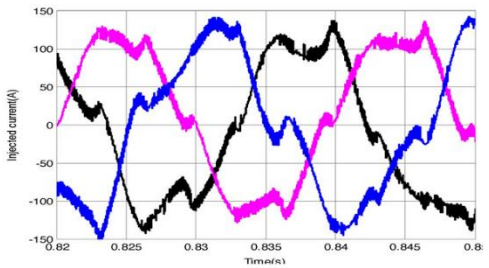

Figure 5. Three phase injected inverter Current.

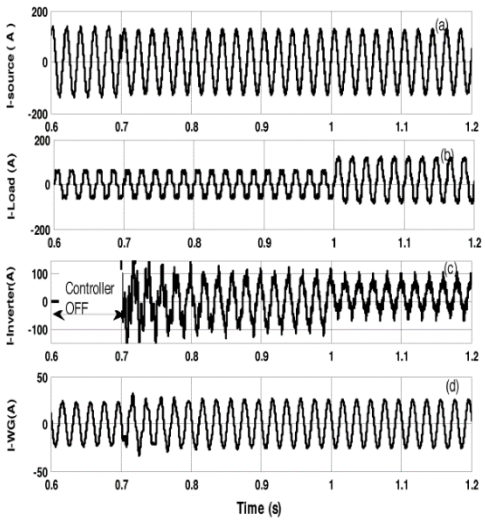

Figure 6. (a) Source Current. (b) Load Current. (c) Inverter Injected Current (d) Wind generator (Induction generator) current.

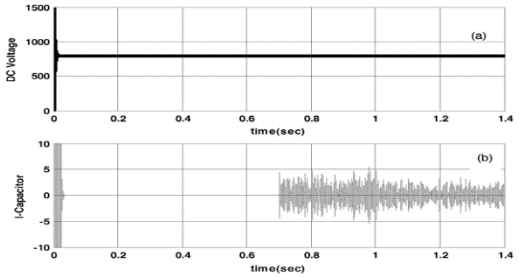

Figure 7. (a) DC link voltage. (b) Current through Capacitor.

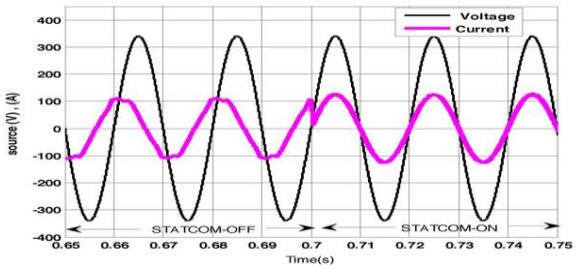

Figure 8. Supply Voltage and Current at PCC.

C. Power Quality Improvement

Power quality is affected by the nonlinear loads as such loads inject harmonics in the grid. Wind generators also have negative impact on power quality. Thus the purity of voltage and current

waveforms on grid side and wind generator side cannot be assured. The STATCOM output voltage and injected current are adjusted as per the power quality parameters sensed by the hysteresis controller from the grid. The high-speed operation of controller ensures reliable power quality norms at the PCC. The STATCOM output voltage is shown in the figure. The source side voltage and the current plot are shown in the figure; the plot clearly shows that power factor becomes near unity when the STATCOM is switched on. The harmonics in the source side current before and after the beginning of STATCOM operation is carried out. When STATCOM is made on significant reduction of harmonics from an initial value of 4.71 % is observed. The source current waveform when STATCOM is on is shown in the figure.

The model not only improves the power quality but also supports the loads with its batteries. It balances the supply and demand. This scheme also has the capabilities to support the loads in case of loss of generation, in such case power from batteries can be supplied to the loads but for a limited time.

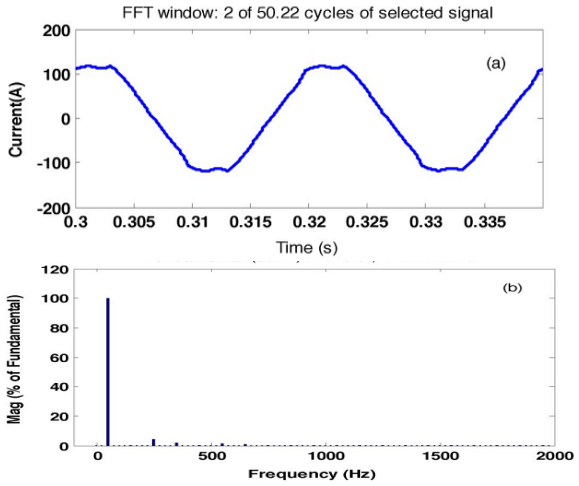

Figure. 9 (a) Source Current. (b) FFT of source current.

VI. Conclusions

The paper presents STATCOM based battery energy storage system. STATCOM is a voltage source inverter having Igbt as its switches. The switching of igbt's is controlled by the hysteresis controller. Therefore the power flow from and to the BESS system is controlled effectively as per the switching command generated by the controller. The entire STACOM-BESS system is modeled in MATLAB/Simulink. When STATCOM is in operation significant improvement in power quality is observed. Issues like voltage sag\ swell, harmonic distortion, power factor voltage profile are properly tackled. When STATCOM in operation it injects current into the power grid at PCC which nullify the harmonic part of the source current. Therefore current and voltage at source side become in phase. A near unity power factor, therefore, can be maintained at the evacuating substation (PCC). By maintaining power quality norms at nearby substations of the wind generating farm forced tripping of connecting lines between pooling substation and evacuating substation can be avoided which improves the plant load factor and in terns revenues.

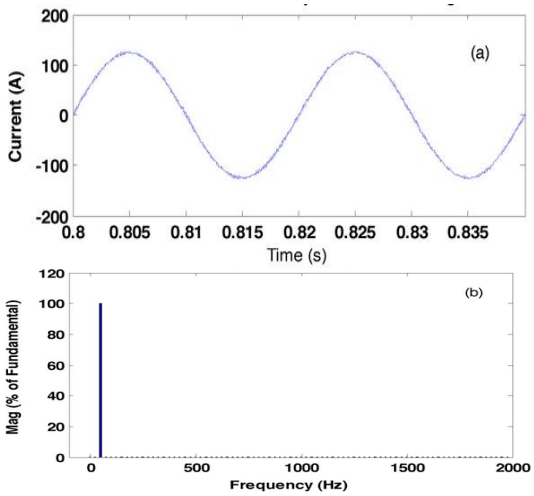

Figure 10. (a) Source Current. (b) FFT of source current.

Acknowledgement

This research did not receive any specific grant from funding agencies in the public, commercial, or not-for-profit sectors.

References

[1] Hook, K. S., Liu, Y., and Atcitty, S. (2006). Mitigation of the wind generation integration related power quality issues by energy storage. *EPQU J.*, *12*(2).

[2] Manel, J. (2006). Power electronic system for grid integration of renewable energy source: A survey. *IEEE Trans. Ind. Electron.*, *53*(4), 1002–1014.

[3] Han, C., Huang, A. Q., Baran, M., Bhattacharya, S., and Litzenberger, W. (2008). STATCOM impact study on the integration of a large wind farm into a weak loop power system. *IEEE Trans. Energy Conv.*, *23*(1), 226–232,

[4] Kinjo, T. and Senjyu, T. (2006). Output leveling of renewable energy by electric double layer capacitor applied for energy storage system. *IEEETrans. Energy Conv.*, *21*(1).

[5] Bhatia, R. S., Jain, S. P., Jain, D. K., and Singh, B., Battery energy storage system for power

conditioning of renewable energy sources. *Proc. Int. Conf. Power Electron Drives System*, *1*, 501–506.

[6] Zeng, J., Yu, C. Qi, Q. and Yan, Z. (2004). A novel hysteresis current control for active power filter with a constant frequency. *Elect. Power Syst. Res.*, vol. 68, pp. 75–82, 2004.

[7] J. Barros, De Apraiz, M., and Diego, R. I. (2007). Measurement of Subharmonics in Power Voltages. *Power Tech, IEEE Lausanne*, 1736 – 1740.

[8] Lei, Y., Mullane, A., Lightbody, G., and Yacamini, R. (2006). Modeling of the wind turbine with a doubly fed induction generator for grid integration studies. *IEEE Trans. Energy Conversion*, *21*(1), 257–264.

[9] Lu, C. F., Liu, C. C., and Wu, C. J. (1995). New dynamic models of lead-acid batteries. *IEE Proc.-Gener. Trans. Distrib.*, *142*(4), 429–435.

[10] Salamah, Z. M., Casacca, M. A., and Lynch, W. A., (1992). A mathematical model for lead-acid batteries. *IEEE Trans. Energy Conversion, 7*(1), 93–97.

[11] Yang, Z., Shen, C., Zhang, L., Crow, M. L. and Atcitty, S. (2001). Integration of a STATCOM and battery energy storage. *IEEE Trans. Power Syst., 16*(2), 254–260.

[12] Black, M., and Strbac, G. (2007). Value of bulk energy storage for managing wind power fluctuations. *IEEE Trans. Energy Conversion, 22*(1), 197–205.

[13] Spahic, E., Balzer, G. and Shakib, A. D. (2007). The impact of the 'wind farm battery' unit on the power system stability and control. *Proc. IEEE Power Tech., Lausanne*, *5,* 485–490.

[14] Mohod S. W., and Aware, M. V. (2006). Grid power quality with variable speed wind energy conversion. *Proc. IEEE Int. Conf. Power Electronic Drives and Energy System (PEDES), 1*, 501–506.

[15] Mohod S. W., and Aware, M. V. (2008). Power quality issues & it's mitigation technique in wind energy conversion. *Proc. of IEEE Int. Conf.Quality Power & Harmonic*, *3.*

[16] Milands, M. I., Cadavai, E. R., and Gonzalez, F. B. (2007). Comparison of control strategies for shunt active power filters in three phase four wire system. *IEEE Trans. Power Electron*. , *22*(1), 229–236.

[17] ZOU, C., WANG, B., and BAO, P. (2008). Application of STATCOM in Wind Farm. *Electric Drive*, *12*, 1-10, 2008.

Journal of Contemporary Urban Affairs

2017, Volume 1, Number 3, pages 38– 42

Global Warming and Climate Change: A Critique on International Law and Policy

* Dr. **Lisa P Lukose** [1]

[1] University School of Law and Legal Studies, Guru Gobind Singh Indraprastha University, New Delhi, India

E mail: drlisarobin@ipu.ac.in

ARTICLEINFO:

Article history:

Received 2 August 2017

Accepted 28 August 2017

Available online 12 October 2017

Keywords:

Solar collector;
Thermal storage;
Latent heat storage.

ABSTRACT

Global warming and climate change, a multidisciplinary topic is a matter of international concern. There are some international environmental treaties related to global warming and climate change. The most significant international agreement in this area is - UNFCCC - the United Nations Framework Convention on Climate Change adopted at the Rio Earth Summit in 1992 and ratified by 195 countries. It mainly deals with greenhouse gases emissions mitigation, adaptation and finance starting in the year 2020. The Kyoto Protocol which extends the 1992 UNFCC mandates State Parties to reduce greenhouse gas emissions: its two basic premises are - global warming exists, and human-made CO2 emissions caused global warming. The Kyoto Protocol came into force in 2005 and each COP has served as the 'meeting of parties' to Kyoto Protocol such as COP13 (Bali, 2007), COP15 (Copenhagen, 2009), COP16 (Cancun, 2010), COP17 (Durban, 2011), COP18 (Doha, 2012), COP19 (Warsaw, 2013), COP21 and (Paris, 2015).There are other international legal instruments such as 1979 Geneva Convention on Long-Range Trans-boundary Air Pollution. Against this backdrop, this paper will critically examine the existing international legal regime (treaties, conventions, agreements, etc.) on global warming and climate change.

JOURNAL OF CONTEMPORARY URBAN AFFAIRS (2017) ***1***(3), 38-42.

https://doi.org/10.25034/ijcua.2018.3677

www.ijcua.com

1. Introduction

Global warming and climate change is no longer a problem of the future generation, though it continues to affect future generations. Global warming from carbon dioxide (C02) and other greenhouse gases pose a severe threat to the international community. The Earth's atmosphere is dilapidated at an unprecedented rate. Law plays a critical and important role for the effective and equitable climate change governance. There is some legal framework adopted to address the issues relating to global warming and climate change. However, global warming and climate change is not an isolated topic to address independently. It is connected to all environmental issues. This paper attempts to examine:

1. Why is global warming of serious concern?
2. How does the present international legal regime respond to climate change?
3. What are the lacunae in the existing international laws?

***Corresponding Author:**
University School of Law and Legal Studies, Guru Gobind Singh Indraprastha University, New Delhi, India
E-mail address: drlisarobin@ipu.ac.in

4. How can climate law respond better to the diverse contemporary requirements?

2. Method and Material

The author has adopted a doctrinal and analytical method to develop this paper. The material is drawn from both primary and secondary sources. The primary sources are the legal instruments while secondary sources are offline and online resource materials which are cited in this paper at relevant places.

3. Effect of Global Warming

The immediate effect of global warming is climate change. The impact of global warming is in fact much beyond climate change. It adversely affects human development, and it does have a long-term impact on the environment. Temperature increase, extreme weather events, flood, drought, sea level rise, erratic precipitation, melting glaciers, reduced snow cover are few impacts to mention. Its impact on aquaculture, biological diversity, agriculture, health, and livelihood is dangerous. It also adversely affects a broad range of other human rights *(Workshop in the Context of the UNFCCC COP 20* , 2014), for example, right to food, indigenous peoples right, etc.

A large section of the world population is suffering from the effects of climate change. In 2009 it was estimated that about 300000 people die annually due to the adverse effect of climate change and 325 million are further seriously affected (Annan, 2009). Since developing countries have less financial and technological resources, they are more vulnerable to the impacts of climate change.

4. UNFCCC 1992

The United Nations Framework Convention on Climate Change (one among the three adopted at the Rio Earth Summit-1992)[1] is described as "first steps to a safer future" which was a global response to climate change. Because the global community for the first time recognized and accepted that the climate change is a 'problem' despite having less scientific evidence than now. It is adopted on 9 May 1992 and came into force on 21 March 1994. It is one of the most widely accepted treaties having a near-universal membership. It neither has any binding limit on the emission of green gas for member countries nor has enforcement mechanisms.

The basic aim of UNFCCC is to prevent dangerous human interference with the climate system. By borrowing from the Montreal Protocol 1987, it bounds member states to "act in the interests of human safety even in the face of scientific uncertainty." UNFCCC is an international framework seeking global cooperation to combat climate change by limiting average global temperature increases and the resulting climate change and coping with impacts that were, by then, inevitable. It obliges the members to stabilize greenhouse gas concentrations at a level that would prevent dangerous anthropogenic interference with the climate system. It states how specific international treaties/protocols/Agreements may be negotiated to accomplish UNFCCC objectives.

5. UNFCC to KYOTO

By the agreements adopted in Copenhagen (2009) and Cancun (2010) countries promised to set a goal of maintaining temperature increases below 2 degrees Celsius above pre-industrial levels. It also explored financial options for implementation of REDD-plus actions. The developed countries committed to mobilizing $100 billion a year in public and private finance for developing countries by 2020. COP 17 at Durban (2011) recognized that "smart government policy, smart business investment, and the demands of an informed citizenry, all motivated by an understanding of mutual self-interest, must go hand in hand in pursuit of the common goal."

COP 18 Doha (2012) resulted in an amendment to the Kyoto Protocol establishing a second commitment period from 2013–20. It also added more item to list of greenhouse gases. At COP 19 in Warsaw (2013) the governments were encouraged to submit their intended nationally determined contributions (INDCs) to the Paris Agreement. INDCs represent member country's self-defined mitigation goals from 2020. 190 countries accounting for 99 percent of global emissions have already submitted INDCs to the UNFCCC. At COP 20 in Lima (2014) more than

[1] The other two sister Rio Earth Summit Conventions are (i) the UN Convention on Biological Diversity and (ii) the Convention to Combat Desertification. All the three conventions aim to encourage mutual cooperation for developing synergies in their activities. Now it incorporates Ramsar Convention on Wetlands as well.

190 countries pledged to develop new" urgency towards fast-tracking adaptation and building resilience across the developing world" (*Lima Call for Action*).

6. The Kyoto Protocol

The Kyoto Protocol which was developed under the UNFCCC's charter was adopted in 1997 subsequent to the negotiations from 1995 launched to strengthen the global response to climate change. It is a legally binding international instrument with 192 countries' ratification. The main aim of the protocol is to provide specific emissions reduction targets to industrialized nations whose activities mainly cause global warming. It is known as global climate treaty as it extends UNFCCC by requiring countries to reduce greenhouse gas emissions; based on the fact that global warming exists and human-made CO2 emissions have caused global warming. It is a binding instrument requiring developed nations (35 industrial nations) to reduce the emission of six major greenhouse gases to 5.2 percent below from their 1990 levels since they are historically responsible for the present levels of greenhouse gases in the atmosphere. The first commitment period was from 2008 to 2012 and the second from 2013 to 2020 (Doha Amendment to the Kyoto protocol; 37 countries have binding targets). Countries failing to meet the protocol standards are required to pay a carbon tax. It thus helps the state parties to mitigate global warming.

7. Criticism

The nations are divided over the benefits of the Koyoto protocol. Some countries have refused to ratify the protocol as they increasingly burn fossil fuels for energy. Sudan, Afghanistan and United States are the examples for countries which refused to ratify though the US itself emits 35% of the total greenhouse gases in the universe. When most polluter countries are not participating, the protocol remains an idea. Japan, New Zealand, Canada, and Russia though have participated in first-round, they have not taken have not taken commitments in the second period. Countries like China, Brazil, and India may surpass the United States emissions within 25 to 30 years. Critics opine that in order for the atmosphere to catch up with the greenhouse gases there must be 60 percent reduction of greenhouse gases whereas the treaty demands an average of 5.2 percent reductions. It is also apprehended that the targets set forth by the treaty cannot be reached by members as CO2 emissions are increasing. When the protocol mandates reduction of emission most of the countries is ill-equipped to meet the situation with less access to alternative forms of energy. Further, it is silent about 'climate change-related threats to state sovereignty (Badrinarayana, 2010).

8.2015 PARIS CLIMATE ACCORD

The 2015 Paris Agreement/Climate Accord, which is a separate instrument under the UNFCCC was adopted at the 21st session of the Conference of the Parties to UNFCCC (COP 21) on 12 December 2015 in Paris and came into force on November 4, 2016. 195 countries have adopted this agreement. This is the latest step in the UN climate change regime which charts a new course in the global effort to fight climate change measures to be taken after 2020 when the second Kyoto commitment period ends. The Paris Agreement seeks to accelerate and intensify the actions required for a sustainable low carbon future. Its main purpose is to strengthen global action plan to climate change by maintaining/limiting a global temperature rise below 2 degrees Celsius. It further aims to limit the increase to 1.5°C.

The Agreement also aims to strengthen the ability of countries to deal with the impacts of climate change. The three main components of the Paris Accord are: (i) the Paris Agreement setting common goals, commitments and expectations, (2) the intended "nationally determined contributions" (NDCs) submitted by more than 180 countries and (3) the thousands of contributions offered by companies, states, cities and civil society organizations. The agreement envisages that successive NDC of each party will "represent a progression" than its previous NDC and also "reflect its highest possible ambition."

NDC are however not legally binding obligations. It provides for more transparency and governmental accountability by "reporting to each other and the public on how well they are doing to implement their targets." Other important aspects of the agreement are:

- Parties are committed t to "prepare, communicate and maintain" successive NDCs
- Parties have to "pursue domestic mitigation measures" to achieve NDCs;
- They have to report on emissions and progress in implementing NDCs regularly.

It has two long-term mitigation goals: (i) a peaking of emissions as soon as possible (Since it will take longer for developing countries, and (ii) net greenhouse gas neutrality in the latter half of the century. Countries are in the process of negotiating the detailed rules to be adopted in 2018 to implement the Paris Agreement.

9. Suggestions and Recommendations

Countries have to promote energy efficiency and renewable energy actively. Countries like India, Mexico, South Africa, Saudi Arabia, Brazil, etc. have cut fossil fuel subsidies significantly. The countries have to encourage people to use and convert their energy usage to cleaner energy such as wind power, solar power, hydropower, geothermal power, biomass, etc.

Law and governance improvements must be taken seriously at both national and international levels for climate change mitigation and adaptation. Governments must urge for compensated reduction and compensated conservation wherein carbon can be saved by reducing deforestation and degradation and also carbon is added through conservation, sustainable management of forests and increase in forest cover – afforestation and reforestation (Subramaium, 2016).

Polluting states must have legal and ethical (Mayer, 2013), obligation to compensate – both prospective and retrospective responsibility. This will also help to address the human right issues in climate change regime (Bouthillier, 2012).

There must be more and more diverse interactions between public and private actors. The climate laws negations must ensure more effective participation of members. It is being criticised that out of more than 190 countries only about twenty countries control climate change negations.[2]

The existing climate law does not cover related environmental issues such as the impact of intellectual property rights (IPR) on the environment - for instance, the impact of genetically modified organisms on the environment. The climate law's reach must be extended to cover topics like IPR. (Rimmer, 2011).

Global warming and climate change are two sides of the same coin. However, this is not an isolated issue. It is interlinked with all environmental issues. Hence, it is a part of sustainable development. To reduce the adverse effect of climate change, the countries have to commit themselves to stop deforestation: REDD and REDD Plus envisages that developing countries have to reduce "emissions from deforestation and forest degradation." They have to consider policy approaches for the "conservation, sustainable management of forests, and enhancement of forest carbon stocks in developing countries."

9. Conclusion

150 years of industrialization have rendered the future of the Mother Nature at stake which will drastically change the equation of coming generations. It is predicted that the average temperature of the atmosphere will raise minimum by 10 degrees in the next century. Kyoto protocol has encouraged innovators and inventors to streamline their R&D for technologies that reduce greenhouse gas emissions. Countries have to accelerate research in alternate forms of energy. There must be international cooperation taking into consideration the legitimate requirement of developing and least developing countries to develop without compromising their responsibility for sustainable development. Then only the ultimate objective of UNFCCC- to achieve a level "within a time-frame sufficient to allow ecosystems to adapt naturally to climate change, to ensure that food production is not threatened and to enable economic development to proceed in a sustainable manner" can be achieved. The other two sisters Rio Earth Summit Conventions are (i) the UN Convention on Biological Diversity and (ii) the Convention to Combat Desertification. All the three conventions aim to encourage mutual cooperation for developing synergies in their activities. Now it incorporates Ramsar Convention on Wetlands as well.

References

Annan, K. (2009). *Anatomy of silent Crisis*. Global Humanitarian Forum.

Badrinarayana, D. (2010). Global Warming: A Second Coming for International Law"? .*Washington Law Review, 85*, 254-292.

Bouthillier, Y (Ed.). (2012). *Poverty Alleviation and Environmental Law*. IUCN Academy of Environmental Law series.

Rimmer, M.. (2011). *Intellectual Property and Climate Change: Inventing Clean Technologies*. UK: Edward Elgar Publishing Ltd.

[2] Daniel Bodansky, *The Copenhagen Climate Change Conference: A Post-Mortem*

Subramaium, G. (2016). *Climate Change and Reduction of Emission Issues Relating to Deforestation and Environmental degradation in India.* India: Indian Law Institute.

Mayer, B. (2013). Climate Change and International Law in the Grim Days. *EJIL*, *24*, 947–970.

Workshop in the Context of the UNFCCC COP 20. (2014). LAW, GOVERNANCE AND CLIMATE CHANGE An International Law and Policy. Lima, Peru. Centre for International Governance Innovation and the Centre for International Sustainable Development Law.

Journal Of Contemporary Urban Affairs
2017, Volume 1, Number 3, pages 43– 48

Exergy analysis of a flat plate solar collector with latent heat storage by phase change material for water heating applications at low temperature

* **Angie Rincon Ortega**[1], Dr. **Mauricio Carmona**[2]
[1, 2] Mechanical Engineering Department, Universidad del Norte, Barranquilla, Colombia
[1] E mail: anggier@uninorte.edu.co , [2] E mail: mycarmona@uninorte.edu.co

ARTICLEINFO:
Article history:
Received 2 August 2017
Accepted 27 August 2017
Available online 12 October 2017
Keywords:
Thermal energy storage;
Phase change material;
Exergy analysis;
Flat plate solar collector.

ABSTRACT

An exergy analysis has been performed to determine the potential for useful work in a latent heat storage system with phase change material (PCM) for a flat-plate solar collector. Commercial paraffin wax is used as PCM to store and release energy in the solid-liquid transformation; this material is located in metal containers under the absorber plate on the bottom insulation of the collector. The exergy analysis is performed in outdoor conditions for days of low, medium and high radiation taken from October 2016 to March 2017 at Barranquilla city (latitude: 10º 59' 16" N, longitude: 74º 47' 20" O, Colombia). The system is evaluated throughout charge and discharge periods. The energy and exergy balance equations based on the first and second law of thermodynamics is formulated and solved for each element of the collector system as well as for the PCM. Results obtained show the energy distribution and energetic destruction for each system component and its variation as a time function. It was observed that the average energy and energetic efficiency are 28.7 %, 13.2 % for of low radiation days. 26.9%, 20.56% for of medium radiation days, and 23.2%, 18.6% for of high radiation days, respectively. Results of the analysis are shown in detail in the present paper.

JOURNAL OF CONTEMPORARY URBAN AFFAIRS (2017) ***1***(3), 43-48.
https://doi.org/10.25034/ijcua.2018.3678

www.ijcua.com

1. Introduction

In recent years there is a grown interest in the use of renewable energy due to the scarcity of fossil energy reserves and the environmental impact caused by their management. Among renewable energy sources solar energy has been great attention due to the ease of obtaining and high potentiality in the generation of electricity and heat, the use of solar heating systems has increased on the basis of reasonable initial costs and structure relatively simple (Jafarkazemi,and Ahmadifard, 2013). For any application with solar thermal systems solar collectors constitute an important component, their operation is based on the capture of the radiation coming from the sun, converting it to heat and the transfer of this heat to a circulating fluid through the collector . The collected energy is carried by the fluid directly to a process requiring heat or to a thermal energy storage system and subsequently withdrawn for use (Kalogirou, 2004). There are different forms of storing thermal energy, among them are the storage by sensible heat, by the

***Corresponding Author:**
Mechanical Engineering Department, Universidad del Norte, Barranquilla, Colombia
E-mail address: anggier@uninorte.edu.co

thermochemical reaction and by latent heat (Oliver et al., 2010).

The most common forms used are by sensible heat and latent heat. Energy stored in the form of sensible heat requires a large volume of the material used to store, while latent heat storage such as phase change materials (PCM) provides higher storage density and little temperature variation during phase change. Techniques have been investigated to improve the thermal energy storage performance with the use of phase change materials, in addition to improving the heat transfer with the application of fins and to improve the thermal conductivity with the PCM encapsulation (Nkwetta, and Haghighat, 2014). Thermal performance can be assessed based on the first thermodynamics law of (Energy Conservation) or the second thermodynamics law of (Principle exergy).
The work done by (Li, 2015) shows the review of several techniques to improve energy and exergetic performance. In addition, it concludes that the evaluation of the energetic efficiency is not enough to evaluate the thermal behavior of storage. The weakness of thermodynamics first law analysis is it does not take into account the quality of energy degradation when the energy is converted from one form to another or is exchanged between materials and the currents along of heat transfer processes (Kalogirou et al., 2016). In this context, the second thermodynamics law evaluates the quality energy, and the first law focuses on amount energy. Meanwhile, the exergetic analysis uses the mass conservation and energy principles with the second thermodynamics law, for to design and to analyze energetic systems (Kocca et al., 2007).
In a solar system, energy inlet is solar energy, (Petela, 1964) in his works exposed the formulas for to calculate the exergy of thermal radiation. And presented a discussion of the dependence of exergy of fluid and the radiation on the temperature. On the other hand, the investigations presented by (Kalogirou et al., 2016) are based on basic principles of exergy analysis and show a review of the thermal analysis of solar collectors and the processes to involving collectors as an energy source. (Jafarkazemi,and Ahmadifard, 2013). They performed a theoretical model and experimental validation for the energetic and exergetic analysis for flat-plate solar collectors, finding the effect of different design parameters in the efficiencies for to determine the optimum working condition.

The main purpose of this study is to perform an exergetic analysis for a flat-plate solar collector with thermal storage system with phase change material. It was determined the exergetic efficiency and exergy destruction for each system component and its variation as a time function for days of low, medium and high radiation.

2. Method and materials

In this study, experimental setup consists of a latent heat storage system with phase change material (PCM) for a flat-plate solar collector as shown in Figure 1 wherein its components are listed. Commercial paraffin wax is used as PCM; this material is located in metal containers under the absorber plate on the bottom insulation of the collector. Measurement of collector system temperatures was with thermocouples, located in glass cover, absorber plate and inlet and outlet water in the copper pipe. The energy and exergy performance of the system was analyzed during days of low, medium and high radiation taken from October 2016 to March 2017 in Barranquilla Atlántico. Initially, for to do energy and exergy analysis, inlet and outlet parameters to heat transfer of each component of the system was specified. Figure 1 shows heat transfer terms involved in the solar collector.

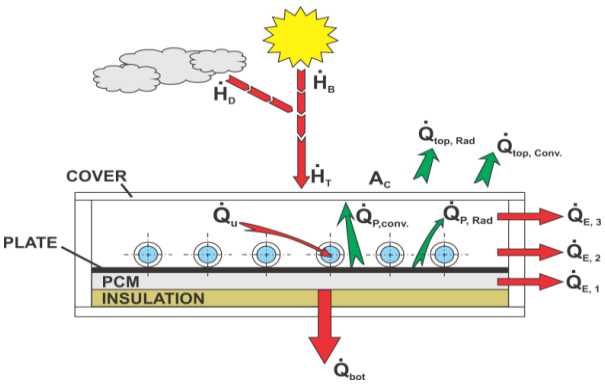

Figure 1. Heat transfer terms involved in solar collector.

The notations and diagrams of the references (Asbik *et al.,* 2016) and (Faramarz Sarhaddi, 2016), was used. In Figure 2. shown the exergy of heat associated with the radiation heat transfer, convection, and conduction in each component of the device. Equations were obtained expressing the exergy destroyed in the glass cover, absorber plate, and the PCM container during charge and discharge of system associates with the heat transfer of exergy equation (Moran and Shapiro, 2004) (1).

$$Ex_q = Q\left(1 - \frac{T_a}{T}\right) \qquad (1)$$

The exergetic efficiency is given by equation (2), which relates the input solar radiation exergy and the exergy transferred to water.

$$n_{Ex} = \frac{Ex_{out}}{Ex_{in}} \qquad (2)$$

In Figure 2. 2a shows that the glass cover absorbs a part of solar exergy and transfers to the environment by convection. 2b. It shows the absorber plate taking into account the charge and discharge processes, during charge process the plate receives solar exergy, transfers by conduction to the PCM and by convection to the water and the glass cover, and during the discharge process receives through the PCM. 2c. It shows the phase change material, during the charge it receives from the absorber plate, during discharge is transferred from the material to the absorber plate to heat the water.

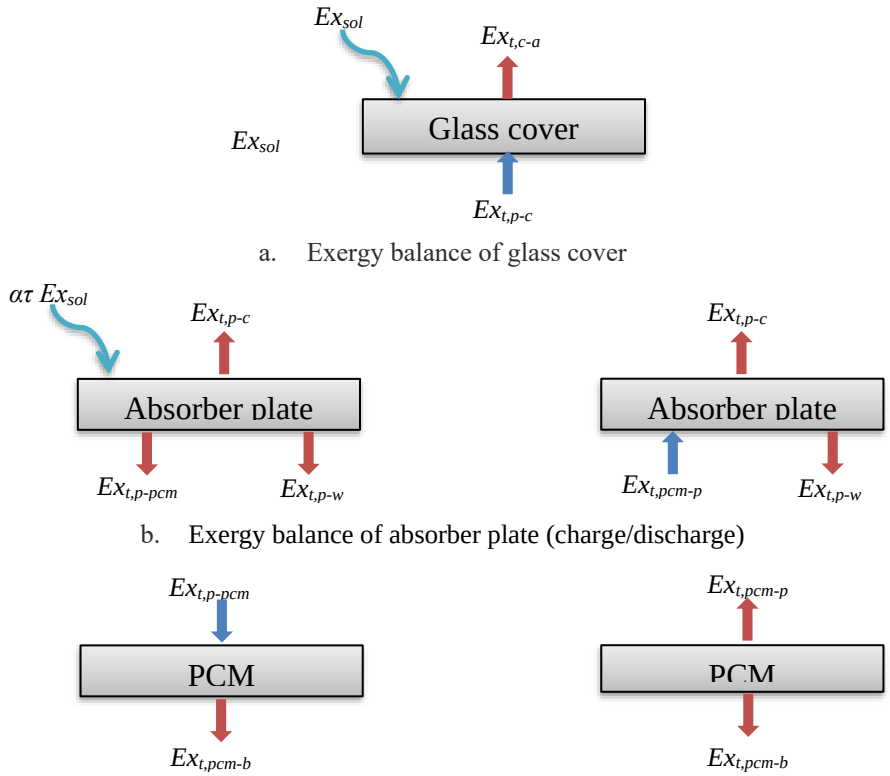

Figure 2. Exergy balance of the solar collector components.

3. Results and discussion

In this section, a comparison the performance of a flat plate solar collector with latent heat storage system with phase change material is carried for days of low, medium and high radiation, for that energetic and exergetic efficiency was calculated. The following figures show solar radiation, stored energy and destroyed exergy for each component and the ambient temperature, water outlet temperature, PCM1 and PCM 2 temperatures. The stored energy for different dates between 8:00 and 20:00 hours for every day is shown in Figure 3. In 3a for the glass cover and 3b for the absorber plate. The results of stored energy show similar variation to the solar radiation during the day.

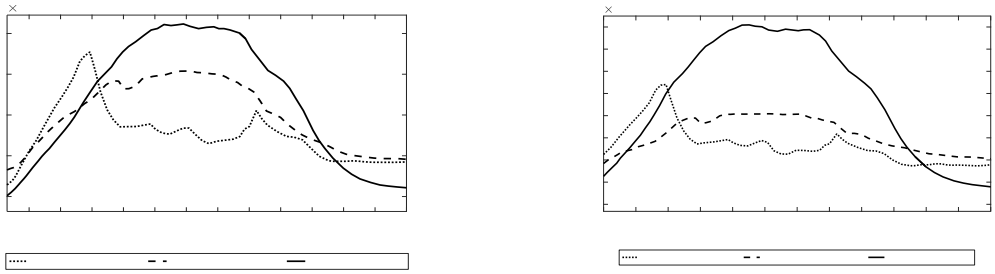

a. Stored energy on glass cover **b.** Stored energy on absorber plate

Figure 3. Stored energy on glass cover and absorber plate.

Another hand, the figures 4a, 5a, 6a show the accumulated radiation during November 28, 2016, December 16, 2016, and February 07, 2017 consecutively. Given that the exergy associate with the heat transfer is depending on temperatures differences between two elements, and understanding the exergy destruction in each component it is necessary to depict the temperature as a function of time for it.

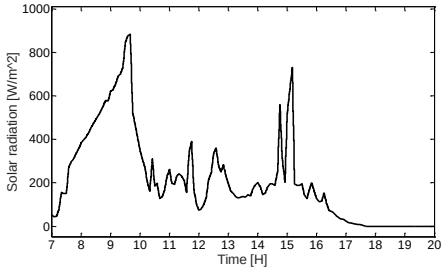

a. Solar radiation for low radiation day

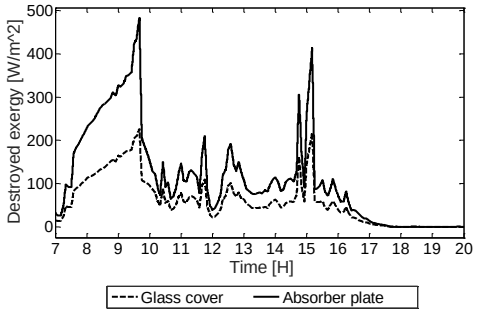

b.Destroyed exergy in glass cover and absorber plate

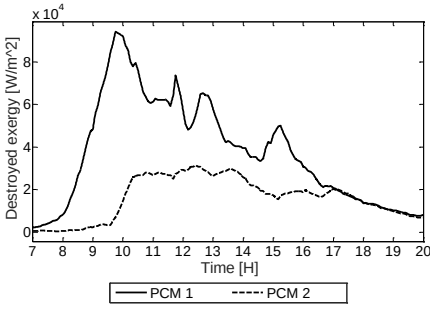

c. Destroyed exergy in PCM1 and PCM 2

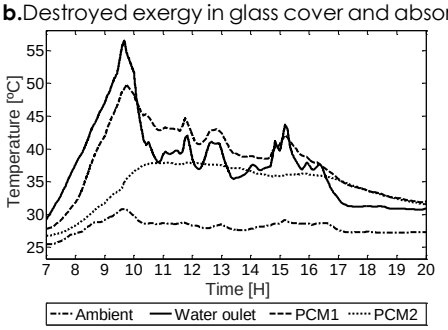

d. Temperatures

Figure 4. Results for November 28, 2016: a. Solar radiation, b. Destroyed exergy in glass cover and absorber plate,c. Destroyed exergy in PCM1 and PCM 2, d. Temperatures

The PCM1 and PCM2 layers temperatures illustrated in figures 4d, 5d, 6d, indicate the behavior of phase change material during everything day. Approximately from 7:00 hours when upsurges temperature of absorber plate, paraffin layers increases the temperature to reach the melting (T=50ºC). In solid state the PCM stores energy as sensible heat and in the liquid phase stores energy as latent heat. As seen in the figures 6d on high solar radiation day, the first and second PCM layers reach the fusion temperature at 12:00 hours when there is more radiation on day. Unlike of low and medium solar radiation days (Figure 4d, 5d) where PCM does not completely melt.

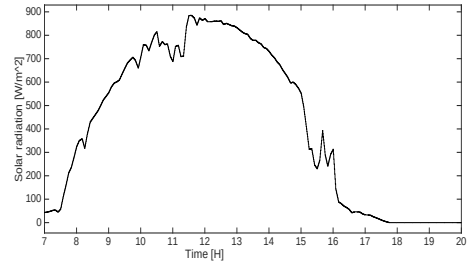

a. Solar radiation for medium radiation day

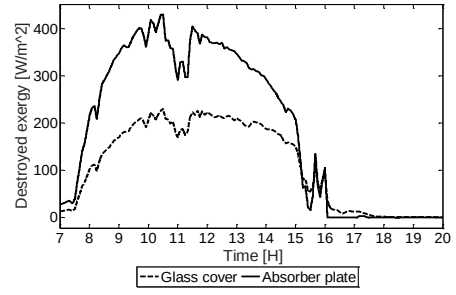

b.Destroyed exergy in glass cover and absorber plate

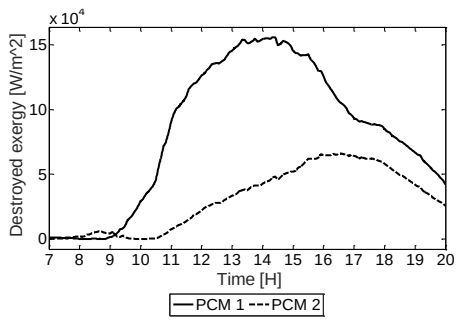

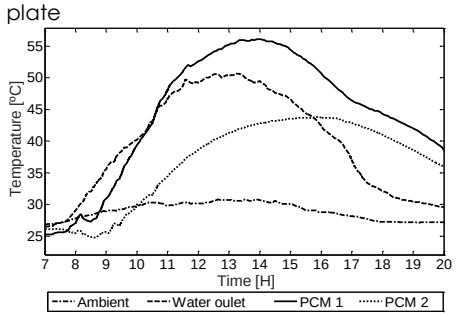

c. Destroyed exergy in PCM1 and PCM 2 **d.** Temperatures

Figure 5. Results for December 16, 2016: a. Solar radiation, b. Destroyed exergy in glass cover and absorber plate,c. Destroyed exergy in PCM1 and PCM 2, d. Temperatures

The destroyed exergy is calculated by the equation (1). As revealed in figure 6c, the exergy destroyed for the PCM is greater when the first PCM layer is in liquid state, during storage latent heat, and for rest of day, irreversibility is created during the charge of material. However at night some of the exergy is destroyed during PCM discharge, that is some of the exergy transmitted to water at night is destroyed. Similarly, for low and medium solar radiation days (Figure 4c, 5c) the destroyed exergy by PCM is greater when it reaches the highest radiation.

Aditional as shown in figures 4b, 5b, 6c the exergy destroyed in the glass cover and absorber plate is superior when there is greater solar radiation. And exergy destruction in absorber plate is greater than in the glass cover because it must transfer heat to water and the PCM during the charge.

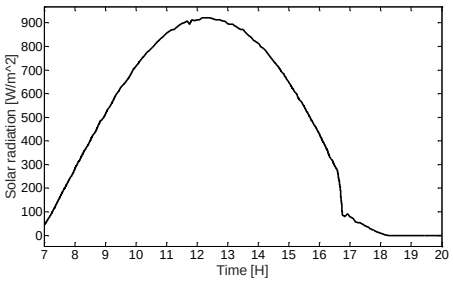

a. Solar radiation for high radiation day

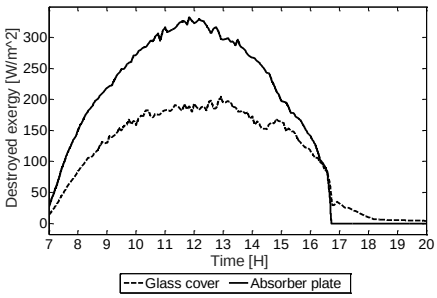

b.Destroyed exergy in glass cover and absorber plate

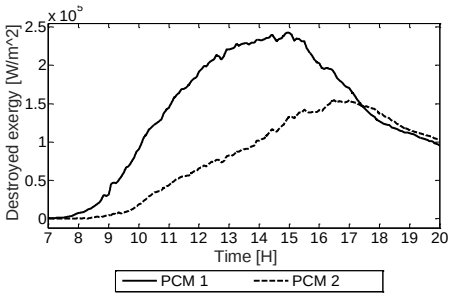

c. Destroyed exergy in PCM1 and PCM 2

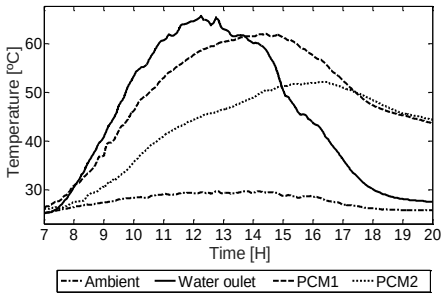

d. Temperatures

Figure 6. Results for February 7, 2017: a. Solar radiation, b. Destroyed exergy in glass cover and absorber plate,c. Destroyed exergy in PCM1 and PCM 2, d. Temperatures

The exergetic efficiency is related to heating of water during the night when the storage heat by paraffin is transmitted during phase change. It is calculated by the equation (2). Owing to low radiation on November 28, the PCM did not reach the fusion temperature and the water outlet temperature after 17:00 hours descended approximately ambient temperature, as seen the figure 1b resulting to an exergetic efficiency of 11.78% for low radiation day. On the contrary, in figure 2d the water outlet temperature during everything day, is greater between 10:00 and 15:00 hours when the radiation is higher. But when the sun hides around at 17:00 hours, the water outlet temperature decreases, but still it remains above ambient temperature. Giving an exergetic efficiency of 20.01% for medium radiation day. On the other hand on March 17 high radiation day, an exergetic efficiency of 28.17% was obtained. Because to heat recovered at night by the PCM was greater, as seen to figure 3d the water outlet temperature is higher than 60°C between at 11:00 and 15:00 hours and stays above during to night.

4. Conclusions

The comparison the performance of a flat plate solar collector with latent heat storage using PCM were performed during charge and discharge period on days of low, medium and high radiation. From that experimental study and calculations, some conclusions are as follows:

- There are more stored energy for each component when the solar radiation is higher
- The results show that destroyed exergy is relevant in absorber plate and PCM medium during the latent heat storage, so it should be

minimalized to increase the performance of the system. Nevertheless, during the latent heat storage, the outlet water temperature is increased.

- According to experimental results and calculations obtained, average exergetic efficiency for low radiation day, medium radiation day, and high radiation days was 13.2 %, 20.56%, and 18.6% respectively. That is, the higher efficiency was for medium radiation days, because the high radiation day more exergy is destroyed on each component.
- As a result low oulet water temperature was obtained for low radiation day, but the oulet temperature for medium and hight radiation day was higher, that is, the PCM storage more energy when the radiation is elevated and during night time,heat is transfered to the absorber plate and the water.

The results show that it is necessary to improve some design parameters to reduce the exergy destruction in the PCM and absorber plate, and increase the exergetic efficiency.

5. Acknowledgments

This investigation has been partially funded by the Colombian Administrative Department of Science, Technology and Innovation-COLCIENCIAS, through the program "es tiempo de volver". Authors wish to express their acknowledgments to COLCIENCIAS and its excellent program.

References

Oliver, A., Neila, F. J., García-Santos ,A.(2010). PCM choosing and classification according to their characteristics for their application for thermal energy storage systems. *Materiales de construccion , 62,* 131-140.

Kocaa,A., Oztop,H.F., Koyun, T., Varol,Y. (2007). Energy and exergy analysis of a latent heat storage system with phase change material for a solar collector. *Renewable Energy ,33*, 567-574.

Nkwetta, D.N., Haghighat,F. (2014). Thermal energy storage with phase change material- A state of the art review. *Sustainable Cities and Society,10*, 87-100.

Jafarkazemi,F., Ahmadifard,E. (2013). Energetic and exergetic evaluation of flat plate solar. *Renewable Energy,56,* 55-63.

Kalogirou,S.A.(2004). Solar thermal collectors and applications. *Progress in Energy and Combustion Science, 30*(3), 231-295.

Li, G. (2015). Energy and exergy performance assessments for latent heat thermal energy storage systems. *Renewable and Sustainable Energy Reviews,15,* 926-954.

Asbik.M., Ansari,O.,Bah,A., Zari,N., Mimet,A.,El-Ghetany,H.(2016). Exergy analysis of solar desalination still combined with heat storage system using phase change material (PCM). *Desalination ,381,* 26-37.

Moran, M. J.,Shapiro, H. N.(Ed.). (2004). *Fundamentals of Engineering Thermodynamics*.(4th ed.) .Barcelona: Reverté, S.A.

Petela, R. (1964). Exergy of Heat Radiation. *J. Heat Transfer,86*(2).187-192.

Jegadheeswaran,S., Pohekar, S.D., Kousksou,T.(2010). Exergy-based performance evaluation of latent heat thermal storage system: A review. *Renewable and Sustainable Energy Reviews ,14*(9),2580-2595.

Kalogirou,S.A., Karellas,S.,Braimakis,K., Stanciu,C., Badescu,V. (2016). Exergy analysis of solar thermal collectors and processes. *Progress in Energy and Combustion Science ,56*, 106-137.

Journal Of Contemporary Urban Affairs

2017, Volume 1, Number 3, pages 49– 53

Membrane Permeability Threshold for Osmotic Power Plant Efficiency

* A. Berger[1], A. Lebrun[2], S. Khan[3], Q. Masson-Pilet[4], A. Supizet[5]

[1, 2, 3, 4, 5] ECE Paris School of Engineering, France

[1]E mail: quentin.masson-pilet@edu.ece.fr

ARTICLEINFO:

Article history:

Received 2 August 2017

Accepted 23 August 2017

Available online 12 October 2017

Keywords:

Osmotic Energy,
Membranes,
Permeability,
Osmotic Pressure.

ABSTRACT

In a context of ever-growing electricity consumption and need for less polluting sources of energy, salinity gradient power (SGP) based on osmosis is a promising technology. Salinity difference between two solutions separated by a semi-permeable membrane leads to the pressure increase. The aim of this study is to find the critical permeability threshold of a membrane for the dimensioning an osmotic power plant. Using Spiegler-Kedem equations, the various fluxes across the membrane have been calculated, and delivered power is explicitly derived in terms of system parameters. A necessary condition for economic viability is that its upper bound is larger than a critical threshold value below which osmotic power plant is not profitable. As it is directly proportional to membrane permeability, fixing the optimal membrane permeability value will in turn enable conceive more efficient membranes specifically made for osmotic energy production, as such membranes do not exist today.

JOURNAL OF CONTEMPORARY URBAN AFFAIRS (2017) ***1***(3), 49-53.

https://doi.org/10.25034/ijcua.2018.3679

www.ijcua.com

1. Introduction

The considerable and very fast growing energy consumption consecutive to the economic development of many countries is acutely raising the question of avoiding disastrous environmental consequences which could inevitably occur if only conventional fossil sources are used. To cope with such situation, a large effort has been oriented toward other sources such as less damaging renewable ones (Lewis, *et al.,* 2011; Kumar, *et al.,* 2011). Aside solar, wind, geothermal and hydraulic sources, they also include other less evident ones which may however represent interesting alternatives in specific situations.

Such is the osmotic power which is the process of converting the pressure differential between water with high salinity and water with lower or no salinity into hydraulic pressure (Loeb, 1975; Mishra, 2013; Kho, 2010; The European Commission, 2004; Helfer, *et al.,* 2013; Skilhagen, *et al.,* 2012; Skilhagen, and Aaberg, 2012). The harnessing of this energy for conversion into power can be accomplished by means of Pressure Retarded Osmosis (PRO) (Kim, and Elimelech, 2013; Helfer, *et al.,* 2014; Wang, *et al.,* 2012). This technique uses a semipermeable membrane to separate a less concentrated solution, or solvent, (for example, fresh water) from a more concentrated and pressurized solution (for example sea water), allowing the solvent to pass to the concentrated solution side (Post, 2009). The additional volume increases the pressure on this side, which can be depressurized by a hydro-turbine to produce power and

***Corresponding Author:**
ECE Paris School of Engineering, France
E-mail address: quentin.masson-pilet@edu.ece.fr

electricity (Kleiterp, 2012) .As seventy percent of Earth surface is covered with water, 97 percent of which is saltwater, the process created by mixing seawater with freshwater generates a resulting osmotic power which could serve as both renewable and consistent electricity source. While still in early stages, best estimates of the global production potential of osmotic power exceed 1,600 terawatt-hours, the equivalent of half of Europe entire energy demand. There are two primary sources for osmotic power: 1) natural occurrence where river water meets the sea water, and 2) merging two man-made water sources from processing plants

Both methods can be viable but in 1), seawater averages 40 grams of salt/ liter + River Water, less power is provided than in than 2), where brine (from desalination) averages 60 grams of salt/ liter + treated water. The higher the salinity, the more free energy can be extracted, and the more power can be generated. Today osmotic power is a promising renewable energy source (RES) provided conversion factor from pressure differential can be made large enough (Dinger, *et al.*, 2012; Brœin, *et al.*, 2010; Straub, *et al.*, 2016). In the following, some elements on this question will be discussed in PRO case. In particular, the threshold value for permeability coefficient which characterizes membrane efficiency for viable economic application is determined.

2. Osmosis Pressure Representation

Potential osmotic pressure π, the maximum osmotic pressure in a solution separated from osmosed fluid by a selectively permeable membrane, is given by

$$\pi = CiRT \qquad (1)$$

with π the potential osmotic pressure (Pa), C the solute molar concentration (mol m^{-3}), R = 8,314 $J.mol^{-1}.K^{-1}$, T solution temperature (°K), and I the particle number per entity. Given the solutions, D and F with respective osmotic pressures π_D and π_F, where D is draw solution (most concentrated), and F feed one (less concentrated), osmotic pressure difference $\Delta\pi = \pi_D - \pi_F$ between the two solutions is typically equal to 12 bars for water fluid, ie, 12.10^5Pa. Let $\Delta P = P_D - P_F$ with P_D and P_F the pressures of solutions D and F. With Spiegler-Kedem [18] model flux equations can be integrated and one gets volume and solute fluxes J_v and J_s flowing through the membrane with pressure retarded osmosis

$$J_v = A(\sigma\Delta\pi - \Delta P) \quad ; \quad J_s = -(1 - E_m)^{-1}(J_v C_d E_m - C_i) \ (2)$$

with J_v , J_s ($m.s^{-1}$) the volume and solute fluxes across the membrane, σ the solute reflection coefficient, A($m.Pa^{-1}$ s^{-1}) the membrane fluid permeability, and $E_m = \exp - [(1 - \sigma) J_v L\omega^{-1}]$ with ω the solute permeability. Similarly in the support one gets

$$J_s = -(1 - E_s)^{-1}(J_v C_i E_s - C_f) \ (3)$$

with C_d, C_i and C_f the solute concentration in the draw solution, at the barrier-layer/support interface, and in the feed solution respectively, and $E_s = \exp - [J_v \delta D_e^{-1}]$ with δ the support thickness. Equality of fluxes in the barrier layer and the support gives from (1,2,3) the non-dimensional equation

$$\alpha\{(1-\sigma)(1-E^{1-\sigma})^{-1} + E^{\rho}(1-E^{\rho})^{-1}\} = (1-r)(1-E^{\rho})^{-1} - \sigma \qquad (4)$$

with $\alpha = 1 - C_i/C_d$, σ the solute reflection coefficient, $r = C_f/C_d$, $\rho = \delta\omega/D_eL$, δ the support thickness, L the barrier layer thickness, D_e the effective diffusion coefficient of the solute, $E = \exp - X$, $X = F(\sigma\alpha - <\Delta P>)$, $F = ARTvC_dL/\omega$, ν the salt stoichiometric coefficient and finally $<\Delta P> = (P_d - P_f)/RTvC_d$. For a given dimensionless hydrostatic-pressure difference $<\Delta P>$, (4) is a transcendental equation in α (dimensionless concentration difference across the barrier layer) which determines the operating conditions of the osmotic plant for a given set of system parameters.

3. Osmotic Power Plant Production

The basic energy production system is composed of a compression unit which delivers pressurized salted water injected in a chamber with a filtering membrane across which a flux of salted water J_s is crossing, see Figure 1.

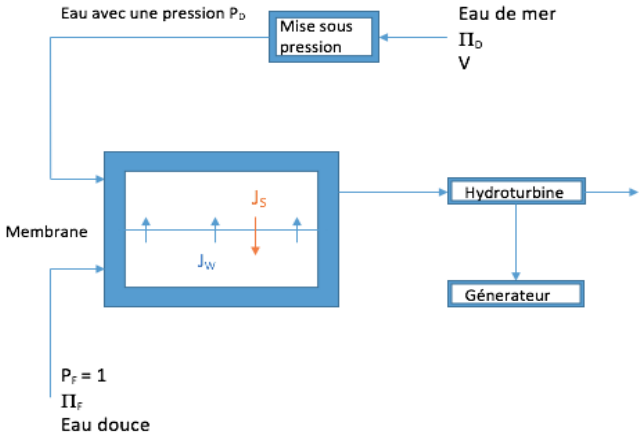

Figure 1. Sketch of Osmotic Plant Balance
J_S is Salt Flux across the Membrane.

The power produced per surface unit of installed membrane is given $W = J_m\Delta P$ with W in Watts/m^{-2}, or else in non-dimensional form

$$<W> = W/A(RTvC_d)^2 = <\Delta P>(\sigma\alpha - <\Delta P>) \qquad (5)$$

<W> is maximum when <ΔP> = σα/2 and is then equal to <W> = $(\sigma\alpha)^2/4$. But this is not necessarily possible as α and <ΔP> are also linked by (4) which imposes a constraint on system coefficients. One effectively gets for z = σα the transcendental equation

$$z\{(1-\sigma)(1-E(z)^{1-\sigma})^{-1} + E(z)^{\rho}(1-E(z)^{\rho})^{-1}\} = \sigma\,(1-r)(1-E(z)^{\rho})^{-1} - \sigma^2 \quad (6)$$

with E(z) = exp−.5Fz which relates "physical" z (concentration performance) to "technical" F (barrier quality). From this different limits can be evaluated for possible power output from the system (Yip, and Elimelech, 2012; Yip, and Elimelech, 2011; Lin *et al.*, 2014). However simple ones are directly obtained from (6) for <W>. In the case of very large ρ for instance, (4) takes the very simple form

$$Y = -(\mathrm{Ln}(1-x))/x \quad (7)$$

where $x = \alpha[1-r((1-\sigma)^{-1}]$ and $Y = \sigma(1-\sigma-r)F/2$. In definition interval $x \in [0,1]$, Y is monotonically increasing from 1 to + ∞, and normalized delivered power $\langle W\rangle = Kx^2$, with $K = \sigma^2/4[1-r((1-\sigma)^{-1}]^2$, varies monotonically between 0 and K, showing that larger <W> corresponds to larger x. More generally parametric dependence of power output W can be obtained from (6) to get best parameter range. When returning to dimensional expression, W is upper bounded by $W_{sup} = KA(RT\nu C_d)^2$, and a necessary condition for economic efficiency is that

$$W_{sup} = KA(RT\nu C_d)^2 \geq W_{crit} \quad (8)$$

where W_{crit} is the threshold value above which the osmotic plant is viable. W_{sup} is larger with larger draw concentration C_d, larger temperature T and larger A, which has to be determined to satisfy economic system efficiency demand, ie here $A \geq A_{crit} = 4W_{crit}\Delta\pi^2$. For usual figure of delivered power $W_d = 5\mathrm{Wm}^{-2}$, and with typical $\Delta\pi = 12.10^5$Pa for water, one gets, for instance, $A \geq A_{crit} = 1.38\ \mathrm{mPa}^{-1}\mathrm{s}^{-1}$. More generally the variation of A_{crit} vs Δπ, sees Figure 2, indicates for $\Delta\pi \in [6.10^5, 20.10^5]$ the "efficiency" interval $A \in [4.910^{-12}, 5.410^{-11}]$ which is still at technical limit today (Straub, *et al.*, 2016; Zhang, and Chung, 2013). To cope with these economic operating constraints, extension of simple osmotic barrier effect have been recently considered (Chou, *et al.*, 2013; Chou, *et al.*, 2012; Yip, *et al*, 2010; Banchik, *et al.*, 2014; Mc Cutcheon, and Elimelech, 2007; Cath, *et al.*, 2013; Chen, *et al.*, 2016; She, *et al.*, 2016 ; Chou, *et al.*, 2013; Hickenbottom, *et al.*, 2016; Dechadilok, and Deen, 2006). A coupled system with solar plant will be discussed elsewhere.

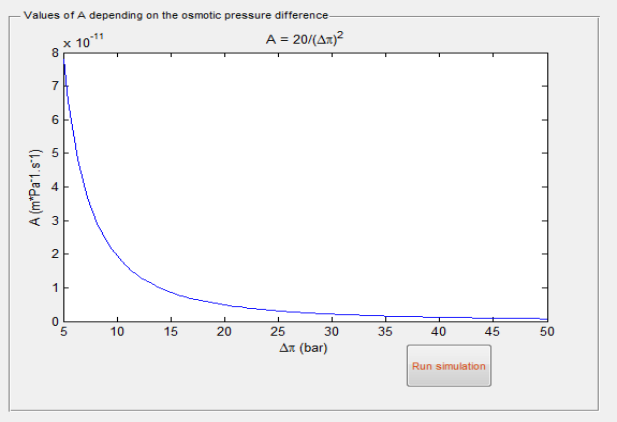

Figure 2 . Permeability Coefficient vs Osmotic Pressure Difference.

4. Conclusion

From analysis of equations representing osmotic physical phenomenon, it is shown that in Pressure Retarded Osmosis case, the harnessing of salinity-gradient energy taking place at the interface between waters of different salt concentration could provide an interesting and almost inexhaustible energy source if systems coefficients satisfy operating conditions which have been explicitly stated within Spiegler-Kedem model. However, even in optimum mode operating case, satisfaction of economic viability condition expressed by fixed specific membrane power output $W_{thres} \cong 5\ \mathrm{Wm}^{-2}$ is not always met. Aside theoretical research on optimizing system operating mode, this weakness is urging further study of membrane physical properties, such as porosity and tortuosity pore length, to design most efficient hydraulic permeability of the barrier layer.

Acknowledgments

The authors are very much indebted to ECE Paris School of Engineering for having provided the necessary setup for the development of the project, to Drs. S. Mouhali for advices during the research and Pr. M. Cotsaftis for help in the preparation of the manuscript.

References

Banchik, L.D., Sharqawy, M.H., Lienhard, J.H. (2014). Limits of Power Production due to Finite Membrane Area in Pressure Retarded Osmosis, J. *Membr. Sci.*, *468*, 81-89.

Brœin, S., Sandvik, Ø.S., Skilhagen, S.E. (2010) .Osmotic Power: from Prototype to Industry–

What Will it Take?, *Proc. 3rd Intern. Conf. on Ocean Energy*, ICOE, Bilbao: Spain.

Cath, T. Y., Elimelech, M., McCutcheon, J. R., Mcginnis, R. L., Achilli, A., Anastasio, D., Brady, A. R., Childress, A. E., Farr, I. V., Hancock, N. T., Lampi, J., Nghiem, L. D., Xie, M. & Yip, N. Yin. (2013). Standard methodology for evaluating membrane performance in osmotically driven membrane processes. *Desalination, 312 (N/A),* 31-38.

Chen, Y., Setiawan, L., Chou, S., Hu, X., Wang, R. (2016). *Identification of Safe and Stable Operation Conditions for Pressure Retarded Osmosis with High-Performance Hollow Fiber Membrane, J. Memb. Sci., 503*, pp.90-100.

Chou, S., Wang, R., Fane, A.G. (2013). *Robust and High-Performance Hollow Fiber Membranes for Energy Harvesting from Salinity Gradients by Pressure Retarded Osmosis. J. Memb. Sci., 448*, 44-54.

Chou, S., Wang, R., Shi, L., She, Q., Tang, C., Fane, A.G. (2012) .Thin-film Composite Hollow Fiber Membranes for Pressure Retarded Osmosis (PRO) Process with High Power Density, *J Membrane Sci,, 389*, 25-33.

Dechadilok, P., Deen, W.M. (2006). *Hindrance Factors for Diffusion and Convection in Pores, Ind. Eng. Chem. Res., 45, 6953–6959*.

Dinger, F., Troendle, T., Platt, U. (2012) . Osmotic Power Plants, *3rd Osmosis Membrane Summit*, Statkraft, Barcelona: Spain

Helfer, F., Sahin, O., Lemckert, C., Anissimov, Y. (2013). Salinity Gradient Energy: a New Source of Renewable Energy for Australia. *Proc. Intern. Conf. of the European Water Resources Association* (EWRA), Porto: Portugal.

Helfer, F., Lemckert, C., Anissimov, Y.G. (2014) . Osmotic Power with Pressure Retarded Osmosis: Theory, Performance, and Trends, *J. Membranes Science*, 453, 337-358.

Hickenbottom, K.L., Vanneste, J., Elimelech, M.A., Cath, T.Y. (2016). *Assessing the Current State of Commercially Available Membranes and Spacers for Energy Production with Pressure Retarded Osmosis, Desalination*, *389*, 108-118.

Kho, J. (2010) .*Osmotic Power: A Primer*. San Francisco, USA: Kachan & Co.

Kim, Y.C., Elimelech, M. (2013). Potential of Osmotic Power Generation by Pressure Retarded Osmosis Using Seawater as Feed Solution: Analysis and Experiments, *J Membrane Sci*, *429*, 330-337

Kleiterp, R. (2012). *The Feasibility of a Commercial Osmotic Power Plant*, Master Thesis, Dept of Hydraulic Engineering, Delft University of Technology, Delft:Netherlands.

Kumar, A., Schei, T., Ahenkorah, A., Rodriguez, R.C., Devernay, J.M., Freitas, M., Hall, D., Killingtveit, Å., Liu, Z. (2011). Hydropower, in: Edenhofer, O., Pichs-Madruga, R., Sokona, Y., Seyboth, K., Matschoss, P., Kadner, S., Zwickel, T., Eickemeier, P., Hansen, G., Schlömer, S., Stechow C. (Eds.). *IPCC Special Report on Renewable Energy Sources and Climate Change Mitigation.* Cambridge and New York, UK &USA: Cambridge Univ. Press.

Lewis, A., Estefen, S., Huckerby, J., Musial, W., Pontes, T., Torres-Martinez, J. (2011). Ocean Energy, in: Edenhofer, O., Pichs-Madruga, R., Sokona, Y., Seyboth, K., Matschoss, P., Kadner, S., Zwickel, T., Eickemeier, P., Hansen, G., Schlömer, S., Stechow C. (Eds.). *IPCC Special Report on Renewable Energy Sources and Climate Change Mitigation*. Cambridge and New York, UK & USA: Cambridge Univ. Press.

Lin, S.H., Straub, A.P., Elimelech, M. (2014). Thermodynamic Limits of Extractable Energy by Pressure Retarded Osmosis, *Energy Environ. Sci., 7*, pp.2706-2714.

Loeb, S. (1975). Osmotic Power Plants, *Science*, *189*, 654-655.

Mc Cutcheon, J.R., Elimelech, M.A. (2007) . *Modeling Water Flux in Forward Osmosis: Implications for Improved Membrane Design, AIChE J., 53*, 1736-1744.

Mishra A. (2013). Osmotic Power–Huge Source of Renewable Energy, *Int J Sci Eng Res*, *4*, 1-6.

Post, J.W. (2009) . *Blue Energy: Electricity Production from Salinity Gradients by Reverse Electro-dialysis*, PhD thesis, Sub-dept of Environmental Technology, Wageningen University, Wageningen: Netherlands.

She, Q., Wei, J., Ma, N., Sim, V., Fane, A. Rong, G., Wang, R., Tang, C.Y. (2016). *Fabrication and Characterization of Fabric-reinforced Pressure Retarded Osmosis Membranes for Osmotic Power Harvesting, J. Memb. Sci., 504*, 75-88.

Skilhagen, S.E., Dugstad, J.E., Aaberg R.J. (2012). Osmotic Power - Power Production Based on the Osmotic Pressure Difference between Waters with Varying Salt Gradients, *Desalination*, *220*, 476-482.

Skilhagen, S.E., Aaberg R.J. (2006) . Power Production Based on the Osmotic Pressure Difference between Fresh Water and Sea Water, *European Seminar on Offshore Wind and Other Marine Renewable Energies in*

Mediterranean and European Seas (Owemes), Owemes, Citavecchia: Italy.

Straub, A.P., Deshmukh, A., Elimelech, M. (2016). Pressure-retarded Osmosis for Power Generation from Salinity Gradients: is it Viable? *Energy Environ. Sci*., *9*, 31–48.

Spiegler, K.S., Kedem, O. (1966): *Thermodynamics of Hyper-filtration (Reverse Osmosis): Criteria for Efficient Membranes, Desalination*, *And 1,311*-326.

The Salinity Project Group, The Salinity Power Project: Power Production from the Osmotic Pressure Difference between Fresh Water and Sea Water - Final Report, (2004). The European Commission, Bruxelles, Lisbon.

Wang, R., Tang, C., Fane, A.G. (2012). Development of Pressure Retarded Osmosis (PRO) Membranes with High Power Density for Osmotic Power Harvesting, in: *3rd Osmosis Membrane Summit*, Statkraft, and Barcelona: Spain.

Yip, N.Y., Tiraferri, A., Phillip, W.A., Schiffman, J.D., Elimelech, M. (2010) . High-Performance Thin-film Composite forward Osmosis Membranes, *Environ Sci Technol*, *44*, 3812-3818.

Yip, N.Y., Elimelech, M. (2012). Thermodynamic and Energy Efficiency Analysis of Power Generation from Natural Salinity Gradients by Pressure Retarded Osmosis, *Environ. Sci. Technol*., *46*, 5230-5239.

Yip, N.Y., Elimelech, M. (2011). Performance Limiting Effects in Power Generation from Salinity Gradients by Pressure Retarded Osmosis, *Environ Sci Technol*, *45*, 10273-10282.

Zhang, S., Chung, T.S. (2013). *Minimizing the Instant and Accumulative Effects of Salt Permeability to Sustain Ultrahigh Osmotic Power Density, Environ. Sci. Technol.*, *47*, 10085-10092.

Journal Of Contemporary Urban Affairs

2017, Volume 1, Number 3, pages 54– 61

A Simple Heliodon System for Horizontal Placed Models

* Dr. **Maged G., Mikhael** [1], Mr. **Mostafa, Metwaly** [2]

[2] Canadian International College (CIC), Egypt

[1]E mail: maged_george@cic-cairo.com ,E mail: mostafa_metwaly@cic-cairo.com

ARTICLEINFO:

Article history:

Received 2 August 2017

Accepted 23 August 2017

Available online 12 October 2017

Keywords:

Heliodon;

Solar path tracking;

Sun's position;

Daylight.

ABSTRACT

Most probably, all our buildings are affected by sunlight. Hence, the ignorance of the sun's impact results in overheating, glare, and missed opportunities for the positive use of daylight, leading to wasted energy. Heliodon is considered to be a powerful tool that can aid students, professionals, building developers and users to better understand the relationship between the sun's path and its effects on the architectural model(s). Most of the heliodons are relatively expensive and complex in operation. Thus, the need to design and build a simple and relatively inexpensive one emerged. It was proposed to work on this heliodon as a team project in the environmental control class "fall-2016". The authors put the design concept and introduced a mathematical calculations table to be used with the physical heliodon, while nine students participated in the manufacturing process. The design concept is based on determining the sun's position by converting the Altitude and Azimuth angels to their corresponding measurements on the (X, Y & Z) coordinates (in relation to the observer's location). One light source can be moved on a set of graded tubes assembled in the shape of a wire frame box (thus the X, Y & Z distances could be measured) to simulate the sun's position and its lighting conditions for any latitude, at any time for any chosen day.

JOURNAL OF CONTEMPORARY URBAN AFFAIRS (2017) ***1***(3), 54-61.

https://doi.org/10.25034/ijcua.2018.3680

www.ijcua.com

1. Introduction

1. Nearly, 40% of the energy produced worldwide is consumed by buildings; this is equivalent to 2500 Mtoe "*million ton oil equivalents*" per one year (Attmann, 2010). In Egypt, 52% of the produced electricity is consumed only by the residential buildings, while 90% of the electric power plants depend on non-renewable energy resources to operate (URL4)(www.moee.gov.eg). Thus, buildings are considered to be one of the main causes of climate change.

Studying the sun's impact on buildings is the first step on the long way of solar-responsive design, where the most important goals are:

- The maximum harvesting of winter sun
- The optimum control of summer sun
- The benefits of the natural daylighting "The natural daylight that a 0.9m × 1.5m window can provide is equivalent to 100 – 60W incandescent lamps" (Lechner, 2008).

Hence, the comprehensive understanding of solar geometry and its consequences is necessary for a successful architectural design.

***Corresponding Author:**
Canadian International College (CIC), Egypt
E-mail address: maged_george@cic-cairo.com

Starting from the very early model made by Dufton-Bachett in 1931, passing by that one developed by George Malcolm Beal in 1953 (Beal, 1957), and till the most recent models of Lechner 2001 and his successors, heliodons have been considered one of the most powerful tools that can aid students, professionals, building developers and users to better understand the relationship between a building and the sun (Lechner, 2001).

Since heliodons have been developed mainly to study the effect of the sunlight on a given building(s) model, three main variables are always the dominant constraints for any heliodon design concept, these variables are:

- Latitude determines the relation between the sun's path and the geographical location on the earth's surface.
- Day of the year: specifies the declination of the sun on a specific day.
- Time of the day: determines the sun's position between the east and the west (Cheung, 2000).

These three variables guide the researcher to obtain two angels that help to allocate the sun's position (Figure 1). These two angels are:

- Altitude (ALT): Measured upwards from the horizon where the observer's location is at the center of the skydome.

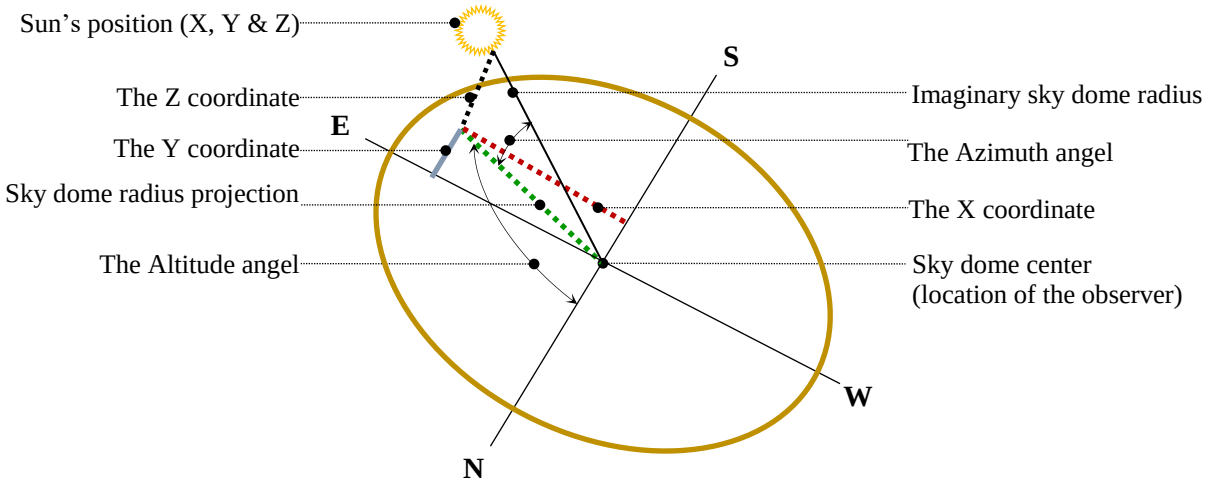

Figure 1. Converting the sun's position parameters from the angels - Altitude & Azimuth - system to the coordinates - X, Y & Z – system.

- Azimuth (AZI): measured in the horizontal plane from north or south (Szokolay, 2008).

Heliodon designs could be classified into two groups, depending on the positions of both of the light source and the building model:

- Tilted / moving building model while the light source (s) is either fixed or moving.
- Fixed (horizontal) building model while the light source is moving (Cheung, 2011).

A quick glance on both of the two types declares that the first type has significant disadvantages: Holding the model in steep angels may result in difficulty in viewing or causing it to slide out of position. Furthermore, it doesn't simulate our everyday experience of the sun moving across the skydome. Meanwhile, the fixed building model types are complicated to manufacture and operate, relatively large (for more accuracy) thus, require larger space during operation and / or storage (most of them), and to somehow more expensive (URL3) (www.heliodon.org).

2. The Need for This Heliodon

Our target in the environmental control class was to encourage the students to build their own heliodon, taking into consideration that it should be easy to understand, can be constructed inside the CIC campus with simple tools, requires a relatively small space during both operation and storage and relatively inexpensive. To achieve the previous goals, the fixed building model type was selected; the concept of converting both of the Altitude and the Azimuth angels to their corresponding (X, Y & Z) coordinates (Figure 1) "with a moving single light source to simulate the sun's position" was chosen. The UPVC pipes and connections were proposed as a construction material for the heliodon, "relatively rigid and cheap", while the 5cm thick rigid foam and 5mm thick white

cardboard were the materials for the base. Design concept and calculations, supervision and the orientation of the manufacturing process were the authors' tasks, while the construction was accomplished by a group of nine students.

3. Solar Position Calculations

The authors relied on external software "SunPosition" to determine the ALT & AZI angels of the sun's position for any latitude, on any day of the year and at any time of the day. Also, to generate the necessary input data to build a calculations table that will be used in the design and manufacturing process of the heliodon(URL5)(www.susdesign.com/sunposition).

The main function of the calculations table is to change the parameters of the sun's position from the "ALT and AZI angles system" to the coordinates system through a series of equations. The "SunPosition" software was chosen for two main reasons:

- It is comprehensive software, but yet, with an easy interface for students' interaction.
- It is open-source software, which can be accessed online easily and freely by students.

3.1The Calculations Table

The authors designed an excel spreadsheet - linked to the "SunPosition" output data file - to generate the main calculations table that will help the students to determine all the needed data and measurements to construct and operate their heliodon. The table was designed with two groups of data as follows:

- **The input data group (Table 1-a):**

Latitude & Longitude: measured in degrees and generated automatically based on the value that was entered manually by the student on the "SunPosition" software to define the exact location for calculation.

Time zone: measured in hours and generated automatically based on the value that was entered manually by the student to the "SunPosition" to define the exact location for calculation.

Date of the day: a unit-less pre-set data, its values represent a predefined range of days for tracking the solar path over the year with one-day interval (1st. of Jan. – 31st. of Dec.).

Time of the day: a pre-set data, measured in hours, its values represent a predefined range of 13 hours for tracking the solar path over the day with one-hour interval (06 – 18).

Zero azimuth direction (North or South): choosing North (N) or South (S) as the zero Azimuth direction (ZAD) is generated automatically based on the selection that was previously entered manually by the student on the "SunPosition", and it is set to the following rule: if the North is the zero Azimuth direction then its value = 1 and the South value = 0, and vice versa.

Original Altitude & Azimuth angles: can be obtained from the "SunPosition" in correspondence with a pre-set time value; it is measured in degrees and entered manually by the student to the calculations table.

- **The output data group (Table 1-b):**

Absolute Azimuth angel: measured in degrees and generated automatically based on the input value of the original Azimuth angle "regardless the zero Azimuth direction".

The correction factor for the Azimuth angel: measured in degrees and generated automatically, its value is either (0 or 180) based on the input value of the Zero Azimuth Direction (180 in case of the ZADN=1 and 0 in case of the ZADS =1).

Corrected Azimuth angle: measured in degrees and generated automatically based on the input value of the zero Azimuth direction (N or S), the output value of the Azimuth angle correction factor and the output value of the absolute angle.

Skydome radius: a pre-set data that is measured in centimeters; its value represents the maximum allowable movement distance of the light source in any direction starting from the heliodon's origin point (Observer's point).

The distances on the (Z) coordinate: measured in centimeters; it is generated automatically based on the output values of the Altitude angle / Sine and the pre-set value of the skydome radius.

The Z Coordinate movement direction: measured in (+) only.

The distances on the (Y) coordinate: measured in centimeters, and is generated automatically based on the values of skydome radius projection on the horizontal plane and the Azimuth angle cosine.

The Y coordinate movement direction: measured either in (+) or in (-); its values are generated automatically based on the output values of Y coordinate distance, the input values of ZAD (N or S) in addition to the output values of absolute Azimuth angel.

The distances on the X Coordinate: measured in centimeters; it is generated automatically based on the output values of skydome radius projection in addition to the output values of the distance of Y coordinate.

The X coordinate movement direction: measured either in (+) or in (-); its values are generated automatically based on the output values of the distance on the X coordinate, the pre-set values of time, the input values of the ZAD (N or S) in addition to the input value of the original Azimuth angle.

4.1VALIDATION OF THE CALCULATIONS TABLE OUTPUT

To validate the output data that was obtained from the calculations table "for specific latitude and a certain time of a certain day" it was important to compare it with a reference data for the same variables. The latitude of 30.04 N (Cairo – Egypt) was chosen and the hours from (6 – 18) for the longest and shortest days of the year (21st. of June and 21st. of December) were selected for the validation. The output data results "the measuring distances on the X, Y and Z coordinates" for Cairo – Egypt at the selected hours on the chosen days were exported to "Grasshopper"software(URL2)(http://www.grasshopper3d.com/) to generate the corresponding solar path diagrams. When the solar path diagrams generated by "Grasshopper" were compared to those generated by reference software "Sun- Path Projections" for the same variables the results were identical (Figure 2).

Table 1-a. Sample of the input data group (The 21st. June & the 21st. December at noon time)

Variables	Latitude	Longitude	Time Zone	Date - Month	Time	Zero Azimuth Direction		Altitude Angle	Azimuth Angle
						North	South	Original	Original
						"1" = Yes	"1" = Yes		
						"0" = No	"0" = No		
Data Type	Input (↕)	Input (↕)	Input (↕)	Pre-set	Pre-set	Input (↕)	Input (↕)	Input (↓)	Input (↓)
Units	"Degrees"	"Degrees"	"Hours"	"---"	"Hours"	"---"	"---"	"Degrees"	"Degrees"
Values	30.0444 N	31.2357 E	GMT 2	21-Jun	12:00	0	1	083.360	006.260
Values	30.0444 N	31.2357 E	GMT 2	21-Dec	12:00	0	1	036.490	001.950

Table 1-b. Sample of the output data group (The 21st. June & the 21st. December at noon time)

Azimuth Angle			Sky Dome Radius	"Z" Coordinate		Sky Dome Radius Projection	"Y" Coordinate		"X" Coordinate	
Absolute	Correction Factor "0" / "180"	Corrected	Hyp. 01	Rate Opp. 01	Direction	Adj. 01 Hyp. 02	Rate Adj. 02	Direction	Rate Opp. 02	Direction
Output (↑)	Output (↑)	Output (↑)	Pre-set	Output (↑)	Output (↑)	Output (↑)	Output (↑)	Output (↑)	Output (↑)	Output (↑)
"Degrees"	"Degrees"	"Degrees"	"cm"	"cm"	"+"	"cm"	"cm"	"+" / "-"	"cm"	"+" / "-"
006.260	0	006.260	100	099	+	012	011	-	001	-
001.950	0	001.950	100	059	+	080	080	-	003	-

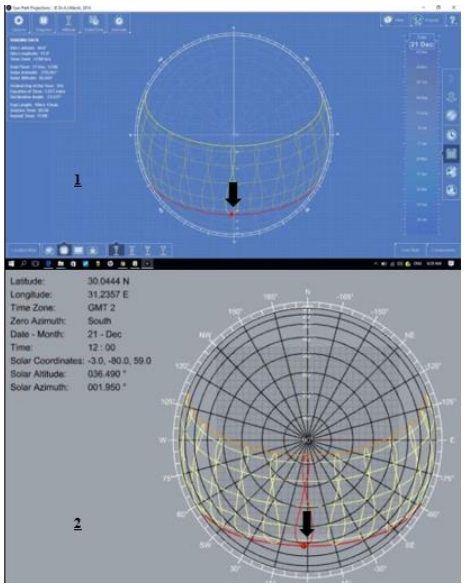

Figure 2. Output data of (Sun-Path Projections - 1 & Grasshopper - 2) at noon time, 21st. December for Cairo – Egypt

4. Heliodon Construction

For the purpose of learning in the environmental control Lab., the skydome radius was selected to be 100cm "this could be greater or smaller according to the available space, the required accuracy and the scale of the model(s) under-study".

The UPVC pipes were cut and assembled "with connections" to construct a wireframe like box "a bit larger to allow the light source to move 100cm in the three coordinates" as shown (Figure 3 & 7). The (Pz1, Pz2, Pz3 & Pz4) pipes were graded (0 to 100cm) "using a sticker measuring tape" to illustrate the measuring units on the Z coordinate, (Px1 & Px2) pipes were graded from their midpoints (0 to 100cm & 0 to -100cm) to illustrate the measuring units (+ & -) on the X coordinate and finally (Py) pipe was graded from its midpoint (0 to 100cm & 0 to -100cm) to illustrate the measuring units (+ & -) on the Y coordinate. Bolts (B1, B2, B3 and B4) can be

loosened to allow (Px1and Px2) pipes to move freely up and down on the (Pz1, Pz2, Pz3 and Pz4) pipes or can be tightened to fix them in the required Z coordinate position (Figure 4). Bolts (B5 and B6) can be loosened allowing the (Py) Pipe to move feely to the right or to the left on (Px1 and Px2) pipes

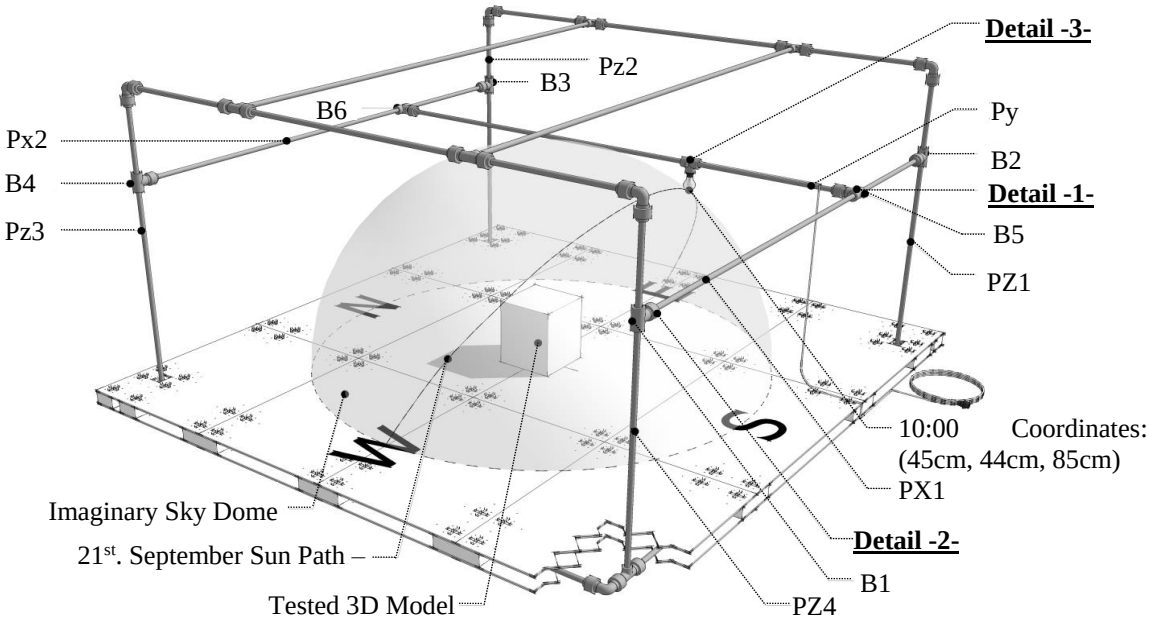

Figure 3. The proposed heliodon illustrates the effect of the sunlight on a building model .

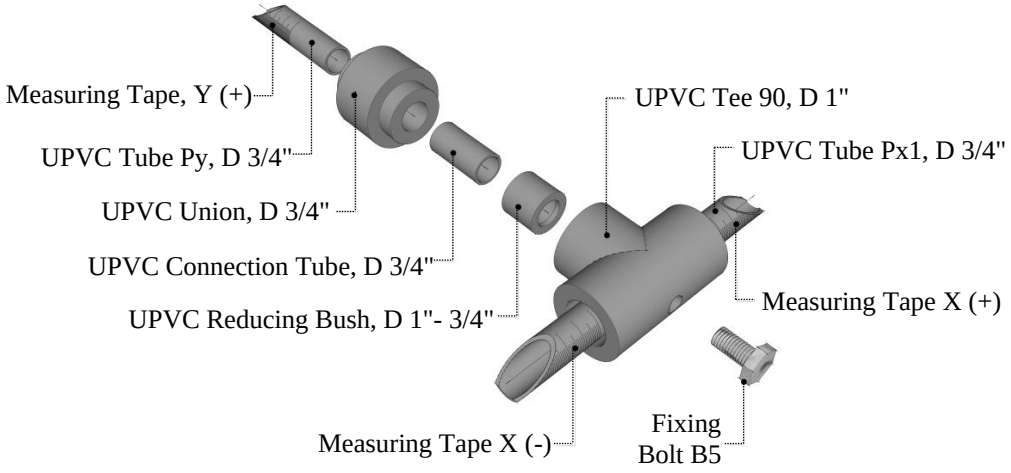

"21st. September at 10:00, Cairo-Egypt"

Figure 4. Detail 1.

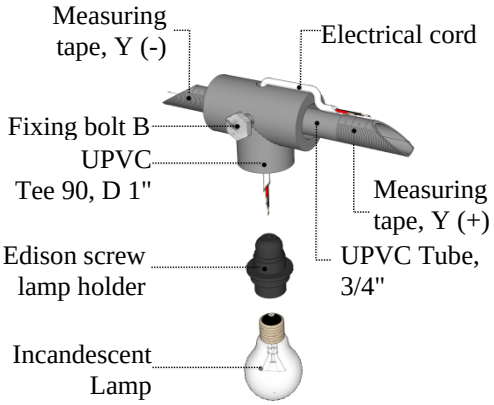

Figure 5. Detail -2-

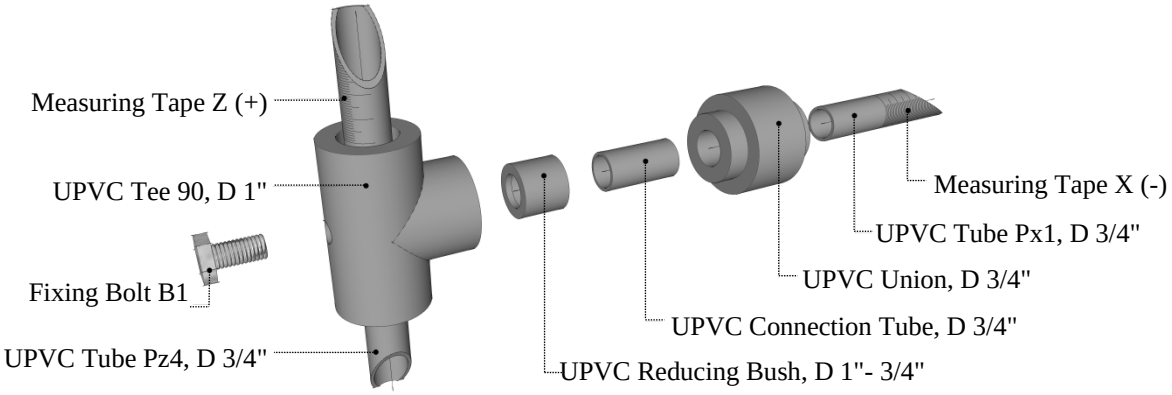

Figure 6. Detail 3.

or can be tightened to fix it in the required X coordinate position (Figure 5). A (100W) incandescent lamp was used as a light source to simulate the sunlight rays and it can move back and forth on the (Py) Pipe to reach the required Y coordinate position and simulate the sun's position (Figure 6). The base was made of 5cm thick rigid foam between two layers of "100cm × 70cm × 5mm" cardboard sheets.

Figure 7. The students during the manufacturing and assembling of the heliodon

4.2Operation of the Heliodon

After the installation process "previously described" the student can follow the next steps to track the solar path and study the effect of the sun light on his building model:

- Prepare the building model and put it in the origin point of the heliodon (the model should be oriented with respect to the four cardinal directions).
- Determine the latitude of the building, date of the day and the time of the selected day.
- Use the previous constrains as input data in the "SunPosition" software (or any similar software) to generate the corresponding Altitude and Altitude angels.
- Use all the predetermined constrains and the generated angles as input data in the designed calculations table to generate the corresponding measuring distances on the X, Y and Z coordinates.
- Adjust the position of the light source according to the generated measures on
- the heliodon.

- Plug in the electrical cable, turn on the lamp and observe the effect of the light on the model (Figure 8).
- After completing the study turn of the lamp and unplug the electrical cable.
- In case of storage for long periods, disassemble the heliodon parts and store it.

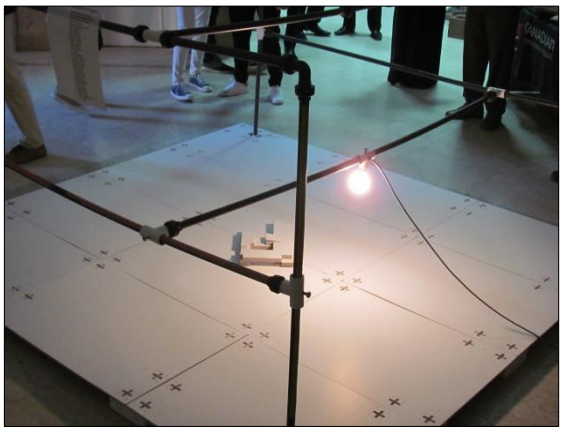

Figure 8. Using the heliodon to test the effect of sunlight on a building model

5. Conclusion

The main target of this work was to encourage the students in the environmental control class to participate in the design and the manufacturing of their own heliodon, hence their awareness of both of the solar geometry and the solar-responsive design could be enhanced. The concept of this heliodon is relatively simple as it depends on the determination of the relationship between the sun's position and its corresponding X, Y and Z coordinates related to the observer's location on the earth's surface. Relying on external software "SunPosition" was necessary to generate both of the Azimuth and Altitude angels for any location on the earth's surface and at any time for any chosen day.

The designed calculations table played a vital role during both of the manufacturing and operation processes.

The Excel sheet that was designed to form the calculations table relied on the output data of the "SunPosition" (Azimuth and Altitude angels) along with the assumption of the sky dome radius to generate the corresponding X, Y, and Z measuring distances on the heliodon. The output data of the calculations table were compared to external reference software - Sun-Path Projections - and the results were identical. Thus the design concept could be verified.

The proposed heliodon was successfully constructed according to the assumed measurements in the calculations table, and the students could use it effectively to study the effect of the sunlight on their building model(s). This heliodon could be designed and constructed with different scales according to the required accuracy; the available space and budget, and can be disassembled and stored in small space for future use.

Tuning & Future Work

We aim to reconstruct this heliodon system with more durable material (stainless steel pipes), more efficient bracing system and a LED light source instead of the incandescent lamp to give more parallel light rays, thus, a more realistic sunlight simulation. Also, we hope we can make a fruitful collaboration with other engineering specializations to make the system fully operated and controlled by a commuter system.

Acknowledgement

We would like to give special thanks to our diligent students who participated in the construction process: Andrew Ghettany, Mahmoud El-Zayaty, Mohamed Wahba, Mohamed Ezz El-Dein, Mohamed Essam, Mostafa Helal, Omar El-Shahawai, Omar Abd El-Gawad and Ziad Hassan.

Also we would like to thank those so special students of the environmental control class "Cohort-2014", a list of their names could be found on the following link: (URL1)(https://drive.google.com/open?id=0B-bNxtEORp3VTUdWVXlaYldLdVk).

References

Attmann, O. (2010). Green Architecture: Advanced Technologies and Materials. *McGraw-Hill Professional*, 11-13.

Beal,G.M.(1957). Natural Light and the Inside-Outside Heliodon, University of Kansas publications. *the bulletin of engineering and architecture*, 38, 12-13.

Cheung, K.P. (2000). A Multi-Lamp Heliodon for Architectural Schools, *International Journal of Architectural Science*, *1*(1), 46-58.

Cheung, K.P. (2011). A Discussion on the Design Principles of a Patented Portable Direct Sunlight Light-Duty Universal Heliodon Mounted on a Camera Tripod. *International Journal of Architectural Science*, *8*(4), 98-113.

Lechner, N. (2001). The Sun Emulator: A Conceptually Clear Heliodon. *Proceedings*

of the ASCA "Association Colligate Schools of Architecture" Technology conference, 116-118.

Lechner, N. (2008). Heating, Cooling, Lighting: Sustainable Design Methods for Architects, 3rd. Ed., NY, USA, John Wiley & Sons,.404.

Szokolay, S.V. (2008). Introduction to Architectural Science: The basis of Sustainable Design, 2nd. Ed., Elsevier, USA, 22-24.

URL1
https://drive.google.com/open?id=0B-bNxtEORp3VTUdWVXlaYldLdVk

URL2
http://www.grasshopper3d.com/

URL3
http://www.heliodon.org

URL4
http://www.moee.gov.eg/english_new/EEHC_Rep/2014-2015en.pdf (pp.18 & pp.43)

URL5
http://www.susdesign.com/sunposition/index.php

Journal Of Contemporary Urban Affairs

2017, Volume 1, Number 3, pages 62– 65

Evaluation Rainfall Regime at the Hydroelectric Power Plant toward Climate Change

* [1] **Francisco Pereira,** [2] **Elison Eduardo Bierhals;** [3] **José Leandro Néris,** [4] **Matheus Rippel,** [5] **Claudinéia Brazil,** [6] **Luciane Salvi,** [7] **Nei Marçal**

[1, 2, 5] Energy Engineering, State University of Rio Grande do Sul, Brazil

[3,4,5,6] Environmental and Sanitary Engineering, Don Bosco College of Porto Alegre, Brazil

E mail: fbp.francisco@gmail.com , E mail: eduardojb_energia@hotmail.com , [3] E mail: matheuslrippel@gmail.com

[4] E mail: leandro_melgar@hotmail.com , [5] E mail: neiabrazil@yahoo.com , [6] E mail: salvi.faculdade@dombosco.net

[7] Email: marcaluergs@gmail.com

ARTICLEINFO:

Article history:

Received 2 August 2017

Accepted 10 August 2017

Available online 12 October 2017

Keywords:

Climate Change;

IPCC-AR5;

Precipitation.

ABSTRACT

The hydroelectric plants are first in the Brazilian energy matrix, so irregularities in the rainfall regime can affect the energy generation, thus evidencing the need to know the rainfall distribution in the studied area. This work aimed to evaluate possible analysis of the impacts of climate change on the rainfall regime in the Machadinho hydroelectric region. For the research development, the IPCC-AR5 pessimistic scenario was used, representing a scenario with a continuous population growth and high carbon dioxide emissions. From the historical series and organized projections, precipitation anomalies were calculated. Analyzing the difference between the average of the month and the climatological normal, it was inferred that the model used presented a positive trend for precipitation in the period from 2026 - 2100, projecting anomalies between 25 and 200 mm per month. A greater amplitude is observed in the precipitation of 2076-2100, indicating an increase in the occurrence of extreme events of precipitation, mainly in the spring period. Considering that the rains in the Machadinho hydroelectric region are increasing in the scenarios analyzed, the average water level in the reservoir of the plant tends to increase.

JOURNAL OF CONTEMPORARY URBAN AFFAIRS (2017) ***1***(3), 62-65.

https://doi.org/10.25034/ijcua.2018.3682

www.ijcua.com

1. Introduction

The global concern about climate change has been increasing, since the emission of gases from human activities contributes to the greenhouse effect in the atmosphere, indicating significant impacts to the planet in the coming years. The changes have been associated with the issue of energy, especially renewable energies, which are directly linked to climate variations. According to Moraes (2013) in 1988, the Intergovernmental Panel on Climate Change (IPCC) was created through an initiative of the World Meteorological Organization (WMO) and the United Nations Environment Program (UNEP). The IPCC was established with the mission of evaluating research, interpreting it, and gathering all relevant information, both technical, scientific and socioeconomic, into comprehensive, easily understood and accessible reports by all in communities,

***Corresponding Author:**
Energy Engineering, State University of Rio Grande do Sul, Brazil
E-mail address: fbp.francisco@gmail.com

including decision makers (Grimm , 2016; Moraes, 2013). According to Nimer (1989), rainfall occurred in Brazil's southern region between 1990 and 2005 can be described as well distributed, with maxima ranging from 1200 to 2100 mm / year.

The hydroelectric plants are in the first position in the Brazilian energy matrix, evidencing, therefore, the need to know the distribution of the pluviometric regime of the region. The main objective of this work is to present an analysis of the impacts of climate change on rainfall in the Machadinho's hydroelectric power plant region, which has an installed capacity of 1,140 MW and is located in the states of Santa Catarina and Rio Grande do Sul.

2. Material and Methods

2.1 Study area description

An evaluation of precipitation projections in the region of the Machadinho Hydroelectric Power Plant, located in the Uruguay River basin (Figure 1). According to Schork et. Al. (2012), a Machadinho Hydroelectric Power Plant is located in the states of Santa Catarina and the Rio Grande do Sul between latitudes 27°31 'and 27°46' south and longitudes 51°47 'and 51°11' west.

The Basin extends between the parallels of 27° and 34° South latitude and the meridians of 49°30 'and 58°5'W. It covers an area of approximately 384,000 km2, of which 174,494 km2 are located in Brazil, equivalent to 2% of the Brazilian territory. According to Andreolli ,(2003) its Brazilian portion is in the southern region, comprising 46,000 km2 of the State of Santa Catarina and 130,000 km2 in the State of Rio Grande do Sul. It is bordered to the north and northeast by the Serra Geral, to the south by the border with the Eastern Republic of Uruguay, east by the Central Depression Riograndense and the west by Argentina.

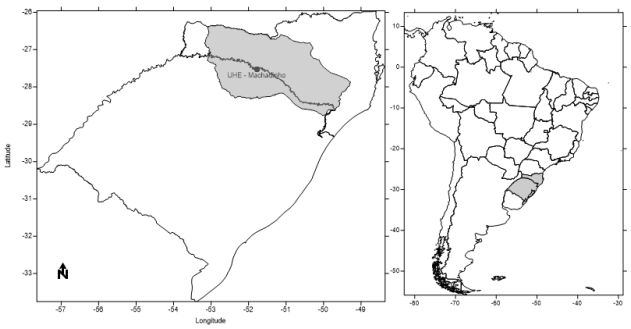

Figure 1. Study area localization.

2.2 Data description and climate model

The scenarios were generated using the models used in the Fifth Report of the Intergovernmental Panel on Climate Change (IPCC-AR5), based on an analysis of the seasonal variability of precipitation and the consequent variation in energy production.

The database used in this research is part of the Phase 5 Intercomparison of Matching Models (CMIP5) and contributed to the preparation of the fifth IPCC-AR5 report. The data were extracted from ACCESS model (The Australian Community Climate and Earth System Simulator). According to Van Vuuren et al., (2011) in AR5 the scenarios are organized according to the RCPs. In this research, RCP 8.5 scenario was used which represents a scenario with a continuous population growth, resulting in high carbon dioxide emissions, with an increase Up to 4 ° C. According to Silveira et al, (2016), this scenario is considered to be the most pessimistic for the 21st century in terms of greenhouse gas emissions, consistent with no policy change to reduce emissions and strong reliance on fossil fuels. The climatic projections of the precipitation series were divided into three scenarios: Scenario-1 (2026-2050), Scenario-2 (2051-2075) and Scenario-3 (2076-2100), the seasonal analysis was done for each of these scenarios.

3. Methodology

The monthly precipitation data were extracted from the IPCC-AR5 database, the information is provided in grid points, and Grads (Grid Analysis and Display System) software were used to extract the results. According to Souza (2004) Grads is a system of visualization and analysis of data in grid points, it works with binary data matrices, in which the variables can have up to four dimensions (longitude, latitude, vertical levels and time). After this stage, the historical data series and the data series with the climatic projections were organized. The projections were divided into three 25-year scenarios: Scenario-1 (2026-2050), Scenario-2 (2051-2075) and Scenario-3 (2076-2100). In the sequence precipitation anomalies were calculated from the following equation:

$$A_{Pre}\ (\%) = ((P_{MM} - P_{MN})/\ P_{MN)}*100 \quad (1)$$

Which:

A_{Pre} (%) is the precipitation anomaly in percentage;

P_{MM} is the mean precipitation of the analyzed month;

P_{MN} is the climatological norm corresponding to the analyzed month.

World Meteorological Organization (WMO) defines climatological normal as averages of climatological data calculated for consecutive periods of 30 years.

4. Results and Discussions

The permanence curve is important for the study of precipitation variability, being possible to verify the probability of occurrence of the events that occur in the watershed. The figures show the permanence curves for Station 1 (Figure 3a) located at -26.25 ° latitude and -52.50 ° longitude and for station 2 (Figure 3b) located at -27.50 ° latitude And -50.63° longitude. In both stations, the trend in the increase of monthly average rainfall for the three scenarios was observed. Analyzing the third scenario of Posto 1, precipitation projections indicated an increase of around 400 mm, compared to scenarios 1 and 2. In relation to the lower precipitation rates scenario 1 presented values below 200 mm in 70% of the analyzed period. For station 2, the maximum precipitation presented values ranging from 600 to 900 mm around 5% of the time.

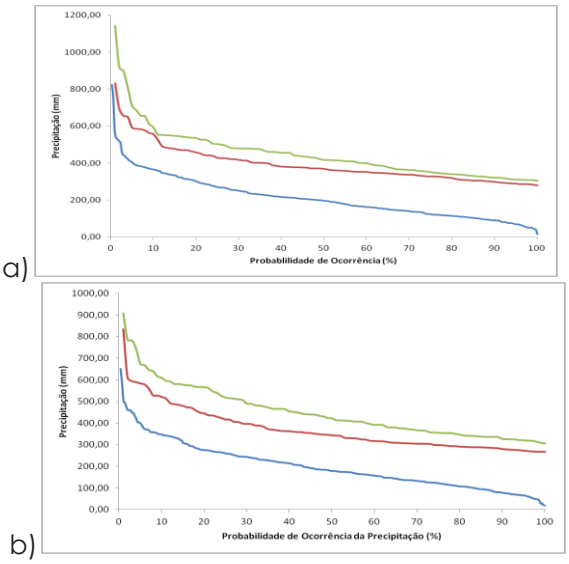

Figure 3. Permanence curve of precipitation projections for scenario 1 (blue line); Scenario 2 (red line); Scenario 3 (green line): a) Post 1 and b) Post 2

Figure 4 shows the positive anomalies in the two stations analyzed indicating a significant increase of the precipitation, mainly for the spring period, with an increase of around 200 mm, for the third scenario. Summer was the period that indicated the smallest increase in precipitation, with values around 30 mm above the climatological norm.

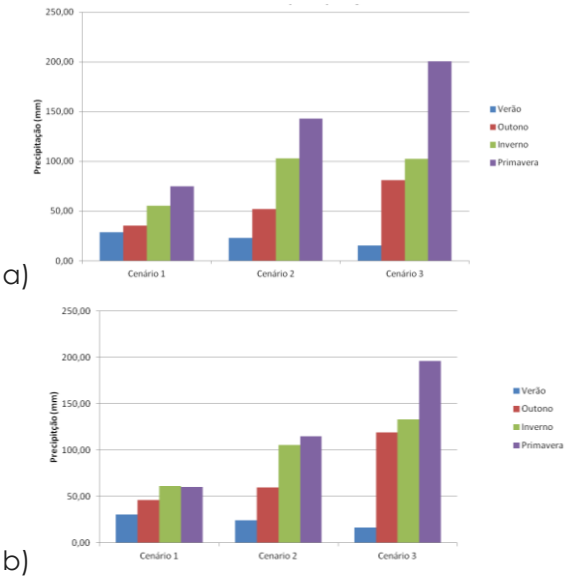

Figure 4. Seasonal Precipitation Anomalies: a) station 01 and b) station 02

Based on the average precipitation projections of the hydrographic basin where the Machadinho HPP is located, it was observed that the highest values of precipitation are found in the western half of the basin, fluctuating around 200 mm for scenario 1 (Figure 5a) .

Scenario 2 (Figure 5b) presented a precipitation projection around 238 mm and an increment around 64 mm for scenario 3 (Figure 5c), in relation to the first scenario analyzed, thus verifying a tendency in the increase of precipitation For the three scenarios in the Hydrographic Region of the Machadinho Hydroelectric Power Plant.

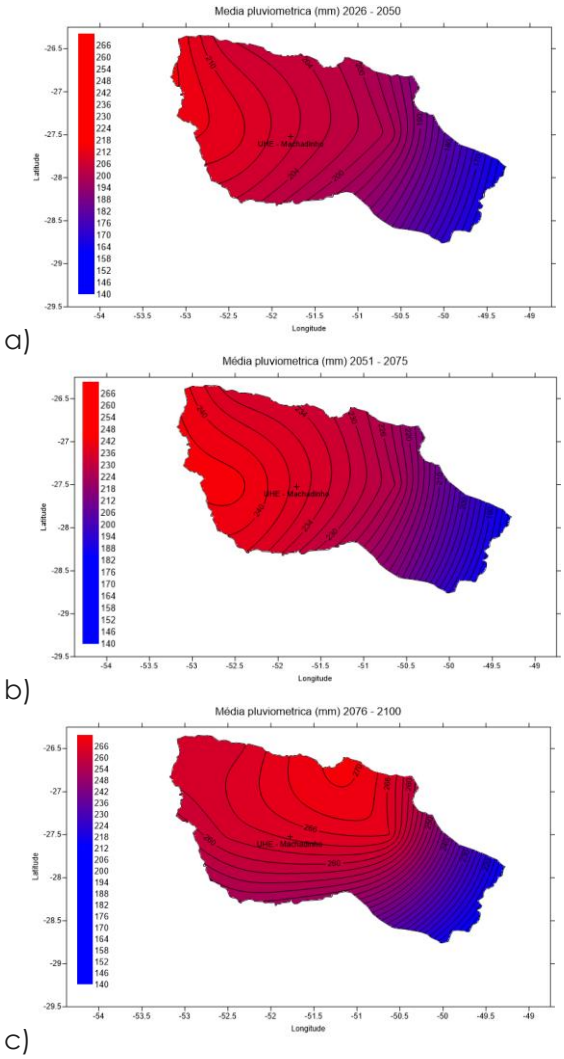

a)

b)

c)

Figure 5. Precipitation projections: a) Scenario 1 (2026 - 2050; b) Scenario 2 (2051 - 2075); C) Scenario 3 (2076 - 2100).

5. Conclusion

The hydroelectric plants are in the first position in the Brazilian energy matrix, evidencing, therefore, the need to know the distribution of the pluviometric regime of the region. The model analyzed in this article presented a positive trend for precipitation in the period from 2026 to 2100, designing anomalies between 25 and 200 mm in each 24 - year period for the precipitation variable. A greater amplitude is observed in the precipitation of 2076-2100, indicating an increase in the occurrence of major precipitation events, mainly in the spring period, considering that the rains in the Machadinho HPP region are increasing in the scenarios analyzed, it is concluded That the level of the reservoir of the plant tends to increase, changing the pluviometric regime of the region.

Acknowledgement

This research did not receive any specific grant from funding agencies in the public, commercial, or not-for-profit sectors.

References

Ivanilto,A.(2003). Previsão de vazão em tempo real no Rio Uruguai com base na previsão meteorológica. Dissertação de Mestrado. Universidade Federal do Rio Grande do Sul.

Grimm, I. J. (2016). Mudanças Climáticas e Turismo: estratégias de adaptação e mitigação. Tese de Doutorado, Pós-graduação em Meio Ambiente e Desenvolvimento da Universidade Federal do Paraná. *Curitiba*, 248.

Moraes,F.(2013). Entenda como são feitos os relatórios do IPCC. Disponível em: <http://www.oeco.org.br/dicionario-ambiental/27621-entenda-como-sao-feitos-os-relatorios-do-ipcc/>. Acesso em: 06 maio 2016.

Nimer, E. (1989) Climatologia do Brasil.(2nd edition). Rio de Janeiro: IBGE.

Schork, G.,Hermes-Silva, S., Beux, L. F., Zaniboni-Filho, E., Nuñer, A. P. O. (2012). Diagnóstico da pesca artesanal na usina hidrelétrica de Machadinho, alto rio Uruguai – Brasil. Bol. *Inst. Pesca, São Paulo, 38*(2),97 –108.

Silveira,S.S., Souza Filho, F., Martins, E. S., Oliveira, J., Costa, Alexandre, Nobrega, M., Souza, S. A. (2011). Climate change in the São Francisco river basin: analysis of precipitation and temperature. *RBRH*, 21, 416 – 428. Porto Alegre abr. /jun. 2016.

Van Vuuren, D. P., Edmonsds, J., Kainuma, M., Riahi, K., Thomsonm, A., Hibbard, K., Hurtt, G. C., Kram T., Krey, V., Lamarque, J. F., Masui, T., Meinshausen, M., Nakicenovic, N., Smith, S. J., Rose, S. K. (2011). The representative concentration pathways: an overview. *Climatic Change*, *109*, 5-31.

Journal Of Contemporary Urban Affairs

2017, Volume 1, Number 3, pages 67– 72

Quality Evaluation and Study of Ecological Toxicity of Heavy Metals in Shadegan Wetland

* Dr. **Samar Mortazavi** [1], Dr. **Mohsen Tizhoosh** [2], Dr. **Zahra Cheraghi** [3]

[1, 2, 3] Department of Environmental Science, Faculty of Natural Recourses and Environmental Science, Malayer University, Iran

[1] E mail: mortazavi.s@gmail.com , [3] E mail: nejatsan@tums.sc.ir

ARTICLEINFO:

Article history:

Received 2 August 2017

Accepted 10 August 2017

Available online 12 October 2017

Keywords:

Sediment quality;

Toxicity; heavy metals;

Shadegan wetland.

ABSTRACT

Wetlands hold a principal position in storing food for primary producers, so they are not able to bear the pressure. The slightest disturbance, hence, may harm wetlands and cause detrimental effects. The present study aims at monitoring heavy metals and evaluation of the sediment quality index of Shadegan wetland in Iran. Thus, a sampling of surface sediments of the wetland was performed at ten stations with three replications; after the preparation of samples with aqua regia, the concentrations of heavy metals were measured by atomic absorption spectroscopy. The quantification of sediment pollution using the contamination factor, contamination degree, pollution load index, ecological risk assessment index, and ecological toxicity of heavy metals in the region were all carried out. The results of Cf and Cd showed that the degree of zinc and copper contamination is low; however, the degree of lead contamination is moderate. Moreover, the obtained PLI was less than 1 indicating a lack of sediments contamination with heavy metals. The RI was less than 150 indicating a low risk of contamination. In addition, comparing the concentrations of elements with National Oceanic and Atmospheric Administration and Sediment Quality Guidelines showed slightly toxic and non-toxic sediments, respectively. Finally, based on a mixture of effect range median, all sediment samples are placed in the first category with less than 12% toxicity probability.

JOURNAL OF CONTEMPORARY URBAN AFFAIRS (2017) ***1***(3), 66-72.

https://doi.org/10.25034/ijcua.2018.3683

www.ijcua.com

1. Introduction

Aquatic ecosystems, as one of the main environmental features, are a key supplier of food and a roof over aquatic organism's head; on the other hand, they are also large sources for a wide range of pollutants. Since these ecosystems withstand a high capacity for development, they are subject to more serious risk due to the pollutants. Domestic and industrial sewage discharges, the growth in urbanization, and industrial activities in coastal areas are severe threats to the safety of the coastal environment and aquatic ecosystems. Among the existing pollutants in the sewage, heavy metals can be mentioned, especially the ones that play important roles in society as the main raw materials for many industries. (Zhuang and

***Corresponding Author:**

Department of Environmental Science, Faculty of Natural Recourses and Environmental Science, Malayer University, Iran,

E-mail address: mortazavi.s@gmail.com

Gao, 2014; Caerio, et l, 2005) Some, such as copper and zinc, play a vital role in the metabolism of the human body. However, in high concentrations, they turn into toxic substances. Being attributable to high persistence toxicity, solubility low absorption and accumulation in the bottom sediments, heavy metals cause contamination in aquatic environments. (Caerio, et al., 2005) The biological toxicity and bio-magnification in food chains have made the issue of heavy metals a significant global problem. (Förstner and Wittmann, 1983) the ways to clean up contaminated sediment are mostly costly, and in some cases impossible. Hence, the evaluation of sediment contamination in the aquatic environment, identifying sources of pollution, applying management policies, and processes to reduce a number of pollutants into the aquatic environment is more important than focusing on clearing techniques.

Many studies have been done in this regard, among which the one carried out by Zarezadeh and Rezai, (2014) can be mentioned through which they have investigated the heavy metals in the sediments bed of mangroves Khurgabrik in Jack Port involving Molar coefficient, the degree of reformed contamination, and ecological risk assessment index. Vaezi et all, (2014) have investigated Mollar environmental index, pollution load, ecological toxicity in sediments in Mosa Firth, Persian Gulf. Chai et al., (2016) explored heavy metal pollution in river sediments in Serbia by calculating the pollution load index and ecological risk assessment. Chai and et al. Sakan and Dordevic, (2015) examined the index of enrichment, molar and ecological risk assessment in Xiangjiang River sediments. In the present study, the types of sediment geochemical index have been determined. Moreover, the ecological risks have been assessed, and ecological toxicity of sediments with heavy metals, namely lead, zinc and copper have been analyzed. The results have been compared with the standards of NOAA and SQG, respectively.

2. Materials and Methods

2.1Area of study

The Shadegan Wetland with an area of approximately 400,000 hectares in the range of coordinates 48 degrees 17 minutes and degrees 50 minutes east, 30 degrees 17 minutes 30 degrees and 58 minutes north is located in Khuzestan province, Iran, and has been recognized as an international wetland in the Ramsar Settlement in 1972. (Nasirian et al., 2015)

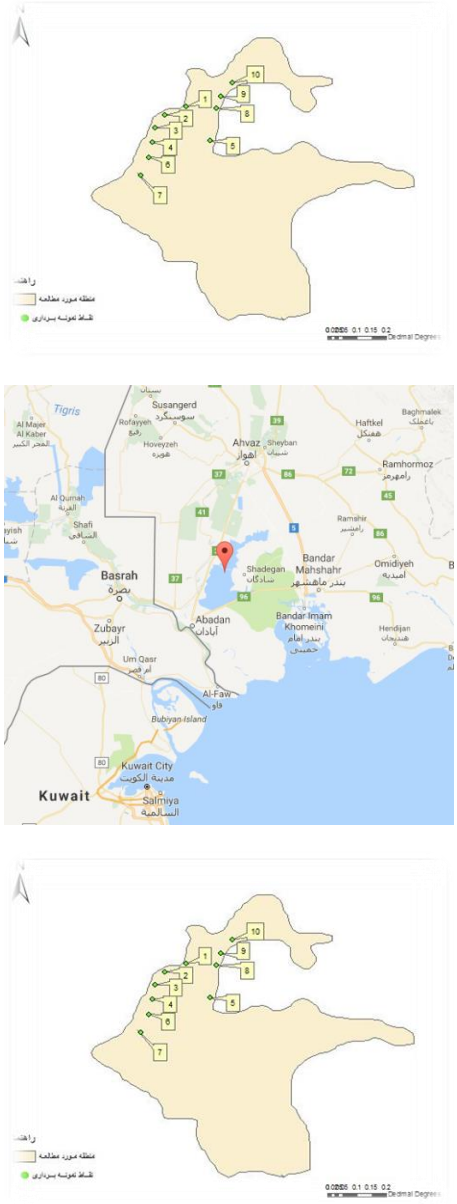

Figure 1. *The location of the Shadegan wetland (left) [Source: Google map], and the locations of the sampling stations within the wetland (right).*

2.2 Sampling and Preparing Samples

As per available access points, a sampling of surface sediments was carried in 10 stations with three replications and recording the geographic coordinates (**table 1**).

For the purpose of preparation, the sediment samples were dried in an oven at a temperature of 105° C. Then, they were crushed in a stone mortar and screened by a 63-micron sieve. For the acid ingestion of sediments, Direct Aqua Regia was employed, following the ingestion; with the contribution of double distilled water in a 25 mL volumetric flask, the volume was delivered. (Yap et al., 2012) To ensure the accuracy of ingestion and elimination of errors

due to sample preparation and to undo the effect of consumed materials on the concentration of metals in each of ingestion operations, a control sample was considered; at the end of atomic absorption ContrAA700analyticjena, the concentration of metals in the samples was read. Detection limit for Cu, Pb and Zn in flame method was 0.23, 0.88 and 0.25 microgram per gram, respectively.

Table 1. Geographical coordinates of the sampling stations within Shadegan wetland.

Land use	Geographical Coordinates	
Road& Entrance of the village	N 66.55 ″ °49′ 30	74.1″ E 48°33′
Rural residential area	N 32.3 ″ 30°48′	34.25″E 48°32′
Rural residential area	N 23.58 ″ 30°45′	18.57″ E 48°31′
Recreation area	N 85.48 ″ 30°43′	87.58″E 48°30′
Recreation area	N 99.38 ″ 30°45′	83.11″E 48°35′
Recreation area	N 12.5 ″ 30°42′	96.47″ E 48°39′
Place& Pleasure Pier refueling	N 87.0 ″ 30°41′	44.15″E 48°27′
Agricultural area	N 16.26″ 30°48′	70.36″E 48°38′
Agricultural area with an area of low	N 16.22″ 30°49′	33.24″ E 48°40′
Agricultural& Wastewater discharge	N 75.20″ 30°50′	87.52″E 48°41′

3. The Investigated Indices

Data geochemical description and choosing the sample ground play an important role in investigations. Many researchers have used the mean of cortical or frequency of data as a base. In the present study, to determine the extent of sediment contamination by heavy metals Shil Mean of Cu, Zn and Pb were 45, 95 and 20, respectively, which are presented by Turkian, and Wedephol, (1964) This index is a benchmark to measure pollution which is achieved by dividing the concentration of the elements to the same concentration of elements in the reference material (Shil average). it shows the amount of sediment contamination by heavy metals. The classification of Hakanson pollution index.(Hakanson,1980) $C_f = M_x/M_b$ (Table 2).

3.1Cp Potential Pollution Index

Potential pollution index is obtained by dividing the maximum amount of each metal in the sediment on the average value of the same metal in the earth's surface and is calculated as follows:

$Cp = \frac{(metal)sample\ Max}{(metal)Background}$,

where Cp <1 indicates a low pollution, 1≤CP <3 moderate pollution, and 3≤Cp severe pollution,Cd[5] Pollution Degree Index. (Davaulter, and Rognerud, 2001).

Table 2. Different contamination factor (Cf) and factor (Cd), (Hakanson,1980)

Cf Value	Contamination factor level	Cd class	Degree of Contamination level
Cf <1	Low	cd<6	Low
1≤ Cf <3	Moderate	6≤cd<12	Moderate
3≤ Cf <6	Considerable	12≤ cd<24	Considerable
6≤ Cf	Very high	24≤cd	Very high

Total coefficients of pollutant contamination which are being studied show the overall degree of sediment contamination called Hakson pollution degree and is obtained from $C_d = \sum_{i=1}^{n} Cf_i$ (Table 2).

3.2 Pollution Load Index (PLI)

Tomlinson, pollution load index, has been the n-th root pollution load factor at one station from all the elements and is determined as = $\sqrt[n]{Cf_1 \times \dots\dots \times Cf_n}$. If 1> PLI, it indicates a low concentration of heavy metals and the lack of pollution; PLI = 0 indicates the proximity of metal concentration to the background concentration, and PLI> 1 indicates contaminated sediment. (Varol, 2001)

3.3 Ecological Risk Assessment Index (RI)

For assessment of ecological risk index deposits in the aquatic environment, Hakansvn,(1980) presented $RI = \sum_{i=1}^{m} E_r$ with $E_r = T_r * C_f$ where E_r is potential ecological risk for each element and RI is potential ecological risk of the total metals (cumulative). Hakanson's theory, (1980), T_r, is defined as the ratio of toxicity in this equation, for Pb, Zn and Cu is 5, 1, and 5, respectively (Table 3).

Table 3. Risk index levels and their effects.

Risk index	Ecological risk criteria of environment
RI<150	Low
150≤R< 300	Moderate
300≤R<600	Considerable
600≤R	Very high

3.4 Estimation of Ecotoxicology

Diverse amounts of pollutants affect the exposed organisms in different ways. In this

regard, in some countries standards for pollutants have been proposed, among which America Standard Quality Sediment NOAA and Canada Guidelines quality sediments SQGS are the best-knowns, and the most widely used ones. The primary purpose of these standards is protecting the fish from the negative impact of organic and inorganic pollutants in sediments, grading and prioritizing contaminated areas for further investigation, and estimating the location of sediment pollution. Two sets of instructions that are commonly used include: Effect Range Low (ERL), Effect Range-Median (ERM), Probable Effect Level (PEl), and Threshold Effect Level (TEL). While the effect range low (ERL or TEL) shows the concentration below which there is no possibility of harmful effects, the major impact range (ERM or PEL) refers to the higher concentrations above which harmful effects and side effects of pollutants are likely to be observed. (MacDonald et al,2000; NOAA,2009) (Table 4).

Table 4. Sediment Quality Guidelines (US and Canada) based on standard values.

Reference	Cu	Zn	Pb	Index	Standard
NOAA,2009	34	150	47	ERL	NOAA
	270	410	218	ERM	
Smith et al,1996	70.35	123	35	TEL	SQGS
	197	315	30.91	PEL	

To obtain more realistic amounts of sediment toxicity effects in living organisms, the probable effective limit coefficient (PELQ) and the average effective limit coefficient (ERMQ) are calculated according to the following equations:

$$PELQ = \frac{\sum_{i=1}^{n} \frac{Mi}{PELi}}{n} \quad \text{and} \quad ERMQ = \frac{\sum_{i=1}^{n} \frac{Mi}{ERMi}}{n}.$$

Here Mi is concentrations in sediment I, PELi and ERMi: The possible effective concentration and average effective concentrations in sediment i, respectively. The variable n is the number of investigated metals in each instance. Correspondingly, the factors associated with the quantity of sediments are reported in Table 5. To calculate the amount of toxicity resulting from the mixture of a group of toxic elements, SQGS is calculated as follows (ERM: mid- effective range, Ci: concentration, N: the number of elements):

$$\mathrm{m-ERM-Q} = \sum_{i=1}^{n} \frac{\mathrm{Ci}/\mathrm{ERMi}}{\mathrm{n}}$$

Table 5. The relationship between sediment toxicity value of ERMQ and PELQ and chance of sediment toxicity classification based on ERM. (Hwang et al ,2008)

Sediment toxicity	ERMQ	PELQ	m-ERM-Q	Possibility of toxicity
non toxic	>0.1	>1.0	>0.1	12%
slightly toxic	0.1-0.5	0.1-1.5	0.5-0.11	30%
moderately toxic	0.5-1.5	1.5-2.3	1/5-0.51	40%
heavily toxic	<1.5	<2.3	<1/5	74%

4. Results

The results of the concentration of zinc, copper and lead in surface sediment samples of Shadegan wetland (in micrograms per gram dry weight) are shown in the Figure 2. The potential contamination index (Cp) values of Pb, Zn and Cu are 1.209, 0.483 and 0.316, respectively.

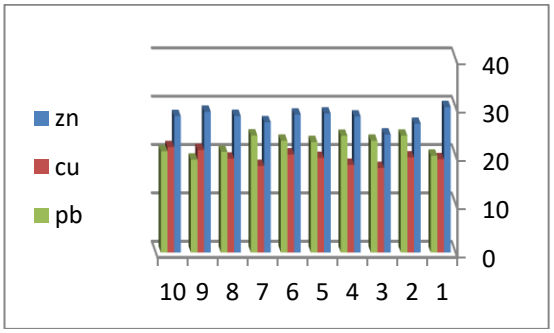

Figure 2. *Average concentration of Zn, Cu and Pb in surface sediment Shadegan wetland (µg/g).*

In order to determine the extent of contamination in the area Cf, Cd, mCd, PLI, RI and m-ERM- Q indices were calculated. The results are presented in Table 6. Ecological toxicity calculation results PELQ and ERMQ were 0.86 and 0.70, respectively, which are indicative of low toxicity and non-toxic sediments of the area in comparison to the studied elements. The results of the calculation of sediment contamination based on the of the ERM and the ERL indices are indicating that, in all the samples, concentrations of Pb, Cu and Zn are less than effective limit (<ERL). The calculated results of all the stations show that m-ERM-Q for the sediment samples exhibit 12% probability to contain toxicity probability.

Table 6. The results of heavy metal pollution in sediments of the Shadegan wetland.

Cd	MCd	10	9	8	7	6	5	4	3	2	1	St.No	
11.08	1.11	1.04	0.96	1.04	1.20	1.15	1.14	1.20	1.15	1.20	1.00	**Pb**	
4.28	0.43	0.48	0.47	0.43	0.39	0.45	0.43	0.402	0.38	0.43	0.42	**Cu**	**Cf**
2.90	0.29	0.29	0.35	0.29	0.28	0.30	0.30	0.29	0.25	0.28	0.31	**Zn**	
-	-	0.52	0.55	0.51	0.51	0.54	0.53	0.52	0.47	0.52	0.51	**PLI**	
-	-	7.89	7.46	7.64	8.23	8.30	8.15	8.44	7.90	8.43	7.41	**RI**	
-	-	0.08	0.08	0.08	0.08	0.08	0.08	0.08	0.07	0.08	0.08	**m-ERM-Q**	

5. Discussion and Conclusion

Investigating the mean concentrations of heavy metals in wetland sediments indicates that Zn> Pb> Cu. The mean concentration of Zn and Cu compared to the permissible concentration of these metals in a global average is lower, and the mean of lead is higher than the average global of the Earth's crust. The cause of this can be the contamination of the sediments to these metals resulting from the discharge of industrial sewage at the sampling stations which is in line with the findings of Hatefi et al, (2016) and Mohammad Saleh et al, (2012) The Cp index results for 1<Pb<3 indicate that the average contamination in Shadegan wetland is in accordance with the results of Chandramohan studies. (Chandramohan, 2016) In this regard, Zn and Cu content is less than 1 which indicates their low pollution in the place.

As it was mentioned in the results section, the pollution index coefficient results (Cf) was less than 1 in all stations for copper and zinc. Hence, they are places in the first category with a low degree of contamination. The results of a lead pollutant index factor were those of average pollution in all stations except for the ninth station; this may be due to the practical usage of this station, which is a small agricultural area. The results are in line with the findings of Mohammad Saleh et al, (2012) and Hatefi et al,(2016) Moreover, based on the results obtained from pollution index factor (Cd), Zn and Cu are ranked first as the two low pollution factors; the Cd factor of lead holds the second rank and has an average pollution factor, a finding which is consistent with the reports of Gholam Dokht Bandari et al,(2015) The obtained mCd index for Zn, Cu, and Pb revealed that all these metal elements are of very low pollution factors; the findings on Zn are similar to those of Zarezadeh and Rezaei,(2014) the results of Cu and Pb are in line with numbers of Gholam Dokht Bandari and Rezaie,(2015) studies. The index rate of PLI of all the stations was less than 1 which is indicative of pollution-free nature of the sediments there; this is consistent with the results found by Chandramohan et al, (2016) and Mohammad Saleh et al, (2012). The ecological risk index shows that, in all stations, the numerical results were less than 150 and that the stations exhibited low ecological risks; this was in harmony with Zarehzadeh and Rezaei, (2000).

Compared with the existing standards of the U.S. and Canada, the results of the present study are representative of low- or non-toxic nature of the sediments for the living organisms in all the stations with low-toxic ratios. Lastly, according to the results of the sediments assessment indices, the prominent role of the destructions of heavy metals in threatening wildlife and the involvement of both human and natural factors on the distribution and concentration of heavy metals, as well as maintaining the balance of ecosystems, reviewing and monitoring the quality of the sediments are among the most important environmental considerations. It is paramount to identify the adverse effects of the pollutants on the environment as prerequisite for a proper management.

Acknowledgement

This research did not receive any specific grant from funding agencies in the public, commercial, or not-for-profit sectors.

References

Zhuang, W., Gao, X L. (2014). Integrated assessment of heavy metal pollution in the surface sediments of the Laizhou Bay and the coastal waters of the Zhangzi Island, China: comparison among typical marine sediment quality indices. *PLoSOne,* 9 (4),94-145.

Caeiro, S., Costa, M.H., Ramos, T.B., Fernandes, F., Silveira, N., Coimbra, A., Medeiros, G., Painho, M. (2005). Assessing heavy metal contamination in Sado Estuary sediment: an index analysis approach. *Ecological Indicators, 5*(2), 151–169.

Förstner, U., Wittmann, G.T. (1983). *Metal Pollution in the Aquatic Environment*, (2nd edition). Berlin, Germany: Springer.

Zarezadeh, A., Rezaee, P. (2014). Study on accumulation of heavy metals in mangrove sediments, Gabrik creek (Jask), *Journal of Nature Environment* ,*69*(1), 61-78.

Vaezi, A., karbasi, A., fakhrai, M., Valikhani samani, A., Heidari, M. (2014). Assessment of sources and contaminations in Marine sediments of Musa Estuary, Persian Gulf, *Journal of Environment studies*, *40*(2), 345-360.

Chai, L., Li, H., Yang,Z ., Min, X,. Liao,Q., Liu,Y., Men,S., Yan,Y., Xu,J.(2016). Heavy metals and metalloids in the surface sedimentsof the Xiangjiang River, Hunan, China: distribution, contamination, and ecological risk assessment. *EnvironSciPollut Res*,*24*(1), 874–885.

Skins., Dordevic,D., (2015). Assessment of pollution with toxic elements in river, sediments by calculating facors of contamination and application of statistical methods. *Naučno-stručničasopis SVAROG br*,*10*, 316-329.

Nasirian, H., Alimohammadi, M., Kamandar, M., Saikhbarahwie, L., Mojadami Moghadam, H., Sheikhi,R. , Asgari, H., Hosseini, S.S., Farhani Ahmadi , F. (2015). water Quality Evaluation of the Shadegan and Hawralazim wetland from Iran. *Indian J.sci.Res*,*6*(2),11-24.

Yap, C.K., Ismail, A., Tan, S.G., Omar H. (2002). Concentrations of Cu and Pb in the offshore and intertidal sediments of the west coast of Peninsular Malaysia. *Environment International, 28*(6). 467–479.

Turkian, K.K., Wedephol, K.H. (1964). Distribution of the elements in some major units of the earth crust, *Geol Soc Am Bull*, 175-192.

Hakanson, L. (1980). "Ecological risk index for aquatic pollution control, a sedimentological approach". *Water Research, 14*, 975–1001.

Davaulter, V., Rognerud, S. (2001). Heavy metal pollution in sediments of the Pasvik River drainage. *Chemosphere, 42*, 9-18.

Varol, M. (2001). Assessment of heavy metal contamination in sediment of the Tigris River (Turkey) using pollution indices and multivariate statistical techniques. *Journal of Hazardous Materials, 195,* 355-364.

MacDonald, D. D., Ingersoll, C. G., Berger, T. A. (2000). Development and evaluation of consensus-based sediment quality guidelines for freshwater ecosystems. *Arch Environ Contam Toxicol*, *39*, 20–31.

NOAA (National Oceanic and Atmospheric Administration). (2009). SQUIRT, Screening Quick Reference Tables for in Sediment, W. 2005. Sediments in the catchment-coast continuum. *J Soil Sediment, 5*, 2-8.

Hwang, H. M., Green, P. G., Young, T. M. (2008). Tidal salt marsh sediment in California, USA: Part 3. Current and historic toxicity potential of contaminants and their bioaccumulation. *Chemosphere*, *71*(11), 2139–2149.

Hatefi, R., Khezri, M., Khodaee, K., Shahsavari, A.A., Modaberi, S., Asadian, F. (2016). Geochemical modeling of environmental chemical pollutions rising from Granitoid Intrusions and mapping potentially hazardous areas: Ahar. *Journal of Earth Science Researcher*, *7*(26), 1-20.

Mohammad Salah, E.A., Zaidan, T.A., Al-Rawi, A.S. (2012). Assessment of Heavy Metals Pollution in the Sediments of Euphrates River, Iraq. *J. of Water Resource and Protection*,*4*, 1009-1023.

Chandramohan, J., Chandrasekaran, A., Senthilkumar, G., Elango,G., Ravisankar, R.(2016). Heavy Metal Assessment in Sediment Samples Collected From Pattipulam to Dhevanampattinam along the East Coast of Tamil Nadu Using EDXRF Technique. *Journal of Heavy Metal Toxicity and Disease,1*(2),8.

Gholam Dokht Bandari, M., Rezaie, P. (2015). Study of some Heavy metal pollutions in the Hormuz Islands coastal sediments and Their origin. *Journal of Oceanoghraghy*, 6(22), 97-106.

Tizhoosh, M., Tizhoosh, H.R. (2016). The Concentration of Zinc, Lead, Cadmium and Copper in Raw Milk Production in Industrial Farms in Khorramabad, Iran. *International Proceedings of Chemical, Biological and Environmental Engineering*, *93*, DOI: 10.7763/IPCBEE. 2016. V93. 16

JCUA | International Journal of Contemporary Urban Affairs

Journal of Contemporary Urban Affairs

Printed: Anglo American Publication LLC